Determinants of HIV-1 Gag Localization to Uropods in Polarized T cells and the Role Uropods Play in Virus Spread

By

George Nicholas Llewellyn

**A dissertation submitted in partial fulfillment
of the requirements for the degree of
Doctor of Philosophy
(Cellular and Molecular Biology)
in The University of Michigan
2012**

Doctoral Committee:

Assistant Professor Akira Ono, Chair
Professor Kathleen Collins
Professor Benjamin Margolis
Professor Richard Miller
Professor Alice Telesnitsky

Table of contents

List of Figures

List of Tables

Abstract

Determinants of HIV-1 Gag Localization to Uropods in Polarized T cells and the Role Uropods Play in Virus Spread

By

George Nicholas Llewellyn

Chair: Assistant Professor Akira Ono

HIV-1 is a deadly virus that kills millions of people around the world each year. One of the primary targets of HIV-1 in the human body is T cells. In lymphoid organs, such as lymph nodes, T cells are highly motile and adopt an elongated or polarized morphology. However, little is known about how HIV-1 localizes, assembles or spreads in polarized T cells. Thus, determining the molecular mechanisms utilized by HIV-1 in polarized T cells can help to understand the virus *in vivo*.

Polarized T cells are characterized by a leading edge at the front and a rear end protrusion called a uropod. In this thesis, it was determined that the HIV-1 structural protein Gag localizes to the uropod in polarized T cells. HIV-1-expressing T cells were found to contact uninfected target cells preferentially via uropods relative to leading edges. Also, uropods participated in virological synapses that mediate cell-to-cell

transmission of HIV-1. Together, these findings indicate that uropods could play an important role in HIV-1 spread *in vivo*. Mutational analyses were also performed to identify the viral determinants of uropod localization of Gag. Nucleocapsid (NC) is a structural domain of Gag that binds and packages viral RNA genomes and can promote multimerization of Gag by using RNA as a scaffold. NC-mediated multimerization, at the level of tetramerization or higher, was found to be required for uropod localization of Gag. In identifying the cellular determinants that mediate Gag localization to uropods, Gag was found to copatch with some uropod markers (CD43, PSGL-1, CD44) even in unpolarized T cells. In contrast, Gag did not copatch with other uropod markers (ICAM-1, ICAM-3, CD59) in unpolarized T cells. These data, along with live cell analyses, indicated that Gag associates with a specific subset of uropod-directed microdomains (UDMs) that could carry Gag to the uropod. The specificity of Gag association with UDMs was found to be determined by matrix (MA), another structural domain of Gag that is responsible for plasma membrane binding.

The observations made in this thesis suggest a working model of HIV-1 replication and spread in polarized T cells: When NC-mediated multimerizaton reaches the level of tetramerization or higher, Gag associates with specific uropod-directed microdomains enriched in CD43, PSGL-1 and CD44 via an MA-mediated mechanism. These Gag-associated UDMs then laterally localize on the membrane to the uropod where virus particles assemble and accumulate. Uropods then mediate contact and VS formation with target cells to facilitate cell-to-cell transmission.

CHAPTER I

Introduction

HIV-1 genome organization

Human Immunodeficiency Virus Type-1 (HIV-1) is an enveloped virus belonging to the family Retroviridae. The HIV-1 genome encodes three large polyproteins, two regulatory proteins and four accessory proteins. The genome itself is roughly 9KB, and expression of the viral proteins requires differential splicing. The three large polyproteins are Gag, Pol and Env, the accessory proteins are Vpu, Vif, Vpr, and Nef, and the regulatory proteins are Tat and Rev (Fig. 1.1A).

The transcribed genome of HIV-1 has several splice variants. First, the HIV-1 polyproteins Gag and Pol are expressed from unspliced viral RNA. Gag is the primary structural polyprotein of HIV-1. Gag is composed of four structural domains and is sufficient to form virus-like particles[1]. Pol is a polyprotein that is translated as a part of a fusion protein (GagPol) by a ribosomal frameshift that occur near the end of the Gag sequence. The efficiency of this frameshifting ranges from 0.8-2.4% in cultured 293T cells and from 4.6-8.5% *in vitro,* depending on HIV-1 subtype[2]. The polyprotein Pol contains the viral enzymes Protease, Reverse Transcriptase and Integrase. Protease cleaves Gag into its four subunits, which is a process required for maturation of the virus into an infectious form. Reverse Transcriptase converts the genomic RNA into double stranded DNA. After transport into the nucleus, Integrase facilitates incorporation of this

double stranded DNA into the host cell chromosome. Unspliced RNA is also used as the viral genome and packaged into new virus particles.

Singly spliced RNA encodes the third viral polyprotein Env and the accessory proteins Vpu, Vpr and Vif. Env (gp160) is composed of a surface subunit (gp120) that binds to the virus receptor CD4[3] and the co-receptors CCR5 or CXCR4[4-6]. Env also contains a transmembrane subunit (gp41) that mediates fusion of the viral and cellular membrane during the virus entry process. Env is cleaved into its gp120 and gp41 subunits by cellular proteases. Vpu binds to and downregulates CD4[7] and a host restriction factor Tetherin[8, 9], facilitating release of the virus from cells. Vpr mediates a delay or arrest of infected cells in the G2 phase of the cell cycle[10, 11]. Vif prevents the incorporation into virus particles of a cellular restriction factor Apolipoprotein B mRNA editing enzyme catalytic polypeptide-like 3G (APOBEG3G)[12], a cytidine deaminase that ultimately converts cytosine to uracil in the viral RNA during reverse transcription often causing deleterious mutations.

Finally, doubly spliced RNA encodes the accessory protein Nef, and the two regulatory proteins Tat and Rev. Tat enhances transcription by binding to the TAR (trans activating response) element of nascent viral RNA genomes, and stabilizing the elongation step as well as recruiting and activating cellular transcription machinery[13]. Rev attaches to the Rev Responsive Element (RRE) on unspliced and singly spliced viral mRNA transcripts and facilitates their export out of the nucleus where they can be translated[14]. Nef has several functions including downregulating CD4 and enhancing immune evasion by downregulating MHC class I[15-18].

HIV-1 Life Cycle

This is a general review of the life cycle of HIV-1. For this thesis, the sections discussing attachment and virus assembly are the most pertinent to the later chapters.

Attachment and fusion

The HIV-1 life cycle is illustrated in Fig. 1.2. HIV-1 primarily infects T cells and macrophages. The surface of an HIV-1 particle is decorated with a glycosylated protein called Env. Env heterodimers (gp120 and gp41) form trimers [19, 20]. Env binds to the host cell receptor CD4[3] and a co-receptor, usually CCR5 or CXCR4[4-6] depending on the cell tropism of the infecting virus. After attachment, the gp41 subunit of Env undergoes a conformational change. This change exposes a fusion peptide[19] that inserts into the target cell membrane. The ectodomains of trimeric gp41 then form a six-helix bundle that brings the two membranes close enough to mediate fusion[21, 22]. HIV-1 can also enter the cell via receptor-mediated endocytosis[23]. However, infection through this pathway still requires fusion of the virus with the endosomal compartment.

Uncoating

After fusion occurs, the core of the virus is released into the cytosol of the target cell. The core is composed of a structural subunit of the Gag polyprotein called capsid (CA), which forms a shell around two copies of the viral RNA genome that are bound by another subunit of Gag called nucleocapsid (NC). The core also contains Reverse Transcriptase. Uncoating of the viral core is required for release of the viral genome.[24, 25] although the exact timing and mechanism of uncoating are still being investigated. A

cellular host restriction factor, tripartite motif-containing protein 5-α (TRIM5-α), was found to bind to the viral core and interfere with the uncoating and reverse transcription processes[26]. This interaction inhibits productive infection, indicating that the uncoating process is required for HIV-1 replication. To overcome this restriction, HIV-1 has evolved mutations in CA, which allow HIV-1 to specifically evade human TRIM5-α[27, 28]. However, these CA mutations do not protect the virus against TRIM5-α proteins from other species. For example, while HIV-1 is insensitive to human TRIM5-α, it is restricted by non-human primate TRIM5-α proteins[29].

Reverse transcription and nuclear entry

If the core is successfully uncoated, reverse transcription of the RNA genome into double stranded DNA is mediated by the viral enzyme Reverse Transcriptase. It is at this stage that another host restriction factor is able to disrupt the virus life cycle. APOBEC3G deaminates cytosines to uracils in the minus strand DNA during reverse transcription, resulting in G→A mutations in the provirus[30, 31]. The HIV-1 viral protein Vif overcomes APOBEC3G-mediated restriction by directly binding to APOBEC3G and triggering its ubiquitination and degradation[12, 32, 33].

During and after reverse transcription, the pre-integration complex (PIC), which is composed of viral DNA and various viral and cellular proteins, is transported to the nucleus. This process is dependent on microtubules[34]. The mechanism by which the viral DNA and Integrase enzyme are imported into the nucleus is still under investigation.

Integration

Once inside the nucleus, multimerized Integrase interacts with the cellular protein lens epithelium derived growth factor (LEDGF) to mediate integration of the viral DNA into a host cell chromosome[35, 36]. This integrated HIV-1 DNA genome is called the provirus. It is thought that LEDGF could promote integration specifically to sites of active transcription[37, 38], although this is still under investigation.

Transcription and RNA export

The provirus is transcribed from a 5` promoter in the long terminal repeat (LTR) region. The HIV-1 protein Tat promotes transcription from this region, specifically by binding the *cis*-acting TAR element of the nascent viral RNA transcripts and recruiting chromatin remodeling complexes[39, 40]. Tat also recruits positive transcription factors such as p-TEFb that phosphorylate and activate DNA polymerase II (Pol II). Pol II then binds the TATA box of the promoter and transcribes the DNA[41]. Tat is also known to enhance initiation and elongation[42, 43]. Doubly spliced RNA that encodes the viral accessory proteins Tat, Rev and Nef are exported to the cytosol where they are translated. Export of the full HIV RNA genome to the cytosol requires the Rev protein, which oligomerizes and interacts with the Rev response element (RRE) sequence[40, 44] as well as the nuclear export protein CRM/Exportin 1 to transport the RNA out of the nucleus[45]. Once enough Rev is made, export of the viral genome can occur and translation and assembly of virus particles ensues.

Assembly

The primary structural protein of HIV-1 is a 55kD precursor polyprotein called $Pr55^{Gag}$(Gag), which contains four structural domains. These structural domains, in order from N to C-terminus, are matrix (MA), capsid (CA), nucleocapsid (NC) and p6[1, 46] (Fig. 1.1B). MA encodes a myristoylation signal at its N-terminus and a highly basic region (HBR), both of which mediate plasma membrane targeting and binding of Gag[47-52]. The myristate moiety is cotranslationally added to the N-terminus of Gag and is normally sequestered inside MA. Exposing the myristate is mediated by trimerization of Gag in a process called the myristoyl switch[49]. The myristate is inserted into the plasma membrane and increases membrane binding. Targeting of Gag to the plasma membrane also requires an interaction between the HBR and a plasma membrane phospholipid phosphatidylinositol-(4,5)-bisphosphate [$PI(4,5)P_2$][50, 53, 54]. This interaction was determined both by NMR studies and by observing Gag mislocalization after treatment of cells with 5phosphataseIV, which depletes $PI(4,5)P_2$[50, 53, 54].. Membrane binding of Gag is also regulated by RNA interactions with the HBR[55].

Assembly of virus particles requires multimerization of Gag on the plasma membrane. Multimerization of Gag is mediated by its CA and NC domains. CA mediates multimerization through a dimerization interface within the C-terminal domain of CA. The residues W184 and M185 are critical for dimerization within this interface[56-61]. NC-mediated multimerization is driven by NC utilizing RNA as a scaffold. This is supported by experiments in which 1) a loss of Gag multimerization was observed when NC was mutated, 2) RNA was required to induce Gag multimerization *in vitro*, and 3)

RNAse treatment disrupts Gag-Gag interactions in another retrovirus, MLV[56, 58, 62-65]. Gag multimerization induces plasma membrane curvature to form virus particles.

Viral genome packaging

During HIV-1 assembly, the viral RNA genome is packaged as a dimer. Genomic RNA dimerization is mediated by a "kissing loop" sequence on both RNAs that specifically interact[66]. This sequence is located within the packaging signal (Ψ). This signal is composed of four stem loops at the 5` end of the viral RNA genome. Packaging of the viral RNA into virus particles is mediated by NC. The specificity of viral RNA packaging by NC, as opposed to most cellular RNA that can also be bound by NC, is mediated by two zinc finger motifs within NC. These zinc fingers recognize and bind the packaging signal[67]. Some cellular RNAs have been found to be randomly packaged[68], while others cellular RNAs such as the small signal recognition particle RNA 7SL[69, 70] are specifically enriched in virus particles. However, the function of these cellular RNAs in virus replication is unknown.

Virus release and maturation

In order for newly formed virus particles to be released from the cell, the cellular ESCRT complex is required. The ESCRT complex facilitates final scission of virions from the plasma membrane[71-74]. The ESCRT complex is recruited by the virus via an interaction between the ESCRT protein TSG101 and the PTAP motif within the p6 domain of Gag[72, 74-76]. The final release of virus particles from the plasma membrane is inhibited by a cellular host restriction factor tetherin[8, 9] through direct binding of

tetherin to virus particles[77-79]. Tetherin restricts the release of several different retroviruses, but the determining how Tetherin mediates restriction of these unrelated viruses is still under investigation. To circumvent tetherin restriction, HIV-1 encodes Vpu[8, 9]. Vpu can bind to tetherin and both remove it from assembly sites and cause its degradation[80, 81]. Another block on the release of virions is the presence of CD4 on the plasma membrane. Even though CD4 is the virus receptor, and is required for attachment and entry of HIV-1, it can also decrease virus release by binding the Env of budding particles. HIV-1 overcomes this restriction by downregulating CD4 with both Nef and Vpu[7, 18] after the cell is infected. Nef also overcomes another source of virus restriction by downregulating MHC class I (MHC-I) on the cell surface[15, 16]. MHC-I presents viral antigens to cytotoxic T lymphocytes that would kill the infected cell.

While Gag is sufficient to form virus-like particles (VLPs)[46], several other proteins are required for a virus particle to be infectious. For example, after an HIV-1 particle is released, Protease cleaves Gag into its component structural subunits MA, CA, NC and p6 in a process known as maturation. This process is required for a particle to be infectious. During maturation, MA forms the outer shell under the HIV-1 membrane and provides the virus with structure. CA forms the virus core that encapsulates the viral genome and enzymes. NC binds to the viral RNA and protects it from degradation by nucleases[82]. Env should be incorporated into virus particles for progeny virions to become infectious. Env incorporation is thought to be mediated by a direct interaction between the cytoplasmic tail of Env and MA[83-85]. However, other factors could also be involved in Env incorporation as well. For example, the cellular protein TIP47 has been observed to bind the cytoplasmic tail of Env and is also implicated in its

incorporation into virus particles[86]. Finally, a cellular protein, cyclophilin A, has been observed to be incorporated into virus particles and has been implicated in early steps of virus replication[87, 88]. Cyclophilin A has also been observed to substantially increase virus infectivity[88, 89].

HIV-1 and Microdomains

The plasma membrane does not contain a homogenous distribution of proteins and lipids. Rather, certain lipids and proteins cluster together in submicroscopic groups called microdomains[90]. Two subgroups of microdomains are lipid rafts and tetraspanin-enriched microdomains (TEMs). Lipid rafts are enriched in cholesterol and glycosphingolipids. Lipid rafts are thought to be dynamic and unstable, with lipid raft proteins rapidly associating and dissociating[91]. Functionally, lipid rafts are thought to serve as platforms for the concentration of proteins to enhance their function in several cellular processes including signaling, protein sorting and cell polarity. Lipid rafts are also important for HIV-1 assembly[92-95]. For example, it was found that HIV-1 Gag is present in detergent resistant membranes (DRMs) and DRM association is considered an indication that a protein is enriched in lipid rafts[93-95]. Also, depleting cholesterol, which disrupts lipid rafts, was found to inhibit Gag membrane binding and virus release of HIV-1[94].

TEMs form when a group of transmembrane proteins called tetraspanins homo- or hetero-oligomerize and recruit other cellular proteins into clusters on the membrane. Gag has been observed to colocalize with several TEMs, including CD9, CD63, CD81 and CD82[96]. TEMs have also been observed to play a role in HIV-1 viral processes.

Specifically, knockdown of the tetraspanin CD81 was observed to increase HIV-1 cell-to-cell transmission[97]. Tetraspanins have been found to be enriched in virological synapses[98] and prevent Env-mediated cell-cell fusion[99]. Interestingly, while knocking down CD81 decreased virus release, it also increased virus infectivity[100]. In contrast, others have found that some TEMs inhibit virus infectivity. Conceivably, this is why TEMs appear to be regulated by HIV-1 and show some reduction in infected cells[97]. Thus, TEMs could serve both positive and negative functions in the life cycle of HIV-1. Further study of TEMs is required to understand their role in virus replication.

As mentioned above, microdomains such as lipid rafts are submicroscopic, measuring only 10-20nm. Thus, lipid rafts are much smaller than the limit of resolution for standard fluorescence microscopy (250nm)[91]. Thus, the optical techniques used to study microdomains have been indirect, and some believe they are potentially flawed[101, 102]. For example, antibody-mediated crosslinking of surface proteins induces stabilization of the microdomains they associate with. This stabilization facilitates formation of larger clusters or patches of microdomains that can be observed by standard fluorescence microscopy. Thus, if two proteins are antibody-crosslinked, the amount of "copatching" between the two should indicate whether they associate with the same microdomain. This copatching assay has been frequently used to determine whether two proteins have a propensity to associate with the same microdomain[103-109]. However, it has been argued that because this is not the native state of the proteins on the cell surface, any conclusions about microdomain association should be treated skeptically. Classifying whether a protein is lipid raft-associated has also been determined biochemically by observing whether that protein partitions into non-ionic

detergent-resistant membrane (DRM) fractions. The rationale is that lipid rafts that contain tightly packed lipids and proteins should be more resistant to detergent treatment than the rest of the plasma membrane and remain intact. These DRMs then float on a sucrose gradient and can be analyzed by western blot. This assay has also been used to determine that HIV-1 Gag associates with lipid rafts[92-94, 110-112]. However, the conclusions about lipid raft association of proteins based on this assay are also subject to debate because the results depend heavily on the strength of the detergent. Also, it has been observed that one of the detergents used in the assay, Triton X, induces formation of solid patches on the membrane[113]. If so, the detergent resistance of some proteins could be an artifact of the detergent treatment itself. Finally, although their relative sensitivities to detergent are different, both lipid rafts and TEMs have been found to reside in DRMs[114-116]. However, while these concerns should be considered, it should also be noted that there have been recent advances in biophysical analysis and new microscopy techniques, such as super resolution microscopy that can observe fluorescent patches at a 10-30nm resolution. This resolution allows visualization of the native state of microdomains, and studies using this technique have lent support to the microdomain model and corroborate copatching analyses[91, 117-119].

Currently, not only lipid-lipid interactions, but also protein-protein and protein-lipid interactions, are thought to be important for microdomain formation [119, 120]. Relevant to this thesis, multimerizing proteins are thought to stabilize or recruit microdomains[121, 122]. HIV-1 Gag multimerizes on the plasma membrane, and this multimerization has been observed to be important for microdomain association[93, 123]. Multimerization could also allow Gag to associate with specific microdomains, and/or

reorganize the membrane by recruiting other microdomains. Recent observations by Hogue et al. on this field are discussed below[124]. Still, the function and even the definition of what constitutes a membrane microdomain require further study.

Other microdomains have also been associated with HIV-1. For example, the Gould group has observed that Gag localizes to exosomes/microvesicles (EMVs), also called endosome-like domains (ELDs), from which exosomes are secreted[123, 125]. They also show that multimerization and membrane binding is sufficient to drive ELD association of a cytoplasmic protein such as Gag [123]. These observations define a specific microdomain with which HIV-1 Gag associates and show that multimerization is sufficient to drive this localization. This study also shows that associating with ELDs facilitates polarization of those proteins. Interestingly, one of the proteins enriched in ELDs is the tetraspanin CD63, suggesting that ELDs could represent the same Gag-associated microdomains discussed above. These studies provide additional supporting evidence for the working model developed in this thesis detailed below and in the following chapters.

TEMs and lipid rafts are distinct microdomains that do not colocalize with each other. However, as just discussed, both TEMs and lipid raft markers have been shown to colocalize with HIV-1 Gag. An interesting development came from recent work in which HIV-1 was observed to coalesce these segregated microdomains together[126] in a step-wise manner[124]. Therefore, it appears that Gag may form its own microdomain by recruiting various cell-surface proteins and microdomains. Work done in this thesis provides insights into uropod-directed microdomains (UDMs) that are enriched in Gag

and several uropod-associated proteins in infected T cells. The mechanism by which Gag associates with or recruits a specific subset of these UDMs is also investigated.

Cell-to-cell transmission

The model of HIV-1 spread that is often described involves HIV-1 virions being released from infected cells after which they travel in extracellular space until they come in contact with a target cell. However, this cell-free transmission route has proven to be highly inefficient[127]. Alternatively, another mode of HIV-1 transmission can occur when an infected cell contacts a target cell and directly transfers the virus. This process is called cell-to-cell transmission. In contrast to cell-free transmission, cell-to-cell transmission of HIV-1 is 10 to several thousand fold more efficient in cultured T cells, and is believed to be the major form of transmission for HIV-1 as well as several other viruses[127-130]. The efficiency of cell-to-cell transmission of HIV-1 was elegantly shown by the Schwartz group, which measured spreading of virus from infected to uninfected cells with or without shaking the cultures. The shaking prevented prolonged contacts between T cells from forming, but not the amount of virus particles released, thus imitating cell-free transmission. Under shaking conditions, the amount of virus spread was found to be minimal compared to without shaking, indicating that cell-cell contacts were vital for the spread of the virus[127].

Cell-to-cell transmission occurs among T cells, dendritic cells, macrophages and other cell types capable of harboring replicating HIV-1[131-135]. For example, in addition to transmission between T cells, cell-to-cell transmission can also occur between T cells and dendritic cells (DCs)[131, 132, 135]. DCs are not efficiently infected by HIV-

1, but they are well known to pass the virus laterally to T cells via cell-to-cell transmission. The contacts formed between T cells and dendritic cells are sometimes called “infectious synapses.” The adhesion molecule ICAM-1 has been observed to be concentrated at this junction and found to be important for transfer of virus particles from DCs to T cells[136]. Interestingly, and relevant to this thesis, ICAM-1 interaction with its binding partner LFA-1 is also implicated in HIV-1 transfer between T cells[137, 138]. Other viruses utilize cell-to-cell transmission to facilitate their spread as well, including another retrovirus that replicates in T cells, human T-lymphotropic virus 1 (HTLV-1)[134, 139-141]. This observation indicates that cell-to-cell transmission is a common means of virus spread among retroviruses. Structurally, cell-to-cell transmission is thought to occur through several mechanisms including traveling along cytonemes or nanotubes or through virological synapses (VSs) that resemble immunological synapses (ISs).

Cytonemes, Latin for “cell thread,” are thin membranous extensions that connect cells together. Cytonemes have been observed to allow particles of Murine Leukemia Virus (MLV), another retrovirus, to travel from infected to uninfected cells[142-144]. Recent live cell imaging showed fluorescently labeled MLV particles appearing to travel along the outside of these long-lived cytoneme protrusions to the target cell. This observation was also made for HIV-1 and avian leukosis virus (ALV), indicating a common transmission pathway for retroviruses in general. However, these studies were conducted using two adherent cell lines as the donor (COS-1) and target (XC) cells[142-144]. Thus, the contribution of cytoneme-mediated transfer to HIV-1 transmission between T cells is unknown.

Nanotubes are closed, actin-filled structures that form when T cells contact each other and pull away. HIV-1 appears to be able to travel on the outside of these nanotube protrusions from infected cells to target cells[145]. Because these structures were observed between cultured T cells, they represent a possible mechanism for cell-to-cell spread of HIV-1 in the body. However, it has yet to be determined whether either nanotubes or cytonemes are formed between T cells *in vivo*.

HIV-1 cell-to-cell transmission also occurs at contact junctions formed between infected and uninfected T cells, which are called virological synapses (VSs)[98, 130, 131, 133, 138, 146-150] due to morphological similarities to immunological synapses. However, recent 3D electron microscopy images have shown that the VS, unlike the IS, is very porous and does not hide viruses from most antibody attacks[147, 151]. Structurally, the VS is enriched in both viral proteins and receptors. The VS is also enriched in TEMs, lipid raft markers as well as adhesion molecules such as LFA-1[97, 98, 130, 138, 149]. The function of these proteins could be to stabilize the VS, although this is still under investigation.

VSs may be common to many retroviruses. For example, this structure was first described for another retrovirus, human T-lymphotropic virus 1(HTLV-1)[134], which was also the first discovered human retrovirus and is propagated solely by cell-to-cell transmission. In the case of HIV-1, VS formation is mediated by the Env-CD4 interaction[152, 153]. One reason virus spread at the VS may be more efficient than cell-free transmission is that, unlike cell-free transmission, the VS is capable of promoting the simultaneous transfer of numerous virus particles[146, 154]. Consistent with this, it has been found that many more copies of the HIV-1 provirus are integrated into the DNA of

infected cells under cell-to-cell transmission compared to cell-free transmission[154]. Thus, cell-to-cell transmission could explain the high number of proviruses detected in the cells of patient samples[155]. The increased number of infection events mediated by cell-to-cell transmission also appears to allow HIV-1 to replicate even in the presence of antiviral drug therapy[156]. Furthermore, the virus particles transferred to target cells via virological synapses can be endocytosed, with maturation occurring inside the endosomes of the target cell. This process can protect the virus from some antibodies targeted to mature particles[157].

Mechanisms of VS formation

While the mechanism of VS formation remains an active subject of study, previous observations indicate that cytoskeletal components and lipid raft integrity are important for VS stability and formation[130, 150, 158]. For example, virological synapses require accumulation of the virus receptor CD4 and coreceptors, which depends on actin[159]. Also, polarization of HIV-1 Env appears to be dependent on the microtubule cytoskeleton[150, 160]. Another cellular protein important for cell-to-cell transmission is Zap70. Zap70 is known to regulate IS formation and cell polarization by controlling cytoskeletal rearrangement and localization of the microtubule organizing center (MTOC)[161]. In the absence of Zap70, HIV-1 infected cells were found to form less VSs and cell-to-cell transmission was decreased[162]. These observations indicate that the cellular cytoskeleton is a vital component of VS formation and cell-to-cell transmission. Because the cellular cytoskeleton can determine lateral localization of proteins on the plasma membrane, it is conceivable that the role of the cytoskeleton could

be to facilitate lateral movement of HIV-1 components to the virological synapse. Consistent with this, it has been observed that HIV-1 Gag can be recruited over the cell surface to the VS after contact is made[146, 149].

The multitude of studies of virological synapses and their role in cell-cell transmission indicate that the VS plays a major role in the spread of HIV-1. However, the relationship between biologically relevant polarized T cells and virological synapses has not been examined. Therefore, this thesis explored the role of polarized T cells in virological synapses and cell-cell transfer of virus particles.

Uropods

Two-photon imaging studies have shown that a majority of T cells in lymph nodes are highly motile and have a polarized or "hand-mirror" morphology[163-168]. The front end of a polarized T cell is called the leading edge, and there is a characteristic protrusion at the rear called a uropod[169-171].(Fig. 1.3) The uropod is a feature common to several cell types including T and B lymphocytes, natural killer (NK) cells, neutrophils, monocytes, granulocytes and dendritic cells[170, 171].

The protrusion of the leading edge is mediated by the small G proteins Rac1, Rac2 and CDC42 that regulate the actin cytoskeleton[172]. For uropod formation, F-actin and uropod-associated proteins are first enriched at one end of the cell[173]. This pole is called the polar cap and is the precursor to uropod formation. F-actin forms filaments in parallel to the long axis of migration. This pattern of F-actin is consistent with the localization pattern of the highly homologous Ezrin/Radixin/Moesin (ERM) proteins. ERM proteins bind and promote polarization to the polar cap of several uropod proteins

including CD43, CD44, P-selectin glycoprotein ligand-1(PSGL-1), Inter-Cellular Adhesion Molecule (ICAM)-1, ICAM-2, and ICAM-3[174-176] The N-terminal domain of ERMs, called the FERM domain, binds both $PI(4,5)P_2$ and the cytoplasmic tails of the aforementioned uropod proteins[177]. $PI(4,5)P_2$ binding then causes a conformational change revealing a phosphorylation site that, when phosphorylated, promotes ERM binding to the actin cytoskeleton via an actin binding domain. This linking of uropod proteins to the actin cytoskeleton facilitates localization of these proteins to the polar cap[174-176]. ERM-mediated localization of these proteins to the polar cap also depends on myosin motor proteins. Protrusion of the polar cap, which leads to formation of the uropod, is mediated by actin rearrangement through RhoA and its downstream effector Rho-p160 coiled-coil kinase (ROCK).[171, 172]. Thus, the ROCK inhibitor Y-27632 depolarizes cells but does not inhibit capping[178], while the myosin light chain kinase inhibitor ML7 morphologically depolarizes cells and disperses uropod proteins[179].

Polar caps that are precursors to uropods also serve an important role in T cell signaling and function. The uropod protein PSGL-1 binds to a family of adhesion molecules called selectins. PSGL-1 primarily binds to P-selectin[180-182] that is usually expressed in endothelial cells. However, PSGL-1 can also bind to L-selectin that is expressed on other T cells[183, 184]. The interaction between PSGL-1 and P-selectin is the first signal for a T cell in the blood to slow down and start rolling on endothelial cell venules. Crosslinking of PSGL-1 sends signals through its cytoplasmic tail that stimulates a Syk-dependent pathway, leading to a conformational change in another major adhesion molecule LFA-1. This signaling pathway leads to an increase in the avidity of LFA-1 to ICAM-1 that further slows T cell rolling velocity[185, 186]. Chemokine signals then

promote further conformation changes that strengthen the LFA-1 interaction with ICAM-1 to arrest cell movement. It is at this step that polarization and uropod formation become necessary for the migration of T cells into the tissue in a process called extravasation. T cells then follow chemotactic signals, especially from CCL21[187].

The uropod can be identified in several ways. For example, uropods are enriched in several cell-surface adhesion molecules including PSGL-1, CD44, CD43, ICAM-1, ICAM-2 and ICAM-3[170, 188-190] and lipid raft markers such as GM1 and CD59[92, 191]. Immunostaining of these proteins can be used to identify uropods in polarized T cells. Uropods can also be identified by the location of the microtubule organizing center (MTOC) that localizes to the base of uropod protrusions. Microtubules are thought to increase the deformability of the cell and increase migration through tight spaces[171, 187]. However, disruption of microtubules does not inhibit uropod formation, in fact it promotes it[192, 193]. Finally, the uropod also features microspikes and microvilli, which are actin-based protrusions known to promote attachment to other cells[179, 190, 194]. In this thesis, uropods are identified primarily by observing the localization of PSGL-1, CD43 and the location of the MTOC.

Functionally, uropods play a role in T cell migration by facilitating deadhesion of adhesion molecules such as LFA-1 that mediates substrate adhesion at the leading edge. While T cell migration, uropods also mediate contact with other T cells[195] and recruit bystander T cells to sites of inflammation[196]. Because the uropod is identified in this thesis as the cell structure to which HIV-1 Gag localizes in polarized T cells, these uropod-mediated contacts between T cells could be taken advantage of by HIV-1 in order

to facilitate its spread *in vivo*. Thus, the role that cell polarization and uropod localization of HIV-1 play in cell-to-cell transfer of the HIV-1 was investigated in this thesis.

Thesis Rationale

HIV-1 infects and kills millions of people every year worldwide. In 2010, 34 million people were living with HIV/AIDS. There were 2.6 million new infections, most of which occurred in Africa. Over 48,000 of these new infections occurred in the United States as well[197]. Most patients who undergo treatment for HIV-1 take a cocktail of anti-HIV-1 drugs in a regimen called highly active anti-retroviral therapy (HAART). Currently, HAART usually includes a cocktail of drugs that target reverse transcription (RTIs) and prevent virus maturation by inhibiting protease (PIs). However, drugs that target fusion of the envelope with the plasma membrane (fusion inhibitors) and integration of the viral genome into the host cell DNA (Integrase inhibitors) have also been developed. Although HAART controls viral loads very well, low levels of virus replication can still occur in the body despite therapy[198, 199]. This low-level virus replication can eventually lead to drug resistant mutations. Also, when patients discontinue HAART therapy, their viral loads rapidly rebound[199-202]. Thus, while HAART has improved the lives of millions of those living with HIV-1, it is not a cure. Currently there is no vaccine or treatments available that cure HIV-1. Thus, further studies into basic HIV-1 biology, especially how HIV-1 replicates and spreads *in vivo*, are required to determine potential new therapy avenues.

As mentioned, current drugs are able to target fusion, reverse transcription, integration and maturation, but there are no inhibitors of several late HIV-1 assembly

steps such as plasma membrane binding or multimerization of Gag. The majority of HIV-1 transmission between cells in the body likely occurs through direct cell-cell contact, yet there is also much that is not understood about how this process occurs *in vivo* and whether drugs need to be tailored better to combat cell-to-cell transmission. For example, cell-cell transmission has been observed to decrease sensitivity to drug treatment[156], which could affect the long-term control of virus by HAART therapy in patients.

T cells in lymphoid organs, where cell-to-cell transmission likely occurs, are constantly migrating and adopting a polarized morphology. However, virological processes, including cell-to-cell transmission, have not been studied in the context of polarized T cells. Therefore, determining how Gag localizes on the plasma membrane in polarized T cells, and the role polarized T cells play in virological processes such as cell-to-cell transmission, would lead to a better understanding of basic HIV-1 biology *in vivo.* This could potentially lead to new drug targets to combat HIV-1. In this thesis it is shown that HIV-1 Gag localizes to uropods in polarized T cells. Therefore, the goal of this thesis is to investigate the role that uropods play in cell-to-cell spread of HIV-1 and the viral and cellular determinants of uropod localization of HIV-1 Gag**.**

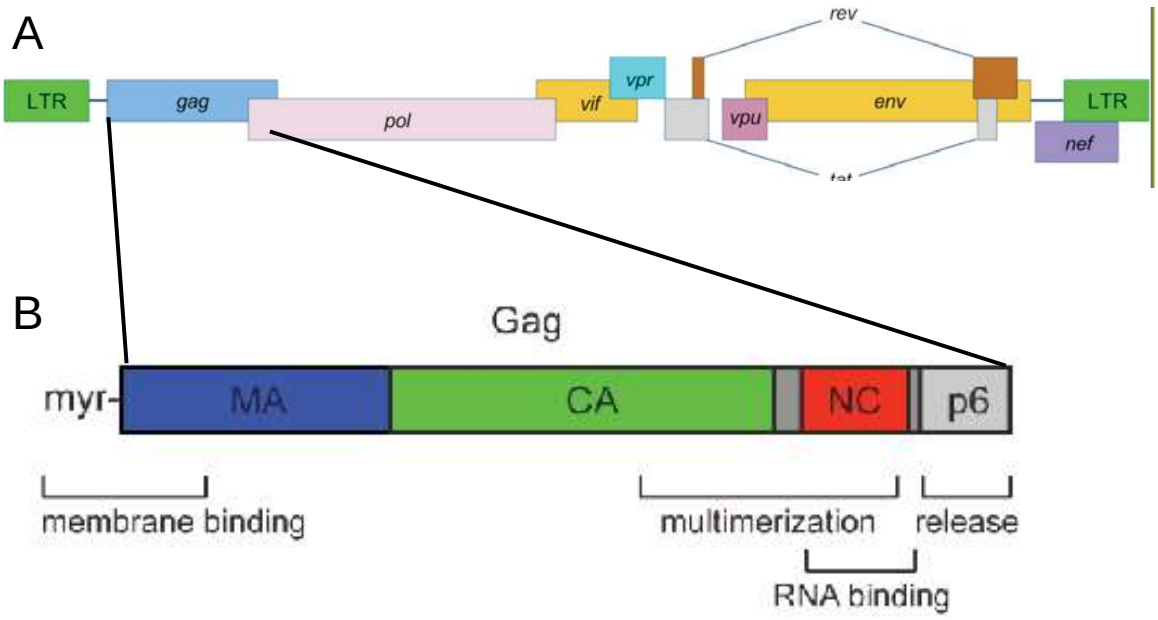

Figure 1.1. HIV-1 genome and Gag organization.
A) Illustration of the HIV-1 genome. HIV-1 encodes 9 proteins generated by differential splicing. Unspliced RNA encodes two of the primary proteins Gag and Pol and is packaged as the viral genome. Singly spliced RNA encodes the third primary protein Env and the accessory proteins VPU, VPR and VIF. Doubly spliced RNA encodes the fourth accessory protein Nef, and the two regulatory proteins Tat and Rev. **B)** The structural polyprotein Gag is composed of four structural domains that are cleaved by protease, MA, CA, NC, and p6. Gag contains four functional domains before it is cleaved. MA mediates membrane binding. CA and NC mediate multimerization. NC also binds and packages viral RNA. p6 recruits cellular ESCRT machinery to facilitate release of viral particles from cells. The diagrams were adapted from the thesis of Ian Hogue, 2010 and Vineela Chukkapalli, 2011.

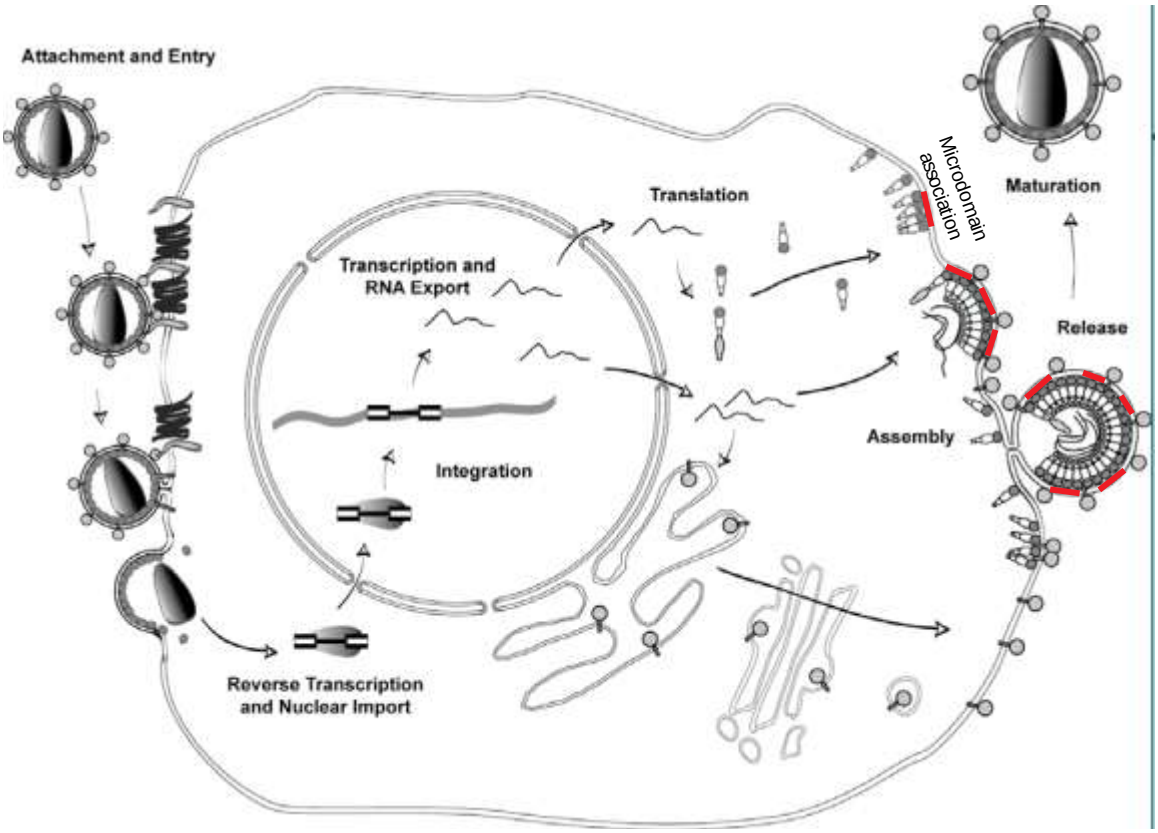

Figure 1.2. The HIV-1 life cycle.
HIV-1 attaches to the cell membrane via an interaction between viral Env protein and the receptor CD4 and coreceptor CCR5 or CXCR4. Fusion of the HIV-1 and plasma membranes releases the genomic RNA into the cytosol. The RNA genome is reverse transcribed into double stranded DNA, transported into the nucleus and integrated into the host cell DNA. This proviral DNA is then transcribed, spliced and exported out of the nucleus where it is translated into viral proteins. The primary structural protein Gag recruits unspliced viral RNA genomes, binds the plasma membrane and multimerizes. Multimerizing Gag causes membrane curvature and the formation of nascent virus particles. Cell machinery is recruited by Gag to facilitate the release of the virions from the cell. After release, the viral protease cleaves Gag into components that form the mature and infectious virus. The illustration was adapted from the thesis of Ian Hogue, 2010.

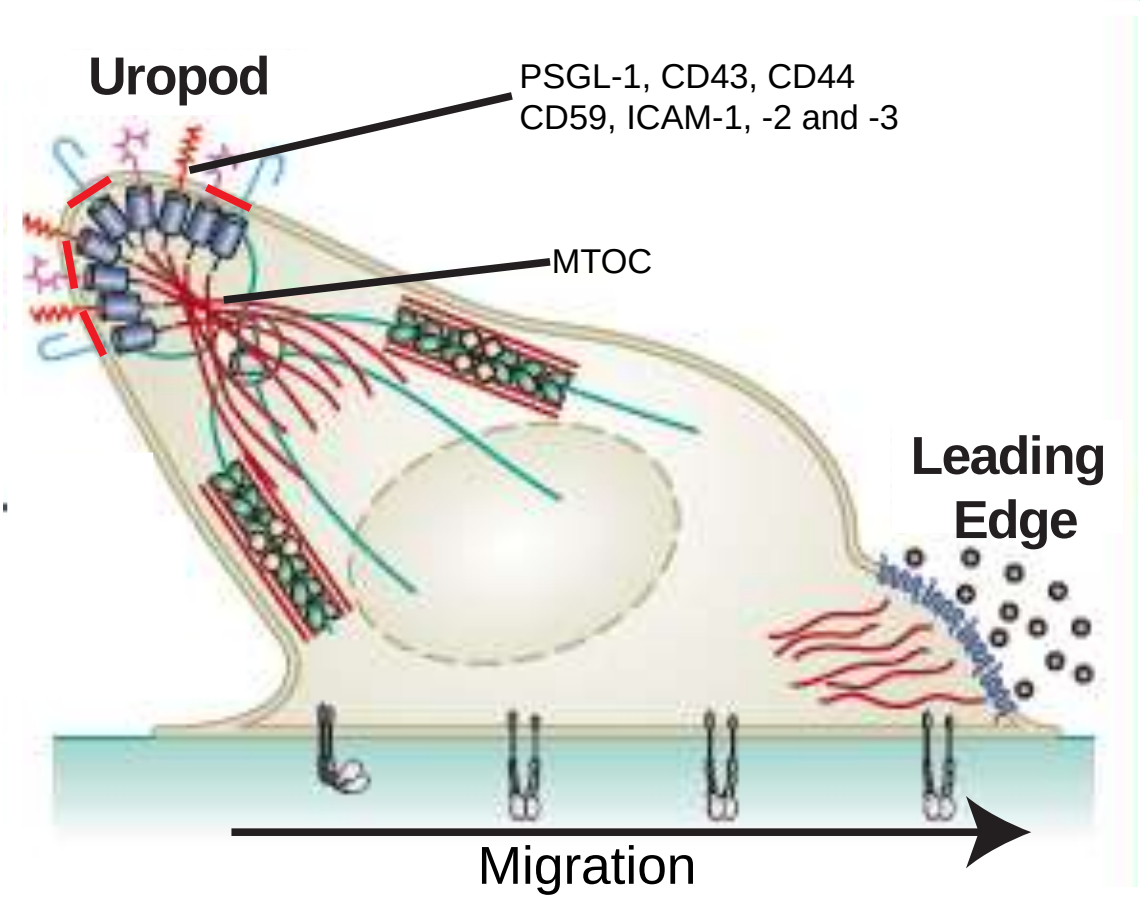

Figure 1.3. Morphology and characteristics of a polarized T cell.
Migrating T cells become morphologically polarized and form two ends. A leading edge at the front and a rear end protrusion called a uropod. The leading edge is enriched in chemokine receptors and the adhesion molecule LFA-1 and drives the direction of migration by sensing chemotactic signals. The rear end uropod is enriched in adhesion molecules, PSGL-1, CD43, CD44, ICAM-1, ICAM-2, and ICAM-3 and lipid raft markers such as CD59 and frequently mediates cell-cell contacts. The microtubule organizing center also localizes to the base of the uropod. The illustration was adapted from Sanchez-Madrid and Serrador, Nature Reviews Cell Biology, 2009.

References

1. Adamson, C.S. and I.M. Jones, *The molecular basis of HIV capsid assembly - five years of progress.* Reviews in Medical Virology, 2004. **14**(2): p. 107-121.

2. Baril, M., et al., *Efficiency of a programmed -1 ribosomal frameshift in the different subtypes of the human immunodeficiency virus type 1 group M.* RNA, 2003. **9**(10): p. 1246-53.

3. Klatzmann, D., et al., *T-lymphocyte T4 molecule behaves as the receptor for human retrovirus LAV.* Nature, 1984. **312**(5996): p. 767-8.

4. Choe, H., et al., *The beta-chemokine receptors CCR3 and CCR5 facilitate infection by primary HIV-1 isolates.* Cell, 1996. **85**(7): p. 1135-48.

5. Deng, H., et al., *Identification of a major co-receptor for primary isolates of HIV-1.* Nature, 1996. **381**(6584): p. 661-6.

6. Dragic, T., et al., *HIV-1 entry into CD4(+) cells is mediated by the chemokine receptor CC-CKR-5.* Nature, 1996. **381**(6584): p. 667-673.

7. Margottin, F., et al., *A novel human WD protein, h-beta TrCp, that interacts with HIV-1 Vpu connects CD4 to the ER degradation pathway through an F-box motif.* Molecular Cell, 1998. **1**(4): p. 565-74.

8. Neil, S.J.D., T. Zang, and P.D. Bieniasz, *Tetherin inhibits retrovirus release and is antagonized by HIV-1 Vpu.* Nature, 2008. **451**(7177): p. 425-U1.

9. Van Damme, N., et al., *The interferon-induced protein BST-2 restricts HIV-1 release and is downregulated from the cell surface by the viral Vpu protein.* Cell Host & Microbe, 2008. **3**(4): p. 245-252.

10. Andersen, J.L., et al., *HIV-1 Vpr-induced apoptosis is cell cycle dependent and requires Bax but not ANT.* Plos Pathogens, 2006. **2**(12): p. e127.

11. Malim, M.H. and M. Emerman, *HIV-1 accessory proteins--ensuring viral survival in a hostile environment.* Cell Host & Microbe, 2008. **3**(6): p. 388-98.

12. Sheehy, A.M., et al., *Isolation of a human gene that inhibits HIV-1 infection and is suppressed by the viral Vif protein.* Nature, 2002. **418**(6898): p. 646-650.

13. Cullen, B.R., *Trans-activation of human immunodeficiency virus occurs via a bimodal mechanism.* Cell, 1986. **46**(7): p. 973-82.

14. Fischer, U., et al., *Evidence That Hiv-1 Rev Directly Promotes the Nuclear Export of Unspliced Rna.* Embo Journal, 1994. **13**(17): p. 4105-4112.

15. Collins, K.L., et al., *HIV-1 Nef protein protects infected primary cells against killing by cytotoxic T lymphocytes.* Nature, 1998. **391**(6665): p. 397-401.

16. Schwartz, O., et al., *Endocytosis of major histocompatibility complex class I molecules is induced by the HIV-1 Nef protein.* Nat Med, 1996. **2**(3): p. 338-42.

17. Guy, B., et al., *Hiv F/3' Orf Encodes a Phosphorylated Gtp-Binding Protein Resembling an Oncogene Product.* Nature, 1987. **330**(6145): p. 266-269.

18. Garcia, J.V. and A.D. Miller, *Serine phosphorylation-independent downregulation of cell-surface CD4 by nef.* Nature, 1991. **350**(6318): p. 508-11.

19. Wyatt, R. and J. Sodroski, *The HIV-1 envelope glycoproteins: fusogens, antigens, and immunogens.* Science, 1998. **280**(5371): p. 1884-8.

20. Zhu, P., et al., *Electron tomography analysis of envelope glycoprotein trimers on HIV and simian immunodeficiency virus virions.* Proc Natl Acad Sci U S A, 2003. **100**(26): p. 15812-7.

21. Chan, D.C., et al., *Core structure of gp41 from the HIV envelope glycoprotein.* Cell, 1997. **89**(2): p. 263-73.

22. Weissenhorn, W., et al., *Atomic structure of the ectodomain from HIV-1 gp41.* Nature, 1997. **387**(6631): p. 426-30.

23. Miyauchi, K., et al., *HIV enters cells via endocytosis and dynamin-dependent fusion with endosomes.* Cell, 2009. **137**(3): p. 433-44.

24. Forshey, B.M., et al., *Formation of a human immunodeficiency virus type 1 core of optimal stability is crucial for viral replication.* J Virol, 2002. **76**(11): p. 5667-77.

25. Arhel, N., *Revisiting HIV-1 uncoating.* Retrovirology, 2010. **7**: p. 96.

26. Towers, G.J., *The control of viral infection by tripartite motif proteins and cyclophilin A.* Retrovirology, 2007. **4**: p. 40.

27. Stremlau, M., et al., *Specific recognition and accelerated uncoating of retroviral capsids by the TRIM5alpha restriction factor.* Proc Natl Acad Sci U S A, 2006. **103**(14): p. 5514-9.

28. Mascarenhas, A.P. and K. Musier-Forsyth, *The capsid protein of human immunodeficiency virus: interactions of HIV-1 capsid with host protein factors.* FEBS J, 2009. **276**(21): p. 6118-27.

29. Sakuma, R., et al., *Rhesus monkey TRIM5 alpha restricts HIV-1 production through rapid degradation of viral Gag polyproteins.* Nature Medicine, 2007. **13**(5): p. 631-635.

30. Mangeat, B., et al., *Broad antiretroviral defence by human APOBEC3G through lethal editing of nascent reverse transcripts.* Nature, 2003. **424**(6944): p. 99-103.

31. Zhang, H., et al., *The cytidine deaminase CEM15 induces hypermutation in newly synthesized HIV-1 DNA.* Nature, 2003. **424**(6944): p. 94-8.

32. Marin, M., et al., *HIV-1 Vif protein binds the editing enzyme APOBEC3G and induces its degradation.* Nat Med, 2003. **9**(11): p. 1398-403.

33. Smith, H.C., *APOBEC3G: a double agent in defense.* Trends Biochem Sci, 2011. **36**(5): p. 239-44.

34. McDonald, D., et al., *Visualization of the intracellular behavior of HIV in living cells.* J Cell Biol, 2002. **159**(3): p. 441-52.

35. Cherepanov, P., et al., *HIV-1 integrase forms stable tetramers and associates with LEDGF/p75 protein in human cells.* J Biol Chem, 2003. **278**(1): p. 372-81.

36. Llano, M., et al., *An essential role for LEDGF/p75 in HIV integration.* Science, 2006. **314**(5798): p. 461-4.

37. Marshall, H.M., et al., *Role of PSIP1/LEDGF/p75 in lentiviral infectivity and integration targeting.* PLoS One, 2007. **2**(12): p. e1340.

38. Meehan, A.M. and E.M. Poeschla, *Chromatin tethering and retroviral integration: recent discoveries and parallels with DNA viruses.* Biochim Biophys Acta, 2010. **1799**(3-4): p. 182-91.

39. Benkirane, M., et al., *Activation of integrated provirus requires histone acetyltransferase. p300 and P/CAF are coactivators for HIV-1 Tat.* J Biol Chem, 1998. **273**(38): p. 24898-905.

40. Seelamgari, A., et al., *Role of viral regulatory and accessory proteins in HIV-1 replication.* Front Biosci, 2004. **9**: p. 2388-413.

41. Garber, M.E. and K.A. Jones, *HIV-1 Tat: coping with negative elongation factors.* Curr Opin Immunol, 1999. **11**(4): p. 460-5.

42. Kao, S.Y., et al., *Anti-Termination of Transcription within the Long Terminal Repeat of Hiv-1 by Tat Gene-Product.* Nature, 1987. **330**(6147): p. 489-493.

43. Barboric, M. and B.M. Peterlin, *A new paradigm in eukaryotic biology: HIV Tat and the control of transcriptional elongation.* PLoS Biol, 2005. **3**(2): p. e76.

44. Edgcomb, S.P., et al., *Protein structure and oligomerization are important for the formation of export-competent HIV-1 Rev-RRE complexes.* Protein Sci, 2008. **17**(3): p. 420-30.

45. Neville, M., et al., *The importin-beta family member Crm1p bridges the interaction between Rev and the nuclear pore complex during nuclear export.* Current Biology, 1997. **7**(10): p. 767-775.

46. Adamson, C.S. and E.O. Freed, *Human immunodeficiency virus type 1 assembly, release, and maturation.* Adv Pharmacol, 2007. **55**: p. 347-87.

47. Bryant, M. and L. Ratner, *Myristoylation-dependent replication and assembly of human immunodeficiency virus 1.* Proc Natl Acad Sci U S A, 1990. **87**(2): p. 523-7.

48. Dalton, A.K., et al., *Electrostatic interactions drive membrane association of the human immunodeficiency virus type 1 Gag MA domain.* Journal of Virology, 2007. **81**(12): p. 6434-6445.

49. Tang, C., et al., *Entropic switch regulates myristate exposure in the HIV-1 matrix protein.* Proc Natl Acad Sci U S A, 2004. **101**(2): p. 517-22.

50. Saad, J.S., et al., *Structural basis for targeting HIV-1 Gag proteins to the plasma membrane for virus assembly.* Proc Natl Acad Sci U S A, 2006. **103**(30): p. 11364-9.

51. Resh, M.D., *A myristoyl switch regulates membrane binding of HIV-1 Gag.* Proc Natl Acad Sci U S A, 2004. **101**(2): p. 417-8.

52. Gottlinger, H.G., J.G. Sodroski, and W.A. Haseltine, *Role of capsid precursor processing and myristoylation in morphogenesis and infectivity of human immunodeficiency virus type 1.* Proc Natl Acad Sci U S A, 1989. **86**(15): p. 5781-5.

53. Chukkapalli, V., et al., *Interaction between the human immunodeficiency virus type 1 Gag matrix domain and phosphatidylinositol-(4,5)-bisphosphate is essential for efficient Gag membrane binding.* Journal of Virology, 2008. **82**(5): p. 2405-2417.

54. Ono, A., et al., *Phosphatidylinositol (4,5) bisphosphate regulates HIV-1 Gag targeting to the plasma membrane.* Proc Natl Acad Sci U S A, 2004. **101**(41): p. 14889-94.

55. Chukkapalli, V., S.J. Oh, and A. Ono, *Opposing mechanisms involving RNA and lipids regulate HIV-1 Gag membrane binding through the highly basic region of the matrix domain.* Proceedings of the National Academy of Sciences of the United States of America, 2010. **107**(4): p. 1600-1605.

56. Burniston, M.T., et al., *Human immunodeficiency virus type 1 Gag polyprotein multimerization requires the nucleocapsid domain and RNA and is promoted by the capsid-dimer interface and the basic region of matrix protein.* J Virol, 1999. **73**(10): p. 8527-40.

57. Gamble, T.R., et al., *Structure of the carboxyl-terminal dimerization domain of the HIV-1 capsid protein.* Science, 1997. **278**(5339): p. 849-53.

58. Hogue, I.B., A. Hoppe, and A. Ono, *Quantitative fluorescence resonance energy transfer microscopy analysis of the human immunodeficiency virus type 1 Gag-Gag interaction: relative contributions of the CA and NC domains and membrane binding.* J Virol, 2009. **83**(14): p. 7322-36.

59. von Schwedler, U.K., et al., *Functional surfaces of the human immunodeficiency virus type 1 capsid protein.* J Virol, 2003. **77**(9): p. 5439-50.

60. Zhang, W.H., et al., *Gag-Gag interactions in the C-terminal domain of human immunodeficiency virus type 1 p24 capsid antigen are essential for Gag particle assembly.* J Gen Virol, 1996. **77 (Pt 4)**: p. 743-51.

61. Datta, S.A.K., et al., *Interactions between HIV-1 Gag molecules in solution: An inositol phosphate-mediated switch.* Journal of Molecular Biology, 2007. **365**(3): p. 799-811.

62. Campbell, S. and V.M. Vogt, *Self-assembly in vitro of purified CA-NC proteins from Rous sarcoma virus and human immunodeficiency virus type 1.* J Virol, 1995. **69**(10): p. 6487-97.

63. Cimarelli, A., et al., *Basic residues in human immunodeficiency virus type 1 nucleocapsid promote virion assembly via interaction with RNA.* J Virol, 2000. **74**(7): p. 3046-57.

64. Dawson, L. and X.F. Yu, *The role of nucleocapsid of HIV-1 in virus assembly.* Virology, 1998. **251**(1): p. 141-57.

65. Muriaux, D., et al., *RNA is a structural element in retrovirus particles.* Proceedings of the National Academy of Sciences of the United States of America, 2001. **98**(9): p. 5246-5251.

66. Paillart, J.C., et al., *A loop-loop "kissing" complex is the essential part of the dimer linkage of genomic HIV-1 RNA.* Proc Natl Acad Sci U S A, 1996. **93**(11): p. 5572-7.

67. D'Souza, V. and M.F. Summers, *How retroviruses select their genomes.* Nature Reviews Microbiology, 2005. **3**(8): p. 643-655.

68. Rulli, S.J., Jr., et al., *Selective and nonselective packaging of cellular RNAs in retrovirus particles.* J Virol, 2007. **81**(12): p. 6623-31.

69. Onafuwa-Nuga, A.A., A. Telesnitsky, and S.R. King, *7SL RNA, but not the 54-kd signal recognition particle protein, is an abundant component of both infectious HIV-1 and minimal virus-like particles.* Rna-a Publication of the Rna Society, 2006. **12**(4): p. 542-546.

70. Keene, S.E., S.R. King, and A. Telesnitsky, *7SL RNA Is Retained in HIV-1 Minimal Virus-Like Particles as an S-Domain Fragment.* Journal of Virology, 2010. **84**(18): p. 9070-9077.

71. Martin-Serrano, J., T. Zang, and P.D. Bieniasz, *Role of ESCRT-I in retroviral budding.* J Virol, 2003. **77**(8): p. 4794-804.

72. Stuchell, M.D., et al., *The human endosomal sorting complex required for transport (ESCRT-I) and its role in HIV-1 budding.* J Biol Chem, 2004. **279**(34): p. 36059-71.

73. Garrus, J.E., et al., *Tsg101 and the vacuolar protein sorting pathway are essential for HIV-1 budding.* Cell, 2001. **107**(1): p. 55-65.

74. Martin-Serrano, J., T. Zang, and P.D. Bieniasz, *HIV-1 and Ebola virus encode small peptide motifs that recruit Tsg101 to sites of particle assembly to facilitate egress.* Nat Med, 2001. **7**(12): p. 1313-9.

75. Im, Y.J., et al., *Crystallographic and Functional Analysis of the ESCRT-I/HIV-1 Gag PTAP Interaction.* Structure, 2010. **18**(11): p. 1536-1547.

76. Huang, M.J., et al., *P6(Gag) Is Required for Particle-Production from Full-Length Human-Immunodeficiency-Virus Type-1 Molecular Clones Expressing Protease.* Journal of Virology, 1995. **69**(11): p. 6810-6818.

77. Hammonds, J., et al., *Immunoelectron microscopic evidence for Tetherin/BST2 as the physical bridge between HIV-1 virions and the plasma membrane.* Plos Pathogens, 2010. **6**(2): p. e1000749.

78. Perez-Caballero, D., et al., *Tetherin inhibits HIV-1 release by directly tethering virions to cells.* Cell, 2009. **139**(3): p. 499-511.

79. Fitzpatrick, K., et al., *Direct restriction of virus release and incorporation of the interferon-induced protein BST-2 into HIV-1 particles.* Plos Pathogens, 2010. **6**(3): p. e1000701.

80. Douglas, J.L., et al., *The great escape: viral strategies to counter BST-2/tetherin.* Plos Pathogens, 2010. **6**(5): p. e1000913.

81. Dube, M., et al., *Modulation of HIV-1-host interaction: role of the Vpu accessory protein.* Retrovirology, 2010. **7**: p. 114.

82. Tanchou, V., et al., *Formation of stable and functional HIV-1 nucleoprotein complexes in vitro.* J Mol Biol, 1995. **252**(5): p. 563-71.

83. Freed, E.O. and M.A. Martin, *Domains of the human immunodeficiency virus type 1 matrix and gp41 cytoplasmic tail required for envelope incorporation into virions.* J Virol, 1996. **70**(1): p. 341-51.

84. Murakami, T. and E.O. Freed, *Genetic evidence for an interaction between human immunodeficiency virus type 1 matrix and alpha-helix 2 of the gp41 cytoplasmic tail.* Journal of Virology, 2000. **74**(8): p. 3548-3554.

85. Wyma, D.J., A. Kotov, and C. Aiken, *Evidence for a stable interaction of gp41 with Pr55(Gag) in immature human immunodeficiency virus type 1 particles.* Journal of Virology, 2000. **74**(20): p. 9381-9387.

86. Lopez-Verges, S., et al., *Tail-interacting protein TIP47 is a connector between Gag and Env and is required for Env incorporation into HIV-1 virions.* Proceedings of the National Academy of Sciences of the United States of America, 2006. **103**(40): p. 14947-14952.

87. Braaten, D., E.K. Franke, and J. Luban, *Cyclophilin A is required for an early step in the life cycle of human immunodeficiency virus type 1 before the initiation of reverse transcription.* Journal of Virology, 1996. **70**(6): p. 3551-3560.

88. Franke, E.K., H.E.H. Yuan, and J. Luban, *Specific Incorporation of Cyclophilin-a into Hiv-1 Virions.* Nature, 1994. **372**(6504): p. 359-362.

89. Thali, M., et al., *Functional association of cyclophilin A with HIV-1 virions.* Nature, 1994. **372**(6504): p. 363-5.

90. Brown, D.A. and J.K. Rose, *Sorting of GPI-anchored proteins to glycolipid-enriched membrane subdomains during transport to the apical cell surface.* Cell, 1992. **68**(3): p. 533-44.

91. Kusumi, A., I. Koyama-Honda, and K. Suzuki, *Molecular dynamics and interactions for creation of stimulation-induced stabilized rafts from small unstable steady-state rafts.* Traffic, 2004. **5**(4): p. 213-30.

92. Nguyen, D.H. and J.E. Hildreth, *Evidence for budding of human immunodeficiency virus type 1 selectively from glycolipid-enriched membrane lipid rafts.* J Virol, 2000. **74**(7): p. 3264-72.

93. Lindwasser, O.W. and M.D. Resh, *Multimerization of human immunodeficiency virus type 1 Gag promotes its localization to barges, raft-like membrane microdomains.* J Virol, 2001. **75**(17): p. 7913-24.

94. Ono, A. and E.O. Freed, *Plasma membrane rafts play a critical role in HIV-1 assembly and release.* Proc Natl Acad Sci U S A, 2001. **98**(24): p. 13925-30.

95. Lindwasser, O.W. and M.D. Resh, *Myristoylation as a target for inhibiting HIV assembly: unsaturated fatty acids block viral budding.* Proc Natl Acad Sci U S A, 2002. **99**(20): p. 13037-42.

96. Nydegger, S., et al., *Mapping of tetraspanin-enriched microdomains that can function as gateways for HIV-1.* Journal of Cell Biology, 2006. **173**(5): p. 795-807.

97. Krementsov, D.N., et al., *Tetraspanins regulate cell-to-cell transmission of HIV-1.* Retrovirology, 2009. **6**: p. 64.

98. Jolly, C. and Q.J. Sattentau, *Human immunodeficiency virus type 1 assembly, budding, and cell-cell spread in T cells take place in tetraspanin-enriched plasma membrane domains.* Journal of Virology, 2007. **81**(15): p. 7873-7884.

99. Weng, J., et al., *Formation of Syncytia Is Repressed by Tetraspanins in Human Immunodeficiency Virus Type 1-Producing Cells.* Journal of Virology, 2009. **83**(15): p. 7467-7474.

100. Grigorov, B., et al., *A role for CD81 on the late steps of HIV-1 replication in a chronically infected T cell line.* Retrovirology, 2009. **6**.

101. Edidin, M., *The state of lipid rafts: from model membranes to cells.* Annu Rev Biophys Biomol Struct, 2003. **32**: p. 257-83.

102. Hancock, J.F., *Lipid rafts: contentious only from simplistic standpoints.* Nat Rev Mol Cell Biol, 2006. **7**(6): p. 456-62.

103. Taylor, R.B., et al., *Redistribution and Pinocytosis of Lymphocyte Surface Immunoglobulin Molecules Induced by Anti-Immunoglobulin Antibody.* Nature-New Biology, 1971. **233**(42): p. 225-&.

104. Revesz, T. and M. Greaves, *Ligand-Induced Redistribution of Lymphocyte Membrane Ganglioside Gm1.* Nature, 1975. **257**(5522): p. 103-106.

105. Spiegel, S., et al., *Direct Visualization of Redistribution and Capping of Fluorescent Gangliosides on Lymphocytes.* Journal of Cell Biology, 1984. **99**(5): p. 1575-1581.

106. Mayor, S., K.G. Rothberg, and F.R. Maxfield, *Sequestration of Gpi-Anchored Proteins in Caveolae Triggered by Cross-Linking.* Science, 1994. **264**(5167): p. 1948-1951.

107. Harder, T., et al., *Lipid domain structure of the plasma membrane revealed by patching of membrane components.* J Cell Biol, 1998. **141**(4): p. 929-42.

108. Janes, P.W., S.C. Ley, and A.I. Magee, *Aggregation of lipid rafts accompanies signaling via the T cell antigen receptor.* J Cell Biol, 1999. **147**(2): p. 447-61.

109. Shvartsman, D.E., et al., *Differently anchored influenza hemagglutinin mutants display distinct interaction dynamics with mutual rafts.* J Cell Biol, 2003. **163**(4): p. 879-88.

110. Ono, A., et al., *Association of human immunodeficiency virus type 1 gag with membrane does not require highly basic sequences in the nucleocapsid: Use of a novel gag multimerization assay.* Journal of Virology, 2005. **79**(22): p. 14131-14140.

111. Holm, K., et al., *Human immunodeficiency virus type 1 assembly and lipid rafts: Pr55(gag) associates with membrane domains that are largely resistant to brij98 but sensitive to Triton X-100.* Journal of Virology, 2003. **77**(8): p. 4805-4817.

112. Halwani, R., et al., *Rapid localization of Gag/GagPol complexes to detergent-resistant membrane during the assembly of human immunodeficiency virus type 1.* Journal of Virology, 2003. **77**(7): p. 3973-3984.

113. Heerklotz, H., *Triton promotes domain formation in lipid raft mixtures.* Biophys J, 2002. **83**(5): p. 2693-701.

114. Claas, C., C.S. Stipp, and M.E. Hemler, *Evaluation of prototype transmembrane 4 superfamily protein complexes and their relation to lipid rafts.* Journal of Biological Chemistry, 2001. **276**(11): p. 7974-7984.

115. Charrin, S., et al., *Differential stability of tetraspanin/tetraspanin interactions: role of palmitoylation.* Febs Letters, 2002. **516**(1-3): p. 139-144.

116. Charrin, S., et al., *Multiple levels of interactions within the tetraspanin web.* Biochemical and Biophysical Research Communications, 2003. **304**(1): p. 107-112.

117. Jacobson K, M.O., Anderson RG, *Lipid rafts: at a crossroad between cell biology and physics.* Nat Cell Biology, 2007. **9**(1): p. 7-14.

118. Mayor, S. and M. Rao, *Rafts: scale-dependent, active lipid organization at the cell surface.* Traffic, 2004. **5**(4): p. 231-40.

119. Douglass, A.D. and R.D. Vale, *Single-molecule microscopy reveals plasma membrane microdomains created by protein-protein networks that exclude or trap signaling molecules in T cells.* Cell, 2005. **121**(6): p. 937-50.

120. Gaus, K., et al., *Condensation of the plasma membrane at the site of T lymphocyte activation.* J Cell Biol, 2005. **171**(1): p. 121-31.

121. Langhorst, M.F., A. Reuter, and C.A. Stuermer, *Scaffolding microdomains and beyond: the function of reggie/flotillin proteins.* Cell Mol Life Sci, 2005. **62**(19-20): p. 2228-40.

122. Parton, R.G. and K. Simons, *The multiple faces of caveolae.* Nat Rev Mol Cell Biol, 2007. **8**(3): p. 185-94.

123. Fang, Y., et al., *Higher-order oligomerization targets plasma membrane proteins and HIV gag to exosomes.* PLoS Biol, 2007. **5**(6): p. e158.

124. Hogue, I.B., et al., *Gag induces the coalescence of clustered lipid rafts and tetraspanin-enriched microdomains at HIV-1 assembly sites on the plasma membrane.* J Virol, 2011. **85**(19): p. 9749-66.

125. Shen, B., et al., *Biogenesis of the Posterior Pole Is Mediated by the Exosome/Microvesicle Protein-Sorting Pathway.* J Biol Chem, 2011.

126. Krementsov, D.N., et al., *HIV-1 Assembly Differentially Alters Dynamics and Partitioning of Tetraspanins and Raft Components.* Traffic, 2010. **11**(11): p. 1401-1414.

127. Sourisseau, M., et al., *Inefficient human immunodeficiency virus replication in mobile lymphocytes.* J Virol, 2007. **81**(2): p. 1000-12.

128. Chen, P., et al., *Predominant mode of human immunodeficiency virus transfer between T cells is mediated by sustained Env-dependent neutralization-resistant virological synapses.* Journal of Virology, 2007. **81**(22): p. 12582-12595.

129. Phillips, D.M., *The Role of Cell-to-Cell Transmission in Hiv-Infection.* Aids, 1994. **8**(6): p. 719-731.

130. Jolly, C. and Q.J. Sattentau, *Human immunodeficiency virus type 1 virological synapse formation in T cells requires lipid raft integrity.* Journal of Virology, 2005. **79**(18): p. 12088-12094.

131. Arrighi, J.F., et al., *DC-SIGN-mediated infectious synapse formation enhances X4 HIV-1 transmission from dendritic cells to T cells.* J Exp Med, 2004. **200**(10): p. 1279-88.

132. Garcia, E., et al., *HIV-1 trafficking to the dendritic cell-T-cell infectious synapse uses a pathway of tetraspanin sorting to the immunological synapse.* Traffic, 2005. **6**(6): p. 488-501.

133. Groot, F., S. Welsch, and Q.J. Sattentau, *Efficient HIV-1 transmission from macrophages to T cells across transient virological synapses.* Blood, 2008. **111**(9): p. 4660-3.

134. Igakura, T., et al., *Spread of HTLV-I between lymphocytes by virus-induced polarization of the cytoskeleton.* Science, 2003. **299**(5613): p. 1713-1716.

135. McDonald, D., et al., *Recruitment of HIV and its receptors to dendritic cell-T cell junctions.* Science, 2003. **300**(5623): p. 1295-1297.

136. Sanders, R.W., et al., *Differential transmission of human immunodeficiency virus type 1 by distinct subsets of effector dendritic cells.* J Virol, 2002. **76**(15): p. 7812-21.

137. Tardif, M.R. and M.J. Tremblay, *LFA-1 is a key determinant for preferential infection of memory CD4(+) T cells by human immunodeficiency virus type 1.* Journal of Virology, 2005. **79**(21): p. 13714-13724.

138. Jolly, C., I. Mitar, and Q.J. Sattentau, *Adhesion molecule interactions facilitate human immunodeficiency virus type 1-induced virological synapse formation between T cells.* Journal of Virology, 2007. **81**(24): p. 13916-13921.

139. Mazurov, D., et al., *Quantitative Comparison of HTLV-1 and HIV-1 Cell-to-Cell Infection with New Replication Dependent Vectors.* Plos Pathogens, 2010. **6**(2).

140. Pais-Correia, A.M., et al., *Biofilm-like extracellular viral assemblies mediate HTLV-1 cell-to-cell transmission at virological synapses.* Nature Medicine, 2010. **16**(1): p. 83-U119.

141. Majorovits, E., et al., *Human T-Lymphotropic Virus-1 Visualized at the Virological Synapse by Electron Tomography.* PLoS One, 2008. **3**(5).

142. Jin, J., et al., *Assembly of the Murine Leukemia Virus Is Directed towards Sites of Cell-Cell Contact.* Plos Biology, 2009. **7**(7).

143. Sherer, N.M., et al., *Retroviruses can establish filopodial bridges for efficient cell-to-cell transmission.* Nature Cell Biology, 2007. **9**(3): p. 310-U106.

144. Sherer, N.M. and W. Mothes, *Cytonemes and tunneling nanotubules in cell-cell communication and viral pathogenesis.* Trends in Cell Biology, 2008. **18**(9): p. 414-420.

145. Sowinski, S., et al., *Membrane nanotubes physically connect T cells over long distances presenting a novel route for HIV-1 transmission.* Nature Cell Biology, 2008. **10**(2): p. 211-9.

146. Hubner, W., et al., *Quantitative 3D video microscopy of HIV transfer across T cell virological synapses.* Science, 2009. **323**(5922): p. 1743-7.

147. Martin, N., et al., *Virological Synapse-Mediated Spread of Human Immunodeficiency Virus Type 1 between T Cells Is Sensitive to Entry Inhibition.* Journal of Virology, 2010. **84**(7): p. 3516-3527.

148. Jolly, C., et al., *HIV-1 cell to cell transfer across an env-induced, actin-dependent synapse.* Journal of Experimental Medicine, 2004. **199**(2): p. 283-293.

149. Rudnicka, D., et al., *Simultaneous Cell-to-Cell Transmission of Human Immunodeficiency Virus to Multiple Targets through Polysynapses.* Journal of Virology, 2009. **83**(12): p. 6234-6246.

150. Jolly, C., I. Mitar, and Q.J. Sattentau, *Requirement for an intact T-cell actin and tubulin cytoskeleton for efficient assembly and spread of human immunodeficiency virus type 1.* J Virol, 2007. **81**(11): p. 5547-60.

151. Felts, R.L., et al., *3D visualization of HIV transfer at the virological synapse between dendritic cells and T cells.* Proceedings of the National Academy of Sciences of the United States of America, 2010. **107**(30): p. 13336-13341.

152. Vasiliver-Shamis, G., et al., *Human immunodeficiency virus type 1 envelope gp120 induces a stop signal and virological synapse formation in noninfected CD4+ T cells.* J Virol, 2008. **82**(19): p. 9445-57.

153. Vasiliver-Shamis, G., et al., *Human Immunodeficiency Virus Type 1 Envelope gp120-Induced Partial T-Cell Receptor Signaling Creates an F-Actin-Depleted Zone in the Virological Synapse.* Journal of Virology, 2009. **83**(21): p. 11341-11355.

154. Del Portillo, A., et al., *Multiploid Inheritance of HIV-1 during Cell-to-Cell Infection.* Journal of Virology, 2011. **85**(14): p. 7169-7176.

155. Jung, A., et al., *Recombination: Multiply infected spleen cells in HIV patients.* Nature, 2002. **418**(6894): p. 144.

156. Sigal, A., et al., *Cell-to-cell spread of HIV permits ongoing replication despite antiretroviral therapy.* Nature, 2011. **477**(7362): p. 95-8.

157. Dale, B.M., et al., *Cell-to-Cell Transfer of HIV-1 via Virological Synapses Leads to Endosomal Virion Maturation that Activates Viral Membrane Fusion.* Cell Host & Microbe, 2011. **10**(6): p. 551-62.

158. Lehmann, M., D.S. Nikolic, and V. Piguet, *How HIV-1 Takes Advantage of the Cytoskeleton during Replication and Cell-to-Cell Transmission.* Viruses, 2011. **3**(9): p. 1757-76.

159. Iyengar, S., J.E. Hildreth, and D.H. Schwartz, *Actin-dependent receptor colocalization required for human immunodeficiency virus entry into host cells.* J Virol, 1998. **72**(6): p. 5251-5.

160. Jolly, C., et al., *The Regulated Secretory Pathway in CD4(+) T cells Contributes to Human Immunodeficiency Virus Type-1 Cell-to-Cell Spread at the Virological Synapse.* Plos Pathogens, 2011. **7**(9).

161. Blanchard, N., V. Di Bartolo, and C. Hivroz, *In the immune synapse, ZAP-70 controls T cell polarization and recruitment of signaling proteins but not formation of the synaptic pattern.* Immunity, 2002. **17**(4): p. 389-399.

162. Sol-Foulon, N., et al., *ZAP-70 kinase regulates HIV cell-to-cell spread and virological synapse formation.* Embo Journal, 2007. **26**(2): p. 516-526.

163. Bajenoff, M., et al., *Stromal cell networks regulate lymphocyte entry, migration, and territoriality in lymph nodes.* Immunity, 2006. **25**(6): p. 989-1001.

164. Hugues, S., et al., *Distinct T cell dynamics in lymph nodes during the induction of tolerance and immunity.* Nature Immunology, 2004. **5**(12): p. 1235-42.

165. Mempel, T.R., S.E. Henrickson, and U.H. Von Andrian, *T-cell priming by dendritic cells in lymph nodes occurs in three distinct phases.* Nature, 2004. **427**(6970): p. 154-9.

166. Miller, M.J., et al., *Autonomous T cell trafficking examined in vivo with intravital two-photon microscopy.* Proc Natl Acad Sci U S A, 2003. **100**(5): p. 2604-9.

167. Miller, M.J., et al., *Two-photon imaging of lymphocyte motility and antigen response in intact lymph node.* Science, 2002. **296**(5574): p. 1869-73.

168. Mrass, P., et al., *Random migration precedes stable target cell interactions of tumor-infiltrating T cells.* J Exp Med, 2006. **203**(12): p. 2749-61.

169. Krummel, M.F. and I. Macara, *Maintenance and modulation of T cell polarity.* Nature Immunology, 2006. **7**(11): p. 1143-1149.

170. Sanchez-Madrid, F. and M.A. del Pozo, *Leukocyte polarization in cell migration and immune interactions.* Embo Journal, 1999. **18**(3): p. 501-511.

171. Sanchez-Madrid, F. and J.M. Serrador, *Bringing up the rear: defining the roles of the uropod.* Nature Reviews Molecular Cell Biology, 2009. **10**(5): p. 353-359.

172. Ridley, A.J., et al., *Cell migration: integrating signals from front to back.* Science, 2003. **302**(5651): p. 1704-9.

173. Coates, T.D., et al., *Relationship of F-actin distribution to development of polar shape in human polymorphonuclear neutrophils.* J Cell Biol, 1992. **117**(4): p. 765-74.

174. Yonemura, S., et al., *Ezrin/radixin/moesin (ERM) proteins bind to a positively charged amino acid cluster in the juxta-membrane cytoplasmic domain of CD44, CD43, and ICAM-2.* J Cell Biol, 1998. **140**(4): p. 885-95.

175. Serrador, J.M., et al., *A novel serine-rich motif in the intercellular adhesion molecule 3 is critical for its ezrin/radixin/moesin-directed subcellular targeting.* Journal of Biological Chemistry, 2002. **277**(12): p. 10400-10409.

176. Serrador, J.M., et al., *A juxta-membrane amino acid sequence of P-selectin glycoprotein ligand-1 is involved in moesin binding and ezrin/radixin/moesin-directed targeting at the trailing edge of migrating lymphocytes.* Eur J Immunol, 2002. **32**(6): p. 1560-6.

177. Bretscher, A., K. Edwards, and R.G. Fehon, *ERM proteins and merlin: Integrators at the cell cortex.* Nature Reviews Molecular Cell Biology, 2002. **3**(8): p. 586-599.

178. Lee, J.H., et al., *Roles of p-ERM and Rho-ROCK signaling in lymphocyte polarity and uropod formation.* J Cell Biol, 2004. **167**(2): p. 327-37.

179. Tibaldi, E.V., R. Salgia, and E.L. Reinherz, *CD2 molecules redistribute to the uropod during T cell scanning: Implications for cellular activation and immune surveillance.* Proceedings of the National Academy of Sciences of the United States of America, 2002. **99**(11): p. 7582-7587.

180. Goetz, D.J., et al., *Isolated P-selectin glycoprotein ligand-1 dynamic adhesion to P- and E-selectin.* J Cell Biol, 1997. **137**(2): p. 509-19.

181. Pouyani, T. and B. Seed, *Psgl-1 Recognition of P-Selectin Is Controlled by a Tyrosine Sulfation Consensus at the Psgl-1 Amino-Terminus.* Cell, 1995. **83**(2): p. 333-343.

182. Sako, D., et al., *A Sulfated Peptide Segment at the Amino-Terminus of Psgl-1 Is Critical for P-Selectin Binding.* Cell, 1995. **83**(2): p. 323-331.

183. Sperandio, M., et al., *P-selectin glycoprotein ligand-1 mediates L-selectin-dependent leukocyte rolling in venules.* J Exp Med, 2003. **197**(10): p. 1355-63.

184. Gallatin, W.M., I.L. Weissman, and E.C. Butcher, *A Cell-Surface Molecule Involved in Organ-Specific Homing of Lymphocytes.* Nature, 1983. **304**(5921): p. 30-34.

185. Miner, J.J., et al., *Separable requirements for cytoplasmic domain of PSGL-1 in leukocyte rolling and signaling under flow.* Blood, 2008. **112**(5): p. 2035-2045.

186. Zarbock, A., C.A. Lowell, and K. Ley, *Spleen tyrosine kinase syk is necessary for E-Selectin-induced alpha(L)beta 2 integrin-mediated rolling on intercellular adhesion molecule-1.* Immunity, 2007. **26**(6): p. 773-783.

187. Ratner, S., W.S. Sherrod, and D. Lichlyter, *Microtubule retraction into the uropod and its role in T cell polarization and motility.* Journal of Immunology, 1997. **159**(3): p. 1063-1067.

188. Alonso-Lebrero, J.L., et al., *Polarization and interaction of adhesion molecules P-selectin glycoprotein ligand 1 and intercellular adhesion molecule 3 with moesin and ezrin in myeloid cells.* Blood, 2000. **95**(7): p. 2413-9.

189. Rosenman, S.J., et al., *Syn-capping of human T lymphocyte adhesion/activation molecules and their redistribution during interaction with endothelial cells.* J Leukoc Biol, 1993. **53**(1): p. 1-10.

190. del Pozo, M.A., et al., *Chemokines regulate cellular polarization and adhesion receptor redistribution during lymphocyte interaction with endothelium and extracellular matrix. Involvement of cAMP signaling pathway.* J Cell Biol, 1995. **131**(2): p. 495-508.

191. Gomez-Mouton, C., et al., *Segregation of leading-edge and uropod components into specific lipid rafts during T cell polarization.* Proc Natl Acad Sci U S A, 2001. **98**(17): p. 9642-7.

192. Brown, M.J., et al., *Rigidity of circulating lymphocytes is primarily conferred by vimentin intermediate filaments.* Journal of Immunology, 2001. **166**(11): p. 6640-6646.

193. Seveau, S., et al., *Leukosialin (CD43, sialophorin) redistribution in uropods of polarized neutrophils is induced by CD43 cross-linking by antibodies, by colchicine or by chemotactic peptides.* J Cell Sci, 1997. **110 (Pt 13)**: p. 1465-75.

194. Serrador, J.M., et al., *CD43 interacts with moesin and ezrin and regulates its redistribution to the uropods of T lymphocytes at the cell-cell contacts.* Blood, 1998. **91**(12): p. 4632-44.

195. Mcfarlan.W and D.H. Heilman, *Lymphocyte Foot Appendage - Its Role in Lymphocyte Function and in Immunological Reactions.* Nature, 1965. **205**(4974): p. 887-&.

196. delPozo, M.A., et al., *ICAMs redistributed by chemokines to cellular uropods as a mechanism for recruitment of T lymphocytes.* Journal of Cell Biology, 1997. **137**(2): p. 493-508.

197. Prejean, J., et al., *Estimated HIV Incidence in the United States, 2006-2009.* PLoS One, 2011. **6**(8).

198. Sturmer, M., et al., *Evolution of resistance mutations during low-level viral replication in HIV-1-infected patients treated with zidovudine/lamivudine/abacavir as a first-line regimen.* Antivir Ther, 2007. **12**(1): p. 25-30.

199. Llewellyn, N., et al., *Continued evolution of HIV-1 circulating in blood monocytes with antiretroviral therapy: genetic analysis of HIV-1 in monocytes*

and CD4+ T cells of patients with discontinued therapy. J Leukoc Biol, 2006. **80**(5): p. 1118-26.

200. Jubault, V., et al., *High rebound of plasma and cellular HIV load after discontinuation of triple combination therapy.* Aids, 1998. **12**(17): p. 2358-9.

201. de Jong, M.D., et al., *Overshoot of HIV-1 viraemia after early discontinuation of antiretroviral treatment.* Aids, 1997. **11**(11): p. F79-84.

202. Havlir, D.V., et al., *Maintenance antiretroviral therapies in HIV-infected subjects with undetectable plasma HIV RNA after triple-drug therapy.* New England Journal of Medicine, 1998. **339**(18): p. 1261-1268.

Chapter II

Nucleocapsid Promotes Localization of HIV-1 Gag to Uropods that Participate in Virological Synapses between T Cells

Abstract

T cells adopt a polarized morphology in lymphoid organs, where cell-to-cell transmission of HIV-1 is likely frequent. However, despite the importance of understanding virus spread in vivo, little is known about the HIV-1 life cycle, particularly its late phase, in polarized T cells. Polarized T cells form two ends, the leading edge at the front and a protrusion called a uropod at the rear. In this chapter, using multiple uropod markers, it was observed that HIV-1 Gag localizes to the uropod in polarized T cells. Infected T cells formed contacts with uninfected target T cells preferentially via HIV-1 Gag-containing uropods compared to leading edges that lack plasma-membrane-associated Gag. Cell contacts enriched in Gag and CD4, which define the virological synapse (VS), are also enriched in uropod markers. These results indicate that Gag-laden uropods participate in the formation and/or structure of the VS, which likely plays a key role in cell-to-cell transmission of HIV-1. Consistent with this notion, a myosin light chain kinase inhibitor, which disrupts uropods, reduced virus particle transfer from infected T cells to target T cells. Mechanistically, it was observed that Gag copatches

with antibody-crosslinked uropod markers even in non-polarized cells, suggesting an association of Gag with uropod-specific microdomains that carry Gag to uropods. Finally, localization of Gag to the uropod was determined to require higher-order clustering driven by the NC domain. Taken together, these results support a model in which NC-dependent Gag accumulation to uropods establishes a preformed platform that later constitutes T-cell-T-cell contacts at which HIV-1 virus transfer occurs.

Introduction

One of the primary natural targets of HIV-1 is the T cell. HIV-1 spread between infected and uninfected T cells likely occurs frequently in densely packed environments such as lymph nodes *in vivo*. Two-photon imaging studies have shown that a majority of T cells in lymph nodes are highly motile and have a polarized morphology [1-6]. Therefore, it is likely that, in lymphoid organs, HIV-1 replicates within and is transmitted by polarized T cells. However, the life cycle of HIV-1 in polarized T cells has not been examined in detail.

HIV-1 assembly occurs at the plasma membrane and is driven by the HIV-1 polyprotein Gag. Gag is the primary structural protein of retroviruses, including HIV-1, and is both necessary and sufficient for formation of virus-like particles [7]. HIV-1 Gag is composed of four structural domains: matrix (MA), capsid (CA), nucleocapsid (NC) and p6. MA mediates Gag targeting and binding to the plasma membrane, primarily through the myristoyl group on the N terminus of MA, which inserts into the plasma membrane, as well as MA basic amino acids that interact with phosphatidylinositol-4,5-bisphosphate [$PI(4,5)P_2$], a plasma-membrane-specific phospholipid [8-20]. CA mediates

Gag dimerization through an interface in its C terminal domain (CTD), in which amino acids W184 and M185 play key roles [21-33]. NC binds specifically to the viral genomic RNA, which is essential for packaging of viral genomes to virions [34]. In addition, NC contributes to multimerization of Gag, whereby RNA is thought to serve as a scaffold [21, 25, 28, 35-43]. p6 contains peptide sequences that recruit cellular endosomal sorting complex required for transport (ESCRT) proteins, which facilitate the release of virus particles [44-46].

A polarized T cell forms a leading edge at the front and a protrusion called a uropod at the rear [47-49]. There are several proteins known to be enriched in the uropod, including intercellular adhesion molecule (ICAM)-1, -2, and -3, P-selectin glycoprotein ligand (PSGL)-1, CD43, and CD44 [50, 51]. The microtubule organizing center (MTOC) is also known to localize to the base of the uropod [49, 52]. Previous studies have observed that in T cells and monocytes, HIV-1 proteins localize to a cell protrusion, which resembles a uropod [53-57]. Furthermore, virus particles are enriched in several uropod-associated proteins, such as ICAM-1, ICAM-2, CD43 and CD44 [58, 59]. A raft-associated lipid known to localize to uropods, GM1 [60], also associates with virus particles [54, 61, 62]. Altogether, these observations suggest that uropods potentially serve as sites of virus assembly in polarized T cells. However, the nature of Gag localization in polarized T cells and its significance to virus spread have yet to be fully determined.

T cell uropods have been shown to mediate contact between T cells and other cells, which is consistent with the observation of adhesion molecule enrichment in uropods [63-65]. Thus, it is possible that HIV-1 accumulation at the uropod may play a

role in cell-to-cell transmission. Cell-to-cell transmission is ten to several thousand times more efficient than cell-free transmission [53, 57, 66-71]. Recent studies have described specific cell contact structures that facilitate cell-to-cell transmission [67, 72-86]. Live cell imaging studies have revealed that particles of HIV-1 and murine leukemia virus (MLV) are transferred from infected cells to uninfected target cells along the surface of filamentous extensions called membrane nanotubes and cytonemes [80-82, 87, 88]. Virological synapses (VS), which appear to structurally resemble immunological synapses [77, 78, 89-97], are also thought to facilitate the direct transfer of budding virus particles from one cell to another [53, 67, 71, 78, 80, 95]. However, the mechanisms leading to the establishment of these transmission routes, especially the VS, remain to be elucidated.

In this chapter, it was determined that the uropod is the cell structure to which membrane-associated Gag accumulates in polarized T cells. Gag-containing uropods mediated frequent contact with uninfected target cells. Virtually all observed VS, defined by accumulation of CD4 and Gag to cell contacts, showed enrichment of the uropod marker CD43, suggesting a major role for HIV-1 localization to the uropod in virus spread. Consistent with this possibility, upon disruption of uropod formation, cell-to-cell transfer of HIV-1 was significantly reduced. Gag on the cell surface copatched strongly with uropod markers not only in polarized T cells but also in non-polarized T cells. Gag-containing patches that were dispersed on the membrane of non-polarized cells appeared to move laterally and to concentrate at the uropod when cells became polarized. These patches maintained colocalization with uropod markers, suggesting that uropod-directed microdomains play a role in polarized Gag localization. Uropod localization of Gag

required higher-order multimerization or clustering mediated by NC. These findings strongly support a model in which multimerization-dependent Gag localization to uropods represents one mechanism by which the VS is formed.

Results

Gag localizes to uropods in polarized T cells.

To examine Gag localization in polarized T cells, a YFP-tagged Gag (Gag-YFP) was expressed in either primary T cells or in a polarized T cell line, P2. To express Gag-YFP, T cells were infected with VSV-G-pseudotyped HIV-1 that encodes Gag-YFP. Two days post-infection, cells were immunostained for uropod markers PSGL-1 or CD43 (Figure 2.1A and B). Alternatively, the MTOC, which localizes to the base of the uropod, was detected using anti-α-tubulin (Figure 2.1C). In both primary $CD4^+$ T cells and P2 cells, approximately 50-60% of cells showed polarized morphology, and infection with VSV-G-pseudotyped HIV-1 did not substantially alter the percentage of polarized cells (Table 2.1). Primary $CD4^+$ T cells expressing Gag-YFP showed strong colocalization of Gag on the plasma membrane with both uropod markers PSGL-1 and CD43, as well as co-polarization with the MTOC in virtually all Gag-positive cells with uropods (Figure 2.1A-C and Table 2.2). In contrast, Gag-YFP showed segregation from LFA-1, a non-uropod-associated protein [98] (Figure 2.1D). Similar to primary T cells, P2 cells also showed strong colocalization of PSGL-1 and Gag-YFP as well as co-polarization of the MTOC and Gag-YFP (Figure 2.1E and F and Table 2.2). In these cells, plasma-membrane-associated Gag-YFP was highly polarized and detected only in the uropod region (Fig. 2.7C). Similarly, untagged Gag detected at the plasma membrane using anti-

Gag antibodies also showed strong colocalization with uropod markers (supplementary Figure 2.S1). These results indicate that Gag localizes to uropods in polarized T cells. To determine whether uropod localization of Gag-YFP is stable, live cell analysis of primary T cells expressing Gag-YFP was performed. It was observed that Gag-YFP maintains localization in the uropod during T cell migration for a minimum of almost 30 min (Figure 2.1G, Supplementary Movie S1).

To determine whether uropod-associated Gag is able to form mature particles, P2 and primary $CD4^+$ T cells were infected with VSV-G-pseudotyped HIV-1 encoding Gag-iYFP. This Gag derivative contains YFP inserted between MA and CA and forms mature Gag proteins and free YFP upon cleavage by viral protease [99]. When cells expressing Gag-iYFP were immunostained with an anti-p17MA antibody, which only recognizes the mature, cleaved matrix domain of Gag [100, 101], the YFP signal was observed to colocalize substantially with p17MA signal at the uropod (Figure 2.2A and Table 2.3). It was also observed that both Gag-iYFP and Gag-YFP colocalize well with HIV-1 Env in the uropod (Figure 2.2B and Table 2.3). These results suggest that at least a subset of Gag localized at uropods is capable of forming Env-containing virus particles that undergo Gag processing essential for virion maturation. It should be noted that Env immunostaining was performed prior to fixation similar to previous studies [61,96]. Thus, the possibility of crosslinking playing a role in Env localization should be considered.

Uropods mediate contact between infected and target T cells.

Uropods in uninfected T cells have been shown to mediate contact between T cells and other cells [63, 65]. Therefore, accumulation of Gag in, and particle formation

at, the uropod may facilitate cell-to-cell transmission of HIV-1. To examine whether contact of HIV-1-infected T cells with target T cells is preferentially mediated by uropods, live cell imaging experiments were performed. Fresh target primary T cells were stained with a blue fluorescent dye, CMAC, and cocultured with Gag-YFP expressing primary T cells. This coculture was then immunostained with anti-PSGL-1, which had been prelabeled with Zenon AlexaFluor594. We observed that the uropod containing Gag-YFP maintained contact with CMAC-stained T cells for over 20 min as the cells moved through the field (Figure 2.3A, Supplementary Movie S2). These observations suggest that HIV-1-infected T cells are able to mediate stable contacts with target cells through their uropods. Newly formed contacts between Gag-YFP-expressing primary T cells and CMAC-stained target primary T cells formed during a 3-h coculture period were then quantified. An example of T cell contacts is shown in Figure 2.3B. We found that the majority of newly formed contacts occur at the uropod (Figure 2.3C), despite the average uropod constituting only approximately 20-30% of the total cell surface (data not shown). These results indicate that Gag-containing uropods stably and preferentially form new contacts with uninfected T cells. In these experiments, when target cells are also polarized, infected cell uropods formed a similar number of contacts with both ends of target cells (data not shown).

Gag-containing uropods of infected cells participate in formation of the VS at which CD4 of target T cells accumulates.

It is possible that cell contacts formed by infected cell uropods observed above actively participate in VS formation. To address this possibility, localization of CD4,

which is known to accumulate to the VS on the cell surface of target cells, was examined. P2 cells infected with VSV-G-pseudotyped HIV-1 expressing Gag-CFP and Env were immunostained for CD43 and mixed with target cells prelabeled with non-blocking, FITC-conjugated anti-CD4. After 3 h of coculture, cells were analyzed by live cell microscopy. When infected P2 cells were in contact with target SupT1 cells, CD4 on the surface of SupT1 cells accumulated to junctions formed between Gag-CFP-positive, CD43-positive uropods and target cells (Figure 2.4A). During quantitative analyses it was found that CD4 accumulation at cell-cell junctions predominantly takes place when Gag-CFP-positive uropods, but not non-uropod regions, of infected P2 cells contact target SupT1 cells (Figure 2.4C). Such CD4 accumulation was rarely observed at junctions formed between Gag-CFP-negative or uninfected P2 cells and SupT1 cells (Figure 2.4A-C). These results suggest that infected T cell uropods are actively involved in recruitment of CD4 to cell junctions, perhaps through accumulation of Env (Figure 2.2). As cell junctions enriched in viral antigens such as Gag and the HIV receptor CD4 are defined as the VS in previous studies [61], these results support a model in which uropods or uropod-derived membrane components specifically participate in formation of the VS.

Myosin light chain kinase inhibitor depolarizes cell morphology and Gag localization and reduces cell-to-cell transfer of Gag-YFP.

In order to explore whether Gag accumulation to uropods facilitates transmission of HIV-1, a cell-to-cell virus transfer assay was performed. In this flow-cytometry-based assay, the transfer of YFP fluorescence, representing virions, from infected P2 cells expressing Gag-YFP to CMTMR-stained SupT1 target cells was measured. Similar

assays have been used in previous studies for analyzing cell-to-cell virus spread [53, 71, 102-104]. Representative flow cytometry plots for control cocultures are shown in Figure 2.5A. Binding of cell-free virions to target cells was undetectable, which is consistent with previous studies [53] (data not shown). Therefore, transfer of fluorescence represents cell-to-cell virus transfer. Consistent with previous reports [53], we observed a significant decrease in virus transfer when cells were cocultured in the presence of an anti-CD4 antibody (Leu3A) that prevents CD4-Env interaction, but not an isotype control IgG (Figure 2.5A and C). These data confirm the importance of Env in cell-to-cell transfer of HIV-1. Using this assay, the effects of cell depolarization on cell-to-cell HIV-1 transfer were examined using a myosin light chain kinase inhibitor, ML7. As expected, treatment of Gag-YFP-expressing P2 cells with this inhibitor disrupted uropod formation and dispersed Gag-YFP on the plasma membrane (Figure 2.5B). ML7 did not have a major impact on efficiency of VLP release by Gag-YFP calculated as the amount of virion-associated Gag as a fraction of total Gag (supplementary Figure 2.S2 and supplementary text). However, because ML7 treatment reduces protein synthesis (data not shown), it was possible that any decrease in cell-to-cell virus transfer by treatment with ML7 may have arisen from reduced Gag expression instead of disruption of cell polarity. To rule out the indirect effect of protein synthesis inhibition on virus transfer, we included 10 μg/ml cycloheximide in all coculture conditions, including those treated with Leu3A and control IgG described above. As shown in Figure 2.5A, substantial virus transfer occurred even in the presence of cycloheximide. Finally, it was observed that in the presence of cycloheximide, ML7 treatment significantly decreased cell-to-cell virus transfer (Figure 2.5C and supplementary Figure 2.S3). Together with the data showing

that the uropod participates in formation of the VS (Figure 2.4), these results suggest that polarized localization of Gag and/or assembling particles at the uropod contributes to cell-to-cell transfer of virus particles to target cells.

Gag localizes to uropod-specific microdomains.

The results presented thus far suggest that Gag-laden uropods play a major role in cell-to-cell virus transmission. Thus, it is important to elucidate the mechanism by which Gag accumulates to uropods. Gag has been shown previously to associate with microdomains, such as lipid rafts and tetraspanin-enriched microdomains (TEMs) [10, 54, 61, 105-112], and these microdomains are observed at the VS [61, 80, 113, 114]. Since subsets of these microdomains are implicated in polarized localization of proteins in leukocytes [49, 60, 115-118], it is conceivable that Gag utilizes uropod-specific microdomains for transport to the uropod. In this case, it would be expected to observe copartitioning of Gag and uropod markers to the same microdomain even in unpolarized cells. A common method to test whether two proteins share a propensity for associating with the same microdomain is to test for colocalization, or "copatching", after crosslinking with antibodies specific to each of the two proteins [119-124]. This assay was used to examine whether Gag-YFP associates with uropod-directed microdomains in unpolarized P2 cells. As Gag forms multimers on its own, antibody-mediated crosslinking was needed only for cell surface marker proteins that include the uropod markers PSGL-1 and CD43 and the non-uropod marker LFA-1. Because Gag has been previously shown to colocalize with TEMs using similar methods [109], we also included the tetraspanin CD81 in the analysis. As observed in previous reports [109], we found

that Gag-YFP copatches with CD81 (Figure 2.6A) [correlation coefficient (CC)=0.46 (see methods); Figure 2.6E]. Relative to CD81, however, the uropod markers PSGL-1 and CD43 copatched more extensively with Gag-YFP (CC=0.69 and 0.70, respectively; Figure 2.6E). On the other hand, even though LFA-1 showed punctate localization as well, we observed a segregation of LFA-1 and Gag-YFP (Figure 2.6D) as indicated by the negative correlation coefficient (CC=-0.14; Figure 2.6E). Because copatching between Gag-YFP and uropod markers was observed even in non-polarized cells (Figure 2.6B and C), these results suggest that Gag localizes to uropod-specific microdomains prior to, and perhaps during, T cell polarization.

To examine whether Gag-YFP localized at uropods had originated from the Gag-YFP-positive patches observed in morphologically unpolarized cells, live-cell microscopy was performed of Gag-YFP-expressing P2 cells that were first depolarized by low temperature treatment prior to image recording at 37ºC. In these experiments, Gag-containing patches were observed to maintain colocalization with PSGL-1 and laterally move on the plasma membrane to the forming uropod as cells re-polarized. (Figure 2.6F, Supplementary Movie S3). Lateral movement of Gag-YFP was also observed in cells that were not immunostained for any marker, indicating that the observed movement was not caused by antibody-mediated crosslinking (supplemental Movie S4). These observations support a model in which Gag associates with uropod-specific microdomains while establishing localization at the rear end of polarized T cells.

Env is not required for Gag localization to the uropod.

It has been shown that Gag and Env interact with each other [125-131]. Furthermore, it has been shown that Env is required for the formation of virological synapses between infected and uninfected T cells [53, 61, 67, 68, 78, 80, 89], unlike those formed between uninfected T cells and infected macrophages [75]. Therefore, Env may play an active role in Gag localization to uropods. To address this possibility, we examined T cells expressing an HIV-1 molecular clone that encodes Gag-YFP but not Env (KFS/Gag-YFP). In these cells, KFS/Gag-YFP co-localized strongly with PSGL-1 and copolarized with the MTOC at the uropod (Figure 2.7A), just as observed in cells expressing both Gag-YFP and Env (Figure 2.1). To examine microdomain partitioning, we also performed copatching assays for KFS/Gag-YFP and uropod markers in unpolarized cells. KFS/Gag-YFP was found to copatch with the uropod markers PSGL-1 and CD43 (Figure 2.7B) at comparable levels to wild type (data not shown). Gag polarization indices was also compared between cells expressing Gag-YFP in the presence (Gag-YFP) or absence (KFS/Gag-YFP) of Env. The Gag polarization index describes the extent of Gag distribution along the plasma membrane from one cell pole to the other (see Materials and Methods). A lower index represents stronger polarization. The polarization index for KFS/Gag-YFP was nearly identical to that for Gag-YFP (Figure 2.7C, $p=0.28$). It was also found that the absence of Env had no impact on the preference for uropod-mediated contact between Gag-YFP-expressing primary T cells and CMAC-stained target primary T cells (Figure 2.7D, $p=0.23$). This finding suggests that Env may not be required for initial contact formation, even while it is required for transfer of virus particles (Figure 2.5) [53, 132] and maintenance of cell-cell conjugates

[53, 68, 78, 80]. Taken together, these results indicate that HIV-1 Env is dispensable for localization of Gag to the uropod.

MA and CA are not required for Gag localization to the uropod.

To identify the molecular determinants of Gag that facilitate its localization to the uropod, a panel of Gag mutants was examined for uropod localization (Figure 2.8). Because MA is essential for specific targeting of Gag to the plasma membrane [11, 12, 100, 133-139], it is conceivable that MA also regulates specific localization of Gag to uropods. To test this possibility, the effect of MA deletion on Gag localization to uropods was examined. As MA is also essential for general membrane binding, to restore Gag membrane binding of the MA deletion mutant, a heterologous membrane binding sequence, an N-terminal 10-amino-acid sequence of Fyn kinase [Fyn(10)] was added to the N terminus of Gag. This sequence contains acylation signals for one myristoyl and two palmitoyl groups, and fully restores Gag membrane binding in the absence of the entire MA sequence [11]. Notably, the Fyn(10) sequence by itself is not capable of targeting proteins to uropods. As shown in Figure 2.9A, CFP attached to the Fyn(10) sequence [Fyn(10)-CFP] localized around the entire plasma membrane. In contrast, Fyn(10)/Gag-YFP localized to the uropod in the same cell (Figure 2.9A). These results indicate that the addition of Fyn(10) did not alter uropod localization of full-length Gag [Fyn(10)/Gag-YFP] in T cells, and that some region in Gag is required for its uropod localization. Notably, it was observed that Fyn(10)/ΔMA/Gag-YFP, in which the entire MA sequence is deleted, still localized to the uropod efficiently in T cells (Figure 2.9B).

Taken together, these results indicate that Gag localization to the uropod requires sequences downstream of MA and not the MA sequence itself.

The downstream sequence of MA includes the CA and NC domains. During virus particle formation, these domains are known to promote the dimerization and multimerization of Gag. To examine the roles played by Gag-Gag interactions in uropod localization, Gag derivatives with changes in either CA or NC was examined for uropod localization. Because Gag multimerization defects also reduce steady-state membrane binding [28, 42, 140], the Fyn(10) sequence was added to the CA and NC mutants. First, the plasma membrane localization of two YFP- and CFP-tagged CA mutants: an amino acid substitution mutant WM184,185AA (Fyn(10)/WMAA/Gag-YFP/-CFP) and a deletion mutant lacking the C-terminal domain (Fyn(10)/delCA-CTD/Gag-YFP/-CFP) was examined. Previously, it was observed by FRET microscopy that these CA mutants are deficient in Gag-Gag interactions in HeLa cells [28]. P2 cells were coinfected with VSV-G-pseudotyped viruses encoding derivatives of Gag-YFP or Gag-CFP, and their localization and multimerization were examined by fluorescence and FRET microscopy, respectively. WT Gag-YFP/-CFP and Fyn(10)/Gag-YFP/-CFP showed high FRET in the uropod, indicating that Gag multimers localize to uropods (Figure 2.10A and B). Notably, both Fyn(10)/delCA-CTD/Gag-YFP/-CFP and Fyn(10)/WMAA/Gag-YFP/-CFP also showed clear localization to the uropod (Figure 2.10C and D) although, as expected, these Gag mutants displayed low FRET (Figure 2.10C and D). The polarization index for Fyn(10)/WMAA/Gag-YFP was also nearly identical to that of Fyn(10)/Gag-YFP (Figure 2.10E). Taken together, these results demonstrate that CA-mediated dimerization is not required for localization of Gag to the uropod.

NC is essential for localization of Gag to the uropod.

To examine the role of NC in Gag localization to uropods, we next analyzed a mutant Gag that lacks most of the NC sequence (Fyn(10)/delNC/Gag-YFP/-CFP). In contrast to the MA and CA mutants that localized to the uropod, Fyn(10)/delNC/Gag-YFP/-CFP localized over the entire plasma membrane (Figure 2.11A). An NC mutant in which 15 NC basic residues essential for RNA binding were substituted with alanine or glycine (Fyn(10)/14A1G/Gag-YFP/-CFP) also showed non-polarized localization (Figure 2.11B). These results indicate that NC is required for Gag localization to the uropod. Pleitropic impacts of NC mutations on Gag assembly precluded obtaining interpretable results regarding the effects of these mutations on cell-to-cell transfer (supplementary Figure 2.S2 and supplementary text).

NC-mediated multimerization is required for Gag localization to the uropod.

As confirmed by FRET microscopy (Figure 2.11A and B), both Fyn(10)/delNC/Gag-YFP/-CFP and Fyn(10)/14A1G/Gag-YFP/-CFP that are defective in polarized localization are also defective in Gag-Gag interaction. Therefore, it is possible that NC-mediated Gag multimerization or clustering plays a key role in Gag localization to the uropod. Alternatively, other functions of NC may facilitate Gag localization to the uropod. To distinguish between these possibilities, a Gag derivative in which NC was replaced by a leucine zipper sequence (LZ) derived from GCN4 (LZ/Gag-YFP/-CFP) was examined for uropod localization. Gag derivatives in which NC is replaced with this LZ sequence, which has no homology to NC, have been shown previously to multimerize efficiently [141-143]. We observed that LZ/Gag-YFP/-CFP localized to the uropod in a

majority of cells expressing this Gag derivative and yielded a WT level of FRET (compare Figure 2.11C with Figure 2.10A). Quantitative analysis of polarization indicated that LZ/Gag-YFP was not as efficiently polarized as WT, but nonetheless significantly more polarized than the NC point mutant Fyn(10)/14A1G/Gag-YFP (Figure 2.11D). These results suggest that NC promotes Gag localization to the uropod through its ability to facilitate higher-order Gag multimerization. As the LZ sequence used above is a dimerization sequence, it would drive higher-order multimerization only in the presence of an additional dimerization motif such as CA-CTD. Thus, it was hypothesized that although Fyn(10)/delCA-CTD/Gag-YFP/-CFP and Fyn(10)/WMAA/Gag-YFP/-CFP localize to uropods (Figure 2.10C and D), in these contexts, LZ in the place of NC would be unable to promote Gag localization to uropods (Figure 2.11E and F). Indeed, cells expressing these constructs, Fyn(10)/WMAA/LZ/Gag-YFP and Fyn(10)/delCA-CTD/LZ/Gag-YFP, showed localization of Gag over the entire plasma membrane, a pattern identical to that of the NC mutants (compare Figure 2.11E and F with A and B). Taken together, these results demonstrate that dimerization mediated by either CA-CTD or LZ alone is insufficient for localization to the uropod. However, NC-mediated higher-order multimerization or clustering of Gag, defined as any multimer higher than a dimer and which likely occurs even in the absence of the CA-CTD dimerization interface, is essential for localization to the uropod.

Discussion

In lymphoid organs, where HIV-1 likely spreads efficiently from infected to uninfected T cells, T cells adopt a polarized morphology and are highly motile. Thus, studying HIV-1 replication in polarized T cells may help to better understand how the virus spreads *in vivo*. In this study, it was found that HIV-1 Gag accumulates to, and forms mature virions at, the uropod in polarized T cells (Figures 2.1 and 2.2). These observations led to the question of whether uropod localization of HIV-1 Gag plays a role in the spread of the virus. In uninfected T cells, uropods are enriched in adhesion molecules and known to mediate contact with other cells [49]. Therefore, polarized virus assembly at uropods could facilitate cell-to-cell transmission of HIV-1. Consistent with this possibility, live cell microscopy and quantitative cell-cell contact analyses showed that HIV-1-infected cells contact target cells preferentially through their uropods (Figure 2.3). Furthermore, a substantial majority of Gag- and CD4-positive cell-cell contacts, which define the VS [61], were observed where uropod-derived (CD43-positive), but not non-uropod (CD43-negative), regions of infected cells mediated contact with target cells (Figure 2.4). Consistent with these microscopy data, it was observed that ML7, a drug that blocks the polarization of T cells and formation of uropods, both dispersed Gag over the cell surface and reduced cell-to-cell transfer of virus particles significantly (Figure 2.5). It should be noted that ML7 may also inhibit some myosin/actin processes besides cell polarization that may affect cell-to-cell virus transfer. Taken together, these results indicate that uropods of polarized T cells play an important role in cell-to-cell transfer of HIV-1. Notably, bone marrow hematopoietic stem cells have been shown to mediate not only contacts with osteoblasts, but also cell-to-cell transfer of plasma-membrane-

associated molecules via their uropods [144]. This process, postulated to mediate intercellular signal transfer, may be a common cell-cell communication mechanism shared among cells of the hematopoietic cell lineage, including T cells. Thus, localization of HIV-1 components to, and subsequent virus assembly at, the uropod may represent yet another example in which viruses hijack cellular processes to facilitate its own replication.

It has been reported by several groups that cell-to-cell HIV-1 transmission occurs via the VS. However, the steps leading to formation of the VS are not well defined. Observations described in this study suggest that at least one path toward establishment of the VS is the accumulation of viral components and assembling virions to the uropod. Uropods could then serve as a pre-formed platform that constitutes a VS upon cell-cell contact (Figure 2.12A). Consistent with this possibility, previous studies showed that disruption of the cytoskeleton, which also impairs cell polarity, reduces Gag accumulation to contact sites between infected and uninfected T cells [77, 78, 80, 145]. It is conceivable that suppression of uropod formation or inhibition of Gag localization to uropods may account for the observed reduction of VS formation upon cytoskeleton disruption.

It is important to note that these observations do not preclude other modes of VS formation. For example, if morphologically unpolarized cells with dispersed Gag make contact with a target cell, Gag could re-localize laterally to the contact site. Consistent with such Gag movement, a recent imaging study showed that most cell conjugate formation precedes Gag redistribution when apparently unpolarized Jurkat cells were used as donor cells [67]. Such lateral movement could also occur in polarized cells that

initially contact target cells through a non-uropod region of the cell (Figure 2.12B). Movement of Gag-containing patches to contact sites has been observed in recent VS studies [67, 80]. It is possible that these patches may have originated at the uropod, although this point remains to be determined by long-term live cell monitoring of polarized T cells. Thus, in either mode of VS formation, prior formation of a platform enriched in Gag and other viral components, which take place at the uropod, may be an important first step in cell-to-cell virus transfer.

Polarized localization of Gag to the uropod appears to play an important role in HIV-1 spread. Thus, determining the mechanism of uropod localization of Gag is important. Previous studies have shown that some cell-surface proteins localize to the uropod upon antibody crosslinking through an undefined mechanism [146-148]. As dimerization and multimerization can be considered to be a form of crosslinking, it was examined whether Gag localization to uropods similarly depends on Gag multimerization. While CA dimerization mutations did not alter localization of Gag to the uropod (Figure 2.10), mutations that disrupt higher-order multimerization mediated by NC-RNA interactions did (Figure 2.11). Mutations in NC caused Gag to localize over the entire plasma membrane despite the presence of the CA dimerization interface. Furthermore, a heterologous dimerization sequence, LZ, restored the uropod localization of NC-deleted Gag. Finally, this LZ-dependent localization required the intact CA dimerization interface, supporting the importance of higher-order Gag multimerization. Therefore, although both CA dimerization and NC-RNA interaction are important for Gag assembly, it is the NC-dependent higher-order multimerization that is essential for Gag localization to the uropod. In this regard, uropod localization of Gag may be driven

by a mechanism similar to the one targeting multimerizing proteins to endosome-like domains reported recently to exist on the plasma membrane [149]. The nature of the NC-dependent higher-order multimer directed to uropods remains to be elucidated; however, as CA dimerization mutants that did not yield substantial FRET signals still localized to uropods (Figure 2.10), it is likely that the uropod targeting process does not require the NC-dependent multimer to be in a highly aligned and packed form. As NC by itself can bind RNA in the absence of CA [150], it is conceivable that Gag clustering through binding to the same RNA molecule is sufficient for localization to uropods.

Protein-protein interactions, which include clustering or multimerization of membrane proteins, are known to stabilize the microdomains with which those proteins associate [151]. In this study, it was observed that Gag copatches moderately with CD81 and strongly with uropod markers PSGL-1 and CD43 even in non-polarized cells (Figure 2.6). Using live cell analysis, it was also observed that Gag/PSGL-1 patches move laterally on the cell surface of unpolarized cells and accumulate at the forming uropod as cells polarize. These results support a model in which Gag, a multimerizing protein, associates with uropod-specific microdomains that carry Gag to the uropod. However, the mechanism by which these microdomains localize to the uropod remains unclear. It is important to note that not all types of microdomain are destined for the uropod. GM3-containing lipid rafts have been shown to localize to the leading edge [60, 118, 152]. Therefore it is likely that there are complex sorting mechanisms by which specific subsets of microdomains are moved to the uropod. In this regard, it is of note that although LFA-1 behaves as a leading edge/non-uropod marker in T cells in suspension [153] (this study), this adhesion molecule redistributes to mid-cell and uropod regions

upon contact with ICAM-1-containing surfaces [154, 155]. Therefore, LFA-1 in infected cells may still modulate uropod-mediated T-cell-T-cell contacts upon encountering ICAM-1-bearing target cells, which would be in agreement with previous studies [96, 103].

While live cell analyses showed that patches of Gag laterally move to the uropod as cells re-polarize, they do not rule out the possibility that in an already polarized cell, *de novo* assembly of viruses preferentially occurs at the uropod or the cell contact without the lateral movement of Gag clusters. A recent study showed that MLV, another retrovirus, preferentially forms particles at contact sites in HEK293 cells [88]. This observation indicates that the site of retrovirus assembly can be polarized upon cell-cell contact formation in otherwise unpolarized cells. Notably, the polarized budding of MLV in HEK293 cells was found to be dependent on the MLV Env cytoplasmic tail. Similarly, the cytoplasmic tail of HIV-1 Env was reported to be important for polarized HIV-1 Gag localization in Jurkat T cells that appeared morphologically unpolarized [156]. In contrast, in this chapter, it was found that in the absence of Env or cell-cell contact, Gag-YFP remained efficiently localized to the uropod in polarized T cells, including P2 and primary $CD4^+$ T cells (Figures 2.1G and 2.7; data not shown). Therefore, it is possible that in T cells with a high propensity to establish front-rear polarity, Gag may not require Env or cell-cell contact to achieve polarized assembly. Further studies will determine the molecular mechanisms by which assembly sites for retroviruses are polarized in different cell types.

Although Env was dispensable for Gag localization to the uropod, formation of stable cell conjugates as well as virus transfer have been shown to require Env-receptor

interaction [53, 67, 68, 78, 80, 132]. Consistent with these findings, an anti-CD4 blocking antibody (Leu3A) diminished cell-to-cell virus transfer (Figure 2.5) and prelabeling infected P2 cells with an anti-Env antibody (b12) reduced formation of cell conjugates with SupT1 cells (data not shown). Therefore, while uropods are enriched in adhesion molecules and form contacts with other cells frequently [49] regardless of the presence of Env, the Env-CD4 interaction is likely to stabilize such contacts during formation of the VS.

In summary, this chapter elucidates a series of molecular events leading to the formation of a VS. The observations made have led to the formation of a working model (Figure 2.12) in which higher-order multimerization, or clustering, mediated by NC is required for Gag association with uropod-specific microdomains. This microdomain association then facilitates localization of the assembling virus to the uropod. According to this model, the uropod, laden with HIV-1 components and particles, then serves as a pre-formed platform that mediates contact with target cells (Figure 2.12A) or redistributes to contacts formed elsewhere (Figure 2.12B). Such contacts could then constitute a VS, which likely facilitates cell-to-cell virus transfer of HIV-1.

Materials and Methods

Plasmids

The HIV-1 molecular clone pNL4-3 [157] and its derivatives encoding Gag-YFP and Gag-CFP fusion proteins (pNL4-3/Gag-YFP/-CFP) [11, 28] were described previously. The latter two constructs contain an extensive deletion of *pol* and silent mutations to reduce ribosomal frameshift to the *pol* reading frame and does not express Vif or Vpr. For YFP and CFP, monomeric Venus [158, 159] and monomeric Cerulean [160] variants were used, respectively. pNL4-3/WM184,185AA/Gag-YFP/-CFP (renamed as pNL4-3/WMAA/Gag-YFP/-CFP), pNL4-3/delCA-CTD/Gag-YFP/-CFP, pNL4-3/14A1G/Gag-YFP/-CFP, pNL4-3/delNC/Gag-YFP/-CFP and the Fyn(10)-modified versions of those plasmids were previously described [28]. In this study, pNL4-3/Fyn(10)fullMA/GagVenus described previously [11, 28] was renamed as pNL4-3/Fyn(10)/Gag-YFP for simplicity. pNL4-3/Fyn(10)/ΔMA/Gag-YFP was previously described [11]. pNL4-3/KFS/Gag-YFP was generated by cloning the XhoI-SalI fragment of pNL4-3-KFS (a kind gift from Dr. Eric Freed [161]) into pNL4-3/Gag-YFP. To construct pNL4-3/LZ/Gag-YFP/-CFP, the sequence encoding GCN4 leucine zipper in the ZWT plasmid, a kind gift from Dr. Heinrich Gottlinger [142], was cloned into pNL4-3/Gag-YFP/-CFP using standard molecular cloning techniques. The double mutants pNL4-3/Fyn(10)/WMAA/LZ/Gag-YFP/-CFP and pNL4-3/Fyn(10)/delCA-CTD/LZ/Gag-YFP/-CFP were generated by cloning a fragment containing the leucine zipper sequence from pNL4-3/LZ/Gag-YFP into pNL4-3/Fyn(10)/WMAA/Gag-YFP/-CFP and pNL4-3/Fyn(10)/delCA-CTD/Gag-YFP/-CFP, respectively. pNL4-3/Gag-iGFP (a kind gift from Dr. Benjamin Chen [99]) was used to construct pNL4-3/Gag-iYFP.

Virus Stocks

Stocks of HIV-1 mutants, pseudotyped with vesicular stomatitis virus G protein (VSV-G), were prepared by transfecting $5.6x10^5$ 293T or HeLa cells with 1.5 μg pNL4-3 derivative encoding a Gag-YFP/-CFP fusion protein, 1.5 μg pCMVNLGagPol-RRE [105], and 0.5 μg pHCMV-G (a kind gift from Dr. J. Burns [162]). Two days post transfection, virus-containing supernatants were filtered through a 0.45 μm filter and used for inoculation of T cells.

Cells

To prepare a polarized T cell line, T cell clones were obtained by limiting dilution of A3.01 T cells (AIDS Research and Reference Reagent Program). Typical A3.01 cell cultures naturally contain 10-20% of cells with a polarized morphology. After limiting dilution, T cell clones were examined for cell morphology and polarized PSGL-1 localization. A cell clone, in which approximately 50-60% of cells were polarized, was designated "P2" and used for experiments. These cell lines, as well as the SupT1 cell line (AIDS Research and Reference Reagent Program), were cultured in RPMI containing 10% fetal bovine serum (FBS)(RPMI-10%FBS). Primary T cells were isolated from buffy coats obtained from the New York Blood Center. The buffy coats were diluted in a 1:1 ratio with phosphate buffered saline (PBS) containing 2% FBS (PBS-2%FBS), and peripheral blood mononuclear cells (PBMCs) were isolated using centrifugation through ficoll (GE Healthcare) according to the manufacturer's instructions. Isolated PBMCs were then plated on polystyrene petri dishes for 2 h to separate the adherent monocytes and non-adherent lymphocytes. Lymphocytes were activated in RPMI-10%FBS

containing phytohemagglutinin (PHA) (Sigma. St. Louis, MO) (6 μg/ml) and IL-2 (20 units/ml) (Roche. Basel, Switzerland) for 2-3 days. Primary $CD4^+$ T cells were isolated with the MACS magnetic antibody bead kit (Miltenyi Biotec. Bergisch Gladbach, Germany) using anti-CD4 beads and MS columns. Cells were then cultured overnight in RPMI-10%FBS and IL-2 (20 units/ml) and used for experiments. IL-2 has been shown to induce a comparable level of T cell polarization and locomotion to those induced by chemokines such as RANTES and MIP-1α [163, 164].

Infection

Cells were infected with virus stocks by spin infection; $3x10^5$ P2 cells or $5x10^5$ primary T cells were resuspended in 200 μl virus stock with 4 μg/ml polybrene and centrifuged at 2500 rpm for 2 h at 15°C. Cells were cultured at 37°C in RPMI-10% FBS for 2-3 days (in the presence of 20 units/ml IL-2 for primary T cells).

Copatching Assay

Mouse anti-PSGL-1, CD43, CD81, or LFA-1 (all from BD Biosciences Pharmingen. San Diego, CA) were prelabeled with the secondary antibody (AlexaFluor-594-conjugated goat anti-mouse IgG (Invitrogen. Carlsbad, California)) for 30 min. Infected cells were cultured in 200 μl of RPMI-10%FBS containing this antibody mixture for 1 h at 37°C, after which they were washed with RPMI-10%FBS and fixed in 1ml 4% paraformaldehyde in PBS (PFA). After washing with PBS-2%FBS, cells resuspended in a small volume (~10 μl) of the same buffer were mixed with equal volume of Fluoromount-G (SouthernBiotech. Birmingham, Alabama), and 3 μl of this mixture was

mounted on glass slides. Images were acquired with a Nikon TE-2000U inverted epifluorescence microscope. Z-series of images were acquired with 0.2 μm intervals between focal planes. Maximum intensity projection images of the z-series images composed of 56 focal planes were obtained with ImageJ software (NIH; downloaded from http://rsbweb.nih.gov/ij/). Copatching quantification was performed using the correlation plot function of the Metamorph 6 software (Molecular Devices. Sunnydale, California). To identify punctate signals objectively and to remove background signals from copatching analyses, the background, calculated as the median intensity of a 32x32-pixel region surrounding each pixel, was subtracted from the original image [165], point noise was removed using a 3x3 median filter [166], and the minimum threshold was set to twice the average fluorescence intensity of the cell of interest and applied to the images. These images were then used for calculation of Pearson's correlation coefficients (CC), representing copatching. Person's correlation coefficients between 0.5 and 1 represent moderate to very strong correlation, between 0 to 0.5 represents low to moderate correlation with 0 representing random distribution, and below 0 represents segregation of the two signals.

Immunostaining

To avoid altering cell morphology, cell suspensions were placed in round-bottom tubes and left still at 37ºC in the presence of 5% CO_2 for at least 1 h prior to fixation. Subsequently, most of the culture supernatant was removed carefully, and cells were fixed in 1ml 4% PFA for 20 minutes. Fixed cells were washed with PBS-2%FBS and then incubated for 1 h in PBS-2%FBS containing primary antibodies against cell surface

molecules (PSGL-1 and LFA-1) followed by washing with PBS-2%FBS. For experiments in which CD43 was used as a uropod marker, cells were first incubated with anti-CD43 for 30 min as done in previous studies [64]. Subsequently, cells were rinsed with RPMI-10%FBS twice, incubated with AlexaFluor 594-conjugated anti-mouse IgG for 30 min, rinsed with RPMI-10%FBS twice, and cultured for an additional 30 min at 37ºC prior to fixation. Detection of Env on the cell surface was performed similarly, except that primary and secondary antibodies used were anti-gp120 (IgG1 b12; AIDS Research and Reference Reagent Program) and AlexaFluor-594-conjugated anti-human IgG (Invitrogen), respectively. For detection of α-tubulin (to identify the MTOC) and mature p17MA, fixed cells were permeabilized by a 10-min incubation in PBS containing 0.2% saponin (Fluka Biohemica. Buchs, Switzerland) and 5% FBS prior to incubation with primary antibodies, anti-α-tubulin (Sigma; clone B-5-1-2) and anti-p17MA (Applied Biotechnologies. Columbia, Maryland), respectively. Primary antibodies were detected by treating cells with AlexaFluor 594-conjugated goat anti-mouse IgG for 30 minutes. Cells were then washed again with PBS-2%FBS and mounted on glass slides, as described above, for microscopy.

Live Cell Microscopy

Cells were infected with VSV-G-pseudotyped HIV-1 encoding Gag-YFP. Two days post-infection, cells were immunostained with anti-PSGL1 prelabeled with the Zenon AlexaFluor 594 reagent (Invitrogen) according to manufacturer's instruction or AlexaFluor 594-conjugated anti-mouse IgG as described for the copatching assay. To morphologically depolarize cells, 4-well chamber coverslips (Nunc. Rochester, NY),

containing Gag-YFP-expressing cells, were placed at 4°C for 30 min. To repolarize cells, the chamber coverslips were then transferred to a pre-warmed (37°C) microscope stage. Time-lapse images were acquired with an interval of 30 s for up to 1 h. The images were then converted to AVI files by ImageJ.

Fluorescence Resonance Energy Transfer (FRET) Analysis

Cells were co-infected with VSV-G-pseudotyped HIV-1 encoding YFP- and CFP-tagged versions of each Gag mutant, cultured and fixed as described above. Cells were subsequently permeabilized, immunostained for α-tubulin, and mounted as described above. Images were collected using four filter combinations: AlexaFluor 594 excitation/AlexaFluor 594 emission, YFP excitation/YFP emission, CFP excitation/CFP emission, and CFP excitation/YFP emission. FRET was calculated using FRET stoichiometry as previously described [28, 167].

Analysis of Cell-cell Contact and VS

$5x10^5$ primary $CD4^+$ T cells were infected with VSV-G pseudotyped HIV-1 encoding Gag-YFP or KFS/Gag-YFP. Two days post infection, $5x10^5$ fresh primary $CD4^+$ T cells were stained with 1 μM CMAC (Invitrogen) for 30 min. Infected T cells were then co-cultured with CMAC-stained target T cells for 3 h in a chamber coverslip at 37°C. Images of 50-60 polarized and YFP-expressing cells were then acquired, and the number of contacts these cells formed with CMAC-labeled cells, which represent newly formed contacts, were quantified and categorized as uropod- or non-uropod-mediated contacts. For analysis of the VS, $2x10^5$ P2 cells were infected with VSV-G-pseudotyped

HIV-1 encoding Gag-CFP. Two days post-infection, cells were immunostained with anti-CD43 and a minimal amount of AlexaFluor-594-conjugated anti-mouse IgG. After extensive washing, $1x10^5$ of these cells or the same number of uninfected P2 cells were mixed with $1x10^5$ target cells (SupT1 cells) that were prelabeled with non-blocking FITC-conjugated anti-CD4 (Clone L120, BD Biosciences. San Jose, California) and cocultured for 3 h in chamber coverslips at 37°C. These cocultures in the chamber coverslips were placed on a microscope stage set at 37ºC, and images were acquired using appropriate excitation and emission filters.

Cell-to-Cell Virus Transfer Assay

$2x10^5$ P2 cells were infected with VSV-G-pseudotyped HIV-1 encoding Gag-YFP. Two days post-infection, $5x10^5$ target SupT1 cells were stained with 1 μM CellTracker CMTMR (Invitrogen. Carlsbad, California) for 15 min, washed with RPMI-10%FBS, incubated for 2 h in RPMI-10%FBS, and washed again in RPMI-10%FBS. Infected donor and CMTMR-stained target cells were cocultured in 0.5 ml RPMI-10%FBS for 3 h in the presence or absence of the myosin light chain kinase (MLCK) inhibitor, ML7 (40 μM) (EMD Biosciences. San Diego, California), or the solvent negative control DMSO. The CD4 blocking antibody Leu3A (0.25 μg/ml) (BD Biosciences) and isotype anti-mouse IgG control antibody (0.25 μg/ml) (Santa Cruz Biotechnology. Santa Cruz, California) were utilized to validate the assay, as it was shown previously using a similar assay that virus transfer was dependent on Env-CD4 interaction [53](Figure 2.4A). To rule out the possibility that inhibitors affect viral protein synthesis and thereby indirectly alter virus transfer, 10 μg/ml cycloheximide,

which abolishes protein synthesis, was added at the beginning of coculture. After 3 h of coculture, cells were fixed in 4% PFA. Double-positive cells, which represent CMTMR-positive target cells that received YFP-containing virus particles, were identified by flow cytometry (see Figure 2.4A for examples). Results were presented as a percentage of double-positive cells compared to total CMTMR-stained target cells.

Quantification of Polarization

To measure morphological polarization of T cells, outlines of Gag-YFP-expressing P2 cells were determined by manually tracing the cell perimeter using the ImageJ program. Circularity values were then calculated based on this outline using the Measure function of ImageJ. The output values range between 0 and 1, with 1 representing a perfect circle. This method has been described previously [168]. Morphologically polarized cells with circularity values below 0.8 were further examined for polarization of Gag localization. To quantify polarity of Gag localization, a 10-segmented grid was placed over each cell along the cell's longest axis. The number of segments that contained plasma-membrane-associated Gag was then used as the polarization index. Lower values correspond to more polarity of Gag on the cell surface. Examples of these quantifications are shown in supplementary Figure 2.S4.

Figure 1

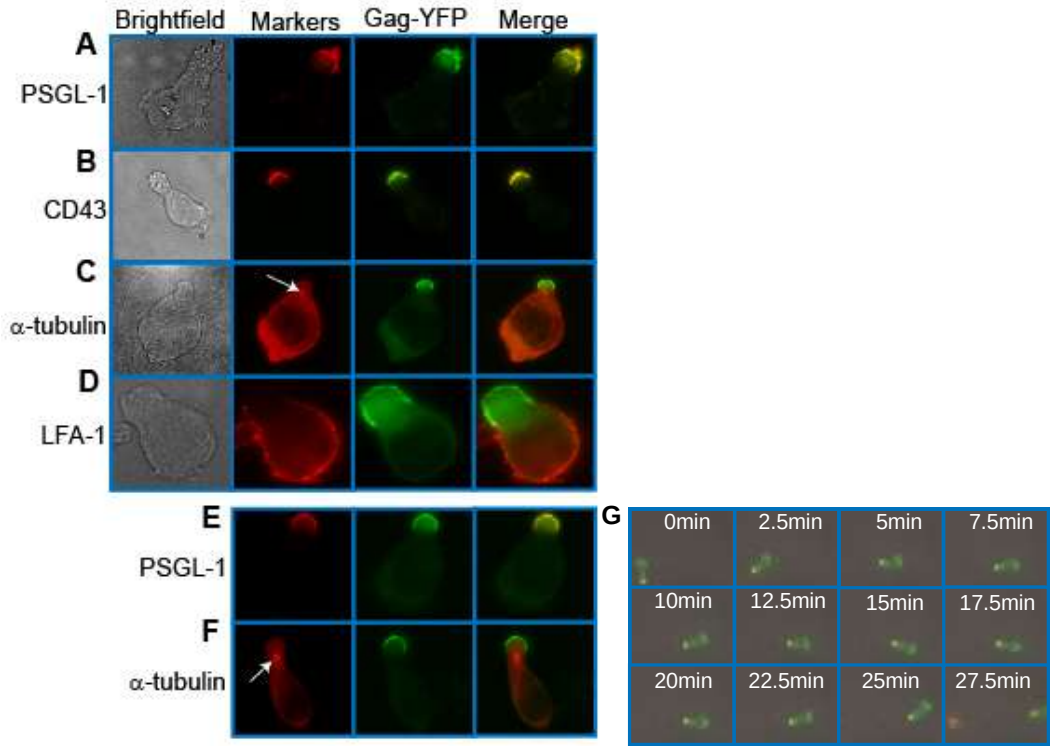

Figure 2.1. Gag stably localizes to the uropod in polarized T cells.
Primary T cells **(A-D)** and P2 cells **(E-F)** expressing Gag-YFP (green) were immunostained for uropod and non-uropod markers as described in the Materials and Methods section, and observed using an epifluorescence microscope. Uropods were identified by the presence of PSGL-1 **(A** and **E)** and CD43 (**B**) as well as by the location of the MTOC determined by immunostaining with anti-α-tubulin **(C** and **F**, arrows**)**. LFA-1 **(D)** is a known non-uropod marker and served as a negative control. **G)** Cells expressing Gag-YFP (green) were immunostained with anti-PSGL-1 prelabeled by AlexaFluor-594-conjugated anti-mouse IgG (red). Images were acquired every 30 s for 30 min as the polarized cell migrates through the field. Yellow color indicates colocalization of PSGL-1 and Gag-YFP.

	Gag-Expressing Cells			Non-Gag-Expressing Cells		
	Polarized (% of total)	Unpolarized (% of total)	Total	Polarized (% of total)	Unpolarized (% of total)	Total
Primary $CD4^+$ T cells	253 (64.4%)	140 (35.6%)	393	530 (56.6%)	406 (43.4%)	936
P2 cells	176 (51.9%)	163 (48.1%)	339	97 (47.1%)	109 (52.9%)	206

Table 2.1. Quantification of T cell Polarization.
Primary $CD4^+$ T cells and P2 cells infected with VSV-G-pseudotyped HIV-1 encoding Gag-YFP were cultured for two days, fixed, immunostained for cellular proteins, and examined by fluorescence microscopy. Gag-YFP-positive and -negative cells were categorized based on cell morphology, and cells in each category were counted. Cells with circularity below 0.8 (see Materials and Methods) were categorized as polarized cells.

	Marker	Gag Polarized		Gag Not Polarized	Total Cell Number
		Copolarized with Marker	Not Copolarized with Marker		
Primary $CD4^+$ T cells	PSGL-1	96%	2%	2%	58
	CD43	100%	0%	0%	58
	MTOC	96%	1%	3%	69
	LFA-1	13%	86%	1%	69
P2 cells	PSGL-1	79%	19%[a]	2%	63
	MTOC	83%	9%[b]	8%	111

Table 2.2. Copolarization of Gag with Cellular Markers.
Primary $CD4^+$ T cells and P2 cells infected with VSV-G-pseudotyped HIV-1 encoding Gag-YFP were cultured for two days, immunostained for cellular proteins, and examined by fluorescence microscopy (see Materials and Methods). Gag-YFP-positive cells that were categorized as polarized cells based on cell morphology were further examined for polarized localization of Gag-YFP and copolarization of Gag-YFP with cellular markers.

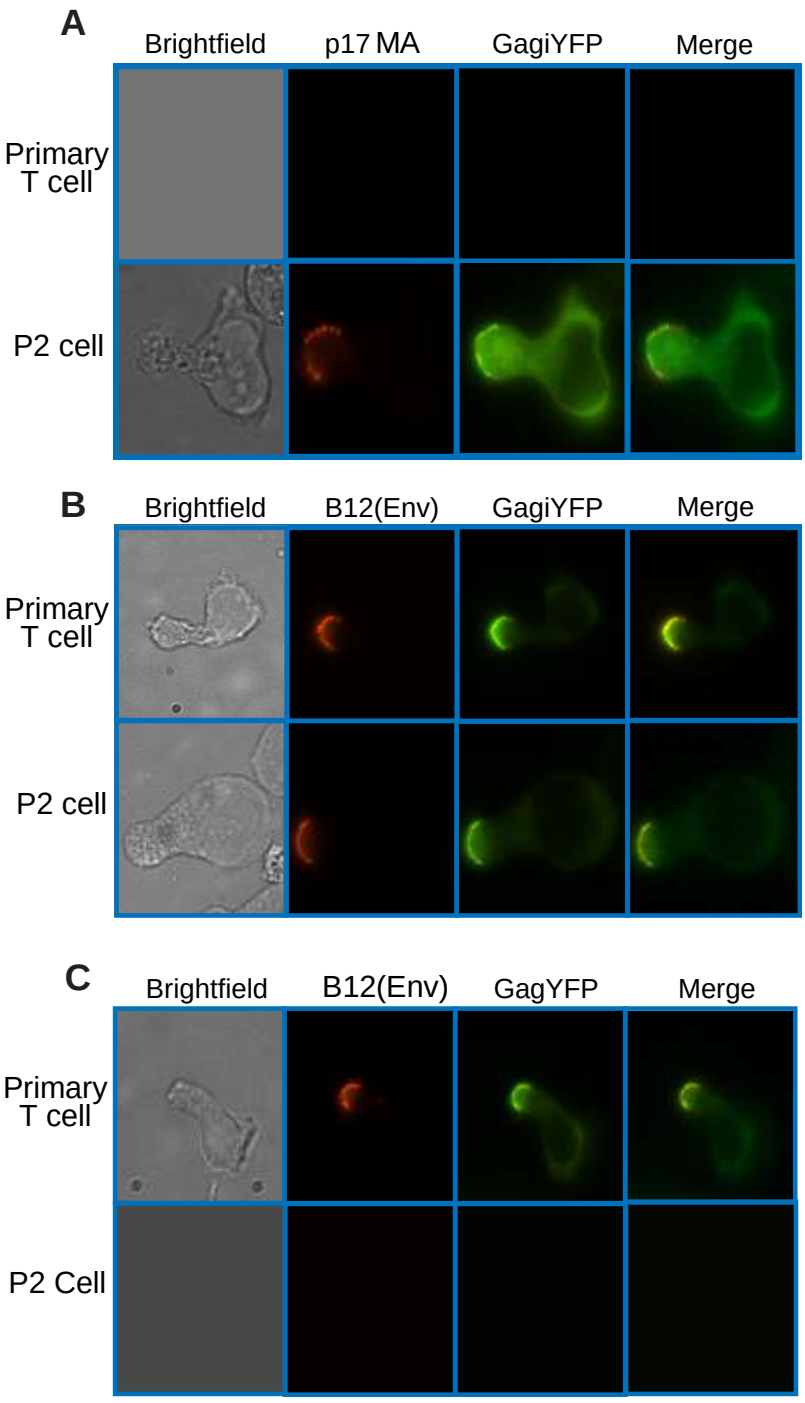

Figure 2.2. Mature Gag and Env localize to the uropod.
Primary $CD4^+$ T cells and P2 cells were infected with a VSV-G-pseudotyped HIV-1 encoding Gag-iYFP (green) (**A** and **B**) or Gag-YFP (green) (**C**). **A**) For detection of mature Gag, cells were fixed, permeabilized, and immunostained with anti-p17MA (red) as described in Materials and Methods and observed with an epifluorescence microscope. **B)** and **C)** For detection of Env on the cell surface, infected cells were incubated with anti-gp120 (IgG1 b12) and subsequently with AlexaFluor-594-conjugated anti-human IgG prior to fixation as described in Materials and Methods.

YFP-Tagged Gag	Antibody	Cell Type	YFP colocalized with antibody signal	YFP not colocalized with antibody signal	Total Cell Number
Gag-iYFP	Anti-p17MA	Primary $CD4^+$ T cells	92%	8%	51
		P2 cells	88%	12%	52
	Anti-gp120 (b12)	Primary $CD4^+$ T cells	92%	8%	50
		P2 cells	92%	8%	61
Gag-YFP	Anti-gp120 (b12)	Primary $CD4^+$ T cells	91%	9%	56
		P2 cells	93%	7%	75

Table 2.3. Colocalization of YFP-Tagged Gag with Antibody-Detected Viral Proteins

Primary $CD4^+$ T cells and P2 cells infected with VSV-G-pseudotyped HIV-1 encoding Gag-iYFP or Gag-YFP were cultured for two days, immunostained for viral proteins, and examined by fluorescence microscopy. YFP-positive polarized cells were examined for colocalization of the cell surface YFP-tagged Gag proteins and viral antigens detected by anti-p17MA or anti-gp120 (b12).

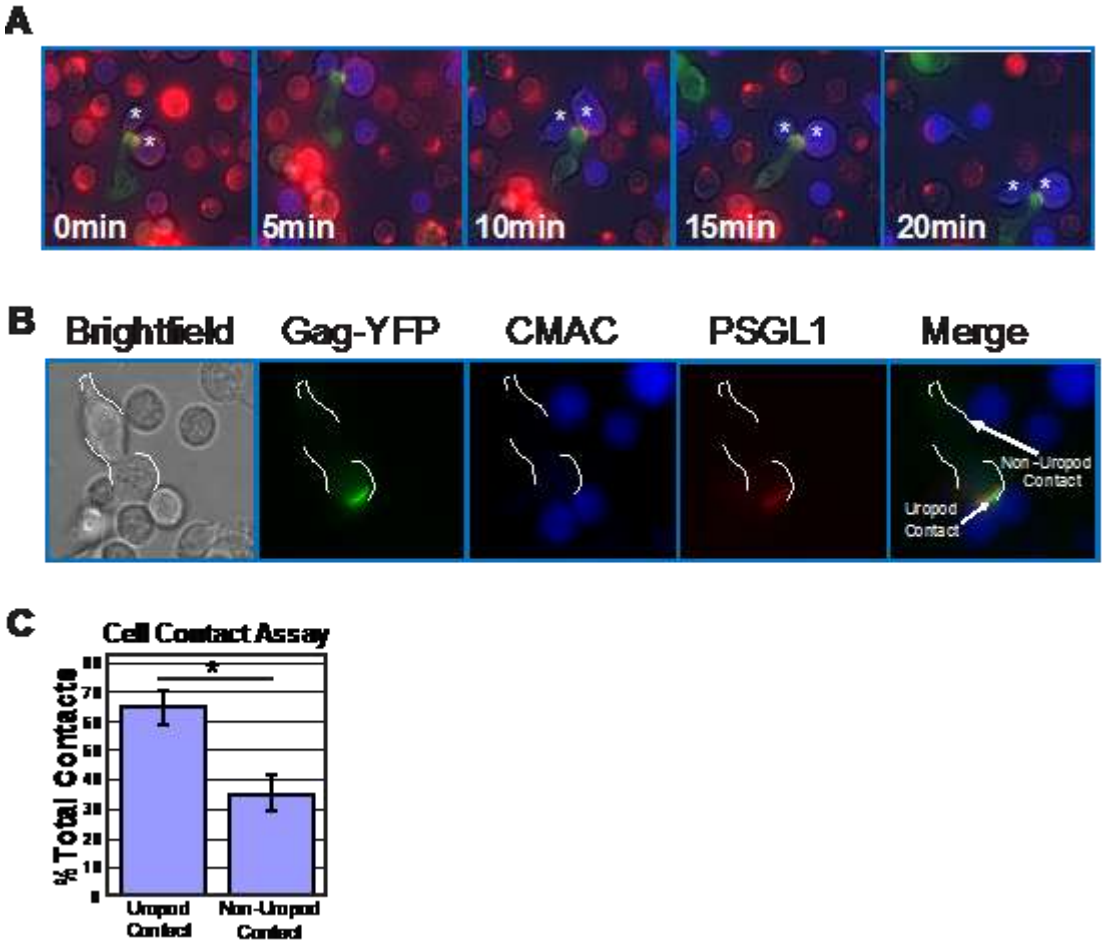

Figure 2.3. Infected polarized T cells form contacts with target cells via their uropods.

A) Primary T cells expressing Gag-YFP (green) were immunostained with an anti-PSGL-1 antibody (red) as described in Figure 2.1G and cocultured with fresh primary T cells from the same donor stained with the fluorescent dye CMAC (blue). Regions of colocalization between Gag and PSGL-1 are shown in yellow. Live cell images were taken every 30 s for 20 min. A series of images with 5-min intervals is shown. Note that the uropod, enriched in Gag-YFP and PSGL-1, mediates stable contacts with target cells (*). **B)** Examples of uropod- and non-uropod-mediated contacts between a Gag-YFP expressing primary T cell (dotted white outline) with CMAC-labeled primary T cells are shown. **C)** Uropod-mediated and non-uropod-mediated contacts were counted for a total of 74 polarized Gag-YFP-positive cells contacting CMAC-labeled cells in two independent experiments. P values were determined using Student's t test. *, $P<0.05$.

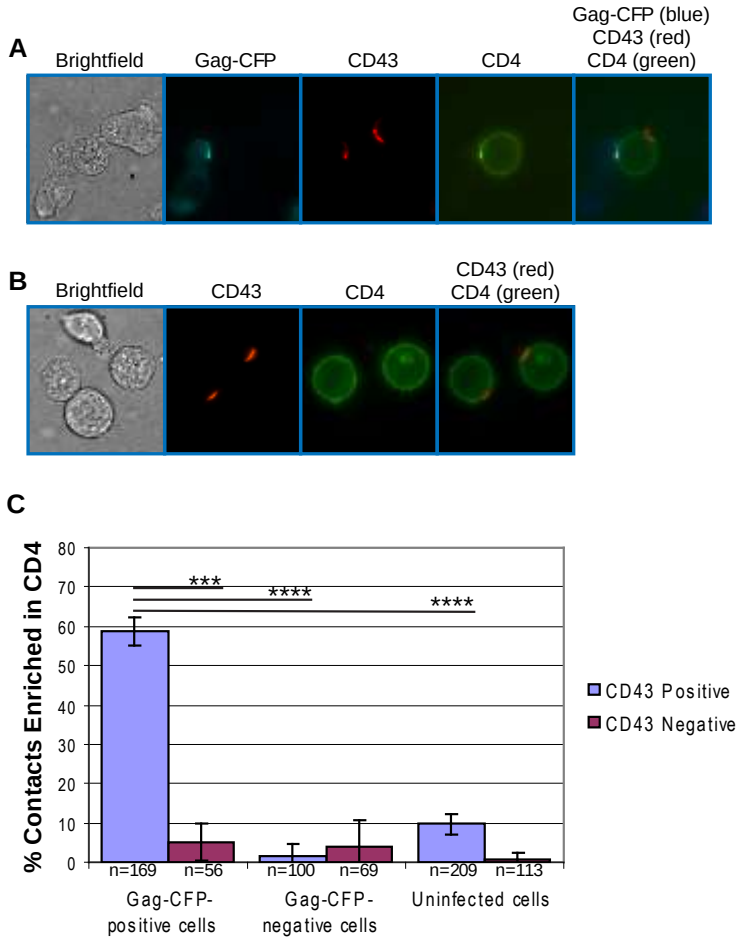

Figure 2.4. Gag-positive uropods form contacts enriched in CD4.
A) P2 cells expressing Gag-CFP (cyan; pseudo-colored in blue in the merge panel) were immunostained with anti-CD43 and AlexaFluor-594-conjugated anti-mouse IgG (red). Subsequently, these cells were cocultured with SupT1 cells prelabeled with FITC-conjugated anti-CD4 (green) for 3 h and examined by live cell microscopy. A target cell (center) in contact with both Gag-CFP-positive (left) and Gag-CFP-negative (right) cells is shown. **B**) Uninfected P2 cells were immunostained with anti-CD43 and co-cultured with SupT1 cells prelabeled for CD4 as done in (A). **C)** In experiments represented in panels A and B, junctions between target SupT1 cells and Gag-CFP-expressing, non-Gag-CFP-expressing, or uninfected P2 cells were classified into uropod-mediated and non-uropod-mediated contacts based on the presence of CD43. The percentage of contacts with accumulation of CD4 relative to total contacts was determined for each category. Data from three independent experiments were shown as means +/-standard deviation. P values were determined using Student's t test. ***, $P<0.001$; ****, $P<0.0001$. Numbers of contacts detected and examined for CD4 accumulation in each of these three experiments are: Gag-CFP-positive/CD43-positve contacts, 56, 56, 57 (total 169); Gag-CFP-positive/CD43-negative contacts, 21,17,18 (total 56); Gag-CFP-negative/CD43-positive contacts, 26, 35, 39 (total 100); Gag-CFP-negative/CD43-negative contacts, 17, 24, 28 (total 69); uninfected/CD43-positve contacts, 56, 67, 86 (total 209); and uninfected/CD43-negative contacts, 20, 38, 55 (total 113).

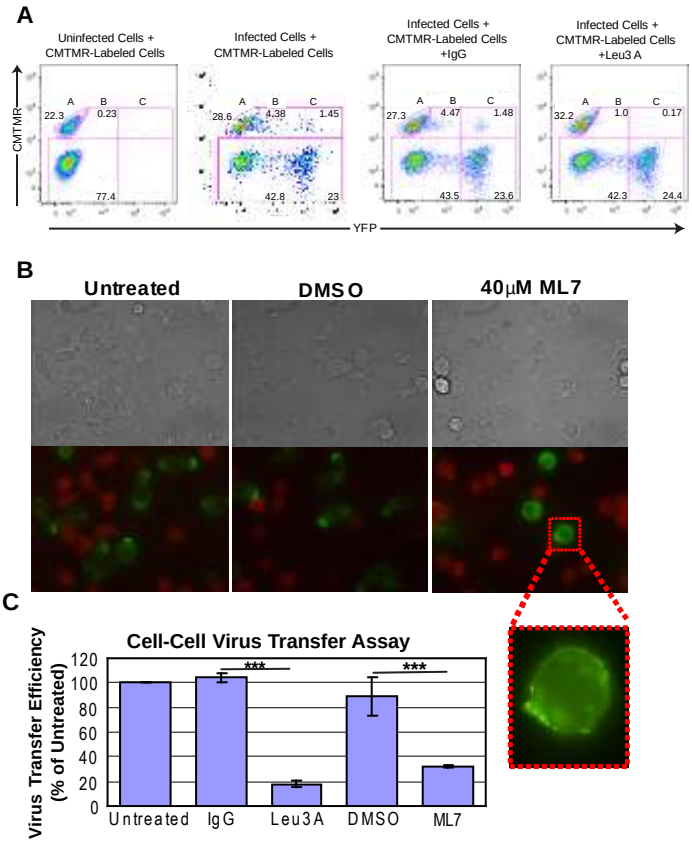

Figure 2.5. ML7 depolarizes cell morphology and Gag localization and reduces cell-to-cell transfer of Gag-YFP.

A) Transfer of Gag-YFP fluorescence from infected P2 cells to CMTMR-stained SupT1 target cells during a 3-h coculture period was measured by flow cytometry. ML7, DMSO, or antibodies, along with 10 μg/ml cycloheximide, were added at the beginning of the coculture period. Flow cytometry plots for CMTMR-labeled target cells co-cultured with uninfected cells as well as CMTMR-labeled target cells cocultured with Gag-YFP-expressing infected cells in the presence or absence of IgG or Leu3A are shown. Gate A, CMTMR-labeled target cells; gate B, double positive cells representing target cells with transferred Gag-YFP particles; and gate C, YFP-expressing cells either fused or conjugated to CMTMR-labeled target cells. **B)** Images of cycloheximide-treated P2 cells expressing Gag-YFP were acquired after 3-h coculture with CMTMR-stained SupT1 cells in the presence or absence of DMSO or ML7. Note that almost all the cells adopt round unpolarized morphology upon treatment with ML7 and that ML7-treated infected cells show dispersed Gag-YFP localization. The latter point is clearer in the higher magnification image (bottom panel) of a region specified in the middle row. Also note that the cell density of the cocultures in experiments shown in panel A (images shown in supplementary Figure 2.S3 and discussed in the supplementary text) is 10 fold higher than in panel B. **C)** Relative efficiencies of cell-to-cell virus transfer were calculated as the percentage of double positive cells out of the total CMTMR-labeled cells (Virus transfer efficiency=B/(A+B+C)*100; error bars represent standard deviation). P values were determined using Student's t test. ***, $P<0.001$.

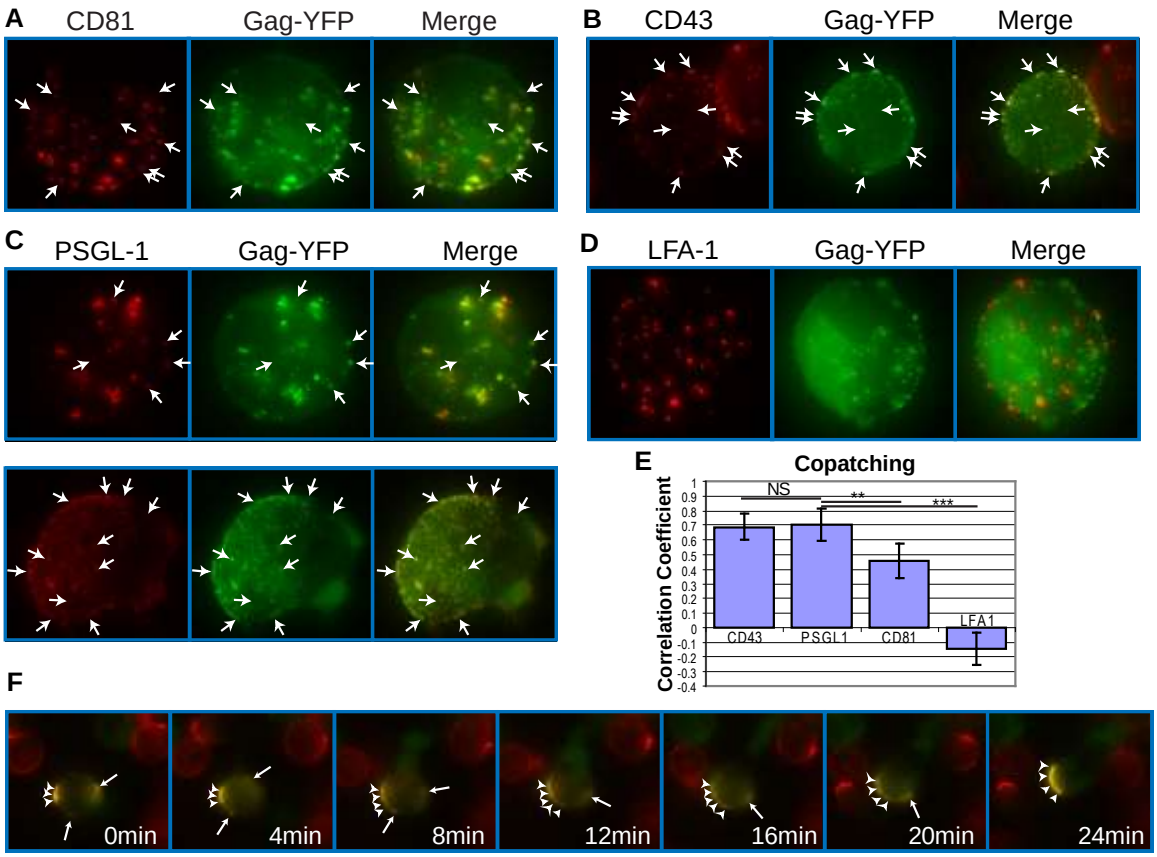

Figure 2.6. Gag associates with uropod-specific microdomains that carry Gag to the uropod.

Unpolarized P2 cells expressing Gag-YFP (green) were examined for copatching with CD81 **(A)**, CD43 **(B)**, PSGL-1 **(C)**, or LFA-1 **(D).** Cells were incubated with specific primary mouse monoclonal antibodies premixed with the fluorescent secondary antibody (red) followed by fixation. Z series of images of morphologically unpolarized cells were acquired and used to generate maximum projection images of each color using Metamorph 6 software. Merged images are shown in the right column of each panel. Several small copatching puncta are indicated by arrows. **E)** Quantification of copatching. Correlation coefficients between Gag-YFP and cell surface marker signals were calculated from a total of 18 cells for each marker. A value of 1 represents perfect colocalization, a value of -1 represents complete segregation, and a value of 0 represents a random distribution. P values were determined using Student's t test. NS, not significant. **, P<0.01. ***, P<0.001. **F)** Time lapse images of a Gag-YFP-expressing T cell during repolarization. Gag-YFP(green)-expressing P2 cells were immunostained for PSGL-1 (red) as described for panels A-D. Cells were then depolarized by incubation at 4°C for 30 min. Approximately 5 min after chamber coverslips containing depolarized cells were transferred to the microscope stage maintained at 37°C, acquisition of live cell images at indicated time points was begun. Note that the small patches (arrows) migrate and coalesce to the large patch (arrowheads) at the cell pole that eventually forms the uropod.

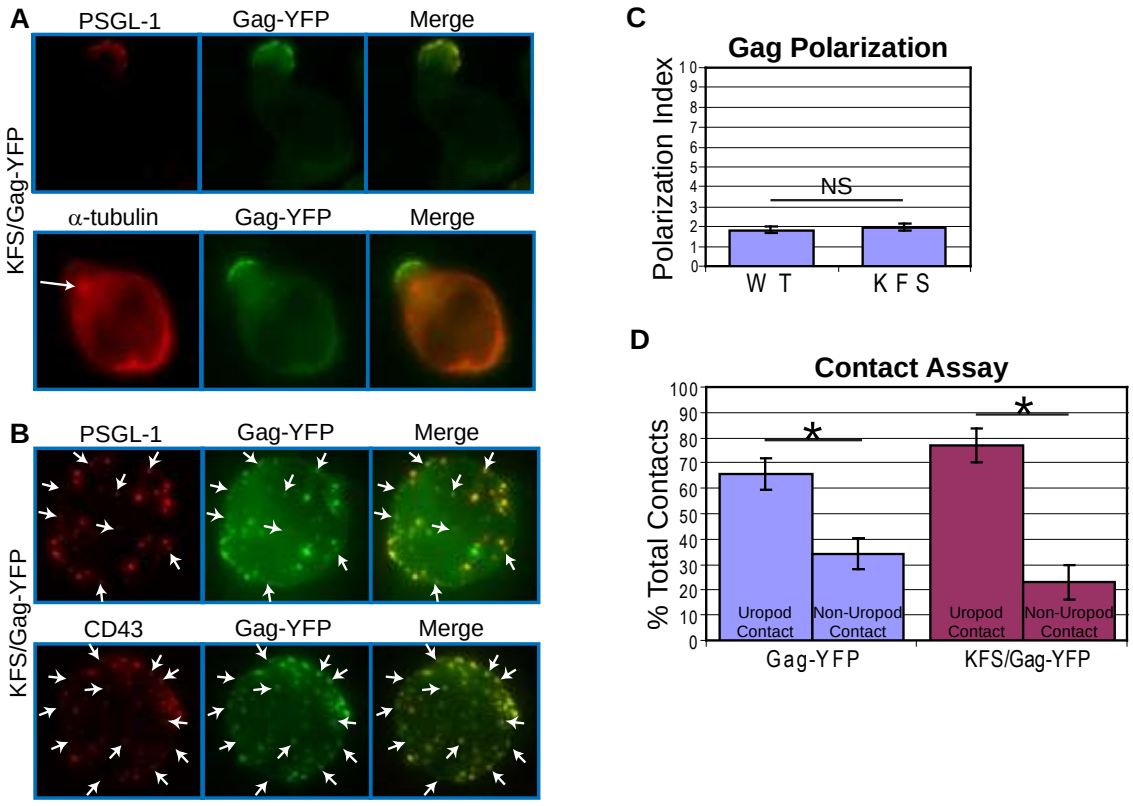

Figure 2.7. Env is not required for Gag localization to the uropod.
A) P2 cells expressing KFS/Gag-YFP (green) were immunostained after fixation with anti-PSGL-1 (red, upper panel) or anti-α-tubulin (red, lower panel, arrow indicates MTOC) as described for Figure 2.1. **B)** KFS/Gag-YFP-expressing P2 cells were immunostained for PSGL-1 or CD43 (red) using the co-patching method as described for Figure 2.6, and Z-series of images of unpolarized cells were acquired. Maximum projections of each color were generated from the Z stacks and merged to examine colocalization (yellow). Several small copatching puncta are indicated by arrows. **C)** The Gag polarization index was determined as described in the Materials and Methods section for cells expressing Gag-YFP and KFS/Gag-YFP. Four separate experiments (32, 23, 39, and 37 cells each) for a total of 131 cells for Gag-YFP and 3 separate experiments (34, 48, and 30 cells each) for a total of 112 cells for KFS/Gag-YFP were used for quantification of Gag polarization. P values were determined using Student's t test. NS, not significant. **D)** Cell-cell contact assays were performed as in Figure 2.3. This graph compares the results of Figure 2.3 to the results obtained with cells expressing KFS/Gag-YFP, which had been obtained concurrently. P values were determined using Student's t test. *, $P<0.05$.

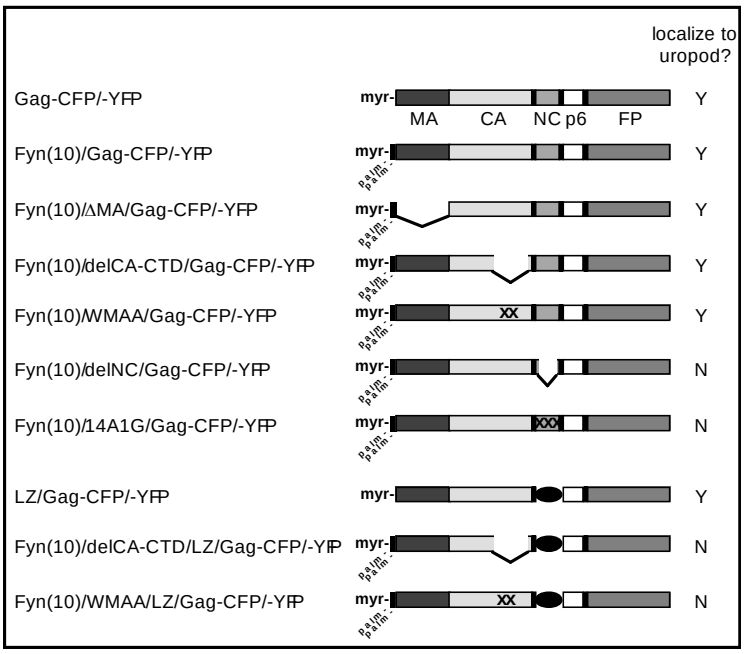

Figure 2.8. Gag derivatives used in this study and their localization pattern.
HIV-1 molecular clones that express Gag-fluorescent protein fusions (WT Gag-YFP/-CFP) were generated. Deletions or amino acid substitutions were created in the MA domain (Fyn(10)/ΔMA/Gag-YFP/-CFP), CA domain (Fyn(10)/delCA-CTD/Gag-YFP/-CFP and Fyn(10)/WMAA/Gag-YFP/-CFP) and the NC domain (Fyn(10)/delNC/Gag-YFP/-CFP, Fyn(10)/14A1G/Gag-YFP/-CFP and LZ/Gag-YFP/-CFP). Gag derivatives containing LZ replacement of NC combined with the CA mutations were also used (Fyn(10)/delCA-CTD/LZ/Gag-YFP/-CFP and Fyn(10)/WMAA/LZ/Gag-YFP/-CFP). The Fyn(10) sequence, a single myristoylation and dual palmitoylation signal, was added to the N terminus of all Gag derivatives except WT Gag-CFP/-YFP and LZ/Gag-CFP/-YFP. Results as to whether these Gag derivatives localize specifically to the uropod (Y) or distribute over the entire cell surface (N) are summarized in the right column.

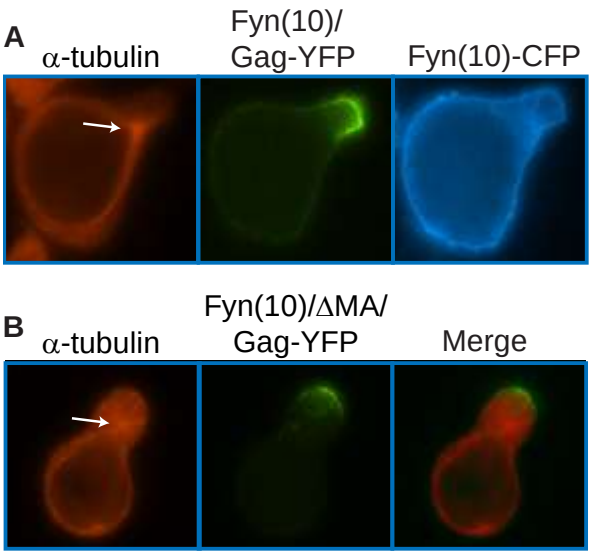

Figure 2.9. The MA sequence is not required for Gag localization to the uropod.
A) P2 cells were co-transfected with plasmids that express Fyn(10)/Gag-YFP (green) and Fyn(10)-CFP (blue). Cells were then stained for α-tubulin (red, arrow indicates MTOC). **B)** Cells expressing Fyn(10)/ΔMA/Gag-YFP (green) were immunostained with anti-α-tubulin (red, arrow indicates MTOC).

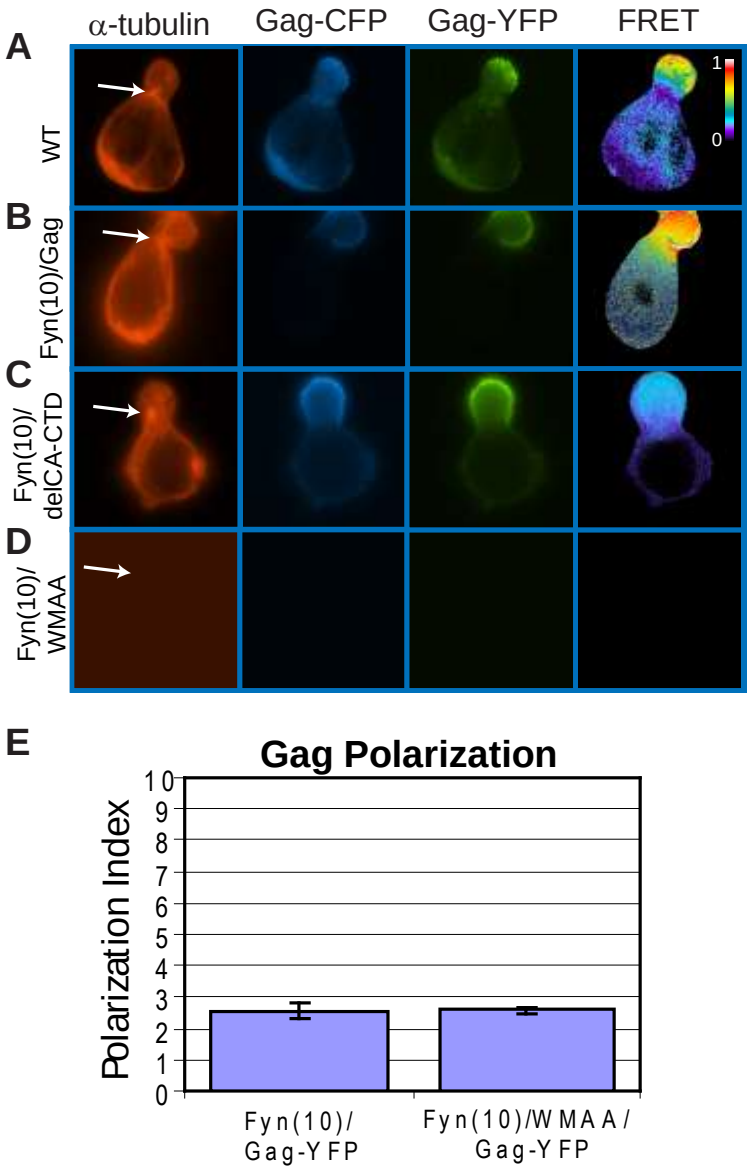

Figure 2.10. CA-mediated dimerization is not required for Gag localization to the uropod.

A-D) P2 cells expressing Gag-YFP (green) and Gag-CFP (blue) or their derivatives were stained for α-tubulin (red) to identify the MTOC. Multimerization efficiency of each Gag mutant was measured by FRET. **A)** WT Gag-YFP/-CFP, **B)** Fyn(10)/Gag-YFP/-CFP, **C)** Fyn(10)/delCA-CTD/Gag-YFP/-CFP, and **D)** Fyn(10)/WMAA/Gag-YFP/CFP. Note that Gag derivatives with CA changes both localize to the uropod but show low FRET. Color scale bar indicates colors associated with high (1) or low (0) FRET. **E)** Polarization indices were calculated for Fyn(10)/Gag-YFP and Fyn(10)/WMAA/Gag-YFP (see Materials and Methods). Three separate experiments (a total of 89 P2 cells for Fyn(10)/Gag-YFP and 78 P2 cells for Fyn(10)/WMAA/Gag-YFP) were used for quantification. Error bars represent standard deviation. P values were determined using Student's t test. NS, not significant.

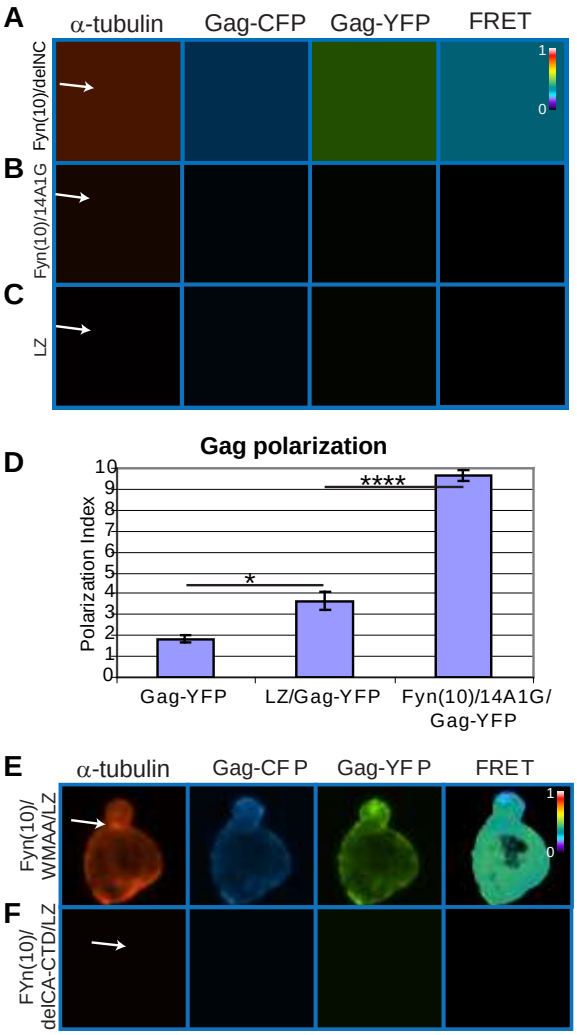

Figure 2.11. Higher-order multimerization mediated by NC is required for Gag localization to the uropod.

A-C) P2 cells expressing Gag-YFP and Gag-CFP that contain an NC deletion or substitutions (green/blue) were immunostained with anti-α-tubulin (red, arrow indicates MTOC). Note that Fyn(10)/delNC/Gag-YFP/-CFP (**A**) and Fyn(10)/14A1G/Gag-YFP/-CFP (**B**) localize over the entire plasma membrane. Both mutants show reduced levels of FRET. In contrast, LZ/Gag-YFP/-CFP (**C**) mostly localizes to the uropod. High FRET is observed indicating that multimerization is rescued as well. **D)** Polarization indices were calculated for LZ/Gag-YFP and Fyn(10)/14A1G/Gag-YFP and compared to WT Gag-YFP. LZ/Gag-YFP is less efficient in polarization, but significantly more efficient than Fyn(10)/14A1G/Gag-YFP. A total of 131 cells for Gag-YFP, 79 cells for LZ/Gag-YFP, and 69 cells for Fyn(10)/14A1G/Gag-YFP from three separate experiments were measured for polarized localization of Gag. Error bars represent standard deviation. P values were determined using Student's t test. *, $P<0.05$. ****, $P<0.0001$. **E)** and **F)** Double mutants containing the LZ sequence with the two different changes in the CA C-terminal domain, Fyn(10)/WMAA/LZ/Gag-YFP/-CFP (E) and Fyn(10)/delCA-CTD/LZ/Gag-YFP/-CFP (F), were expressed in P2 cells. Note that both Gag derivatives fail to localize to the uropod despite the presence of the LZ sequence.

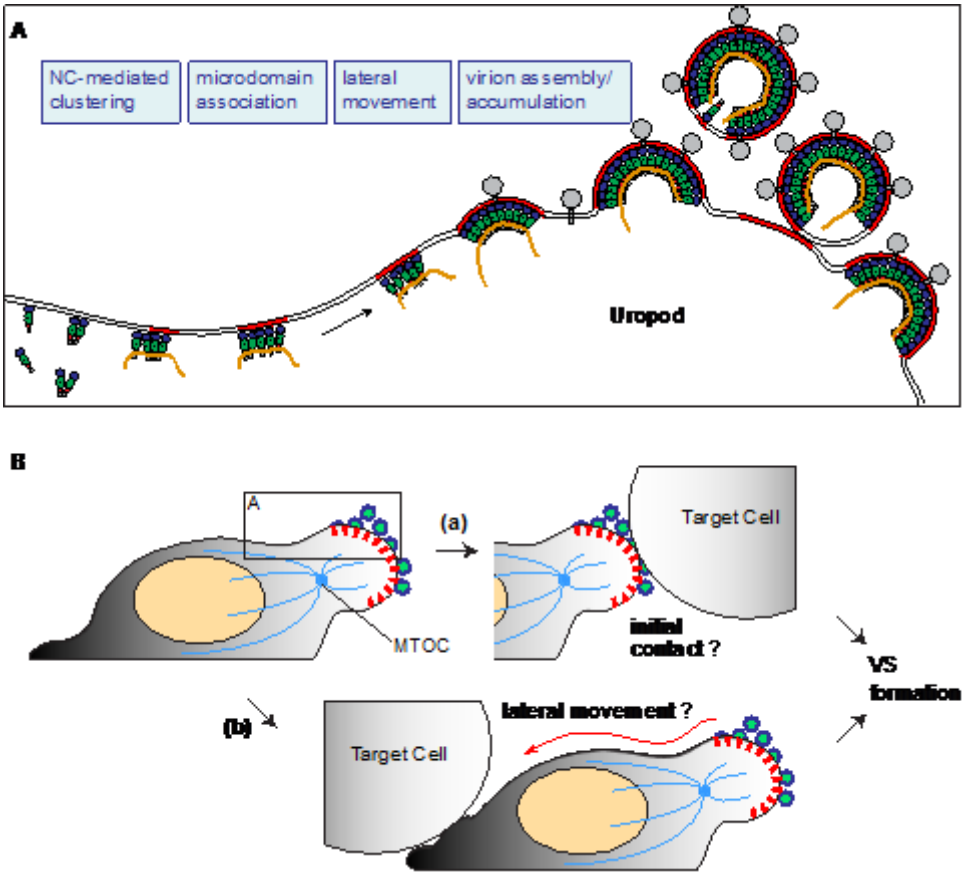

Figure 2.12. Working Model.
A) Based on the findings in this study, we have postulated a working model in which NC-mediated clustering of Gag allows association of Gag with uropod-specific microdomains that facilitate movement to the uropod in polarizing T cells. **B)** The virus-laden uropod, acting as a pre-formed platform that may either mediate contact with target cells (a) or relocalize to contacts formed elsewhere subsequently (b), constitutes a VS that facilitates cell-to-cell transmission of HIV-1.

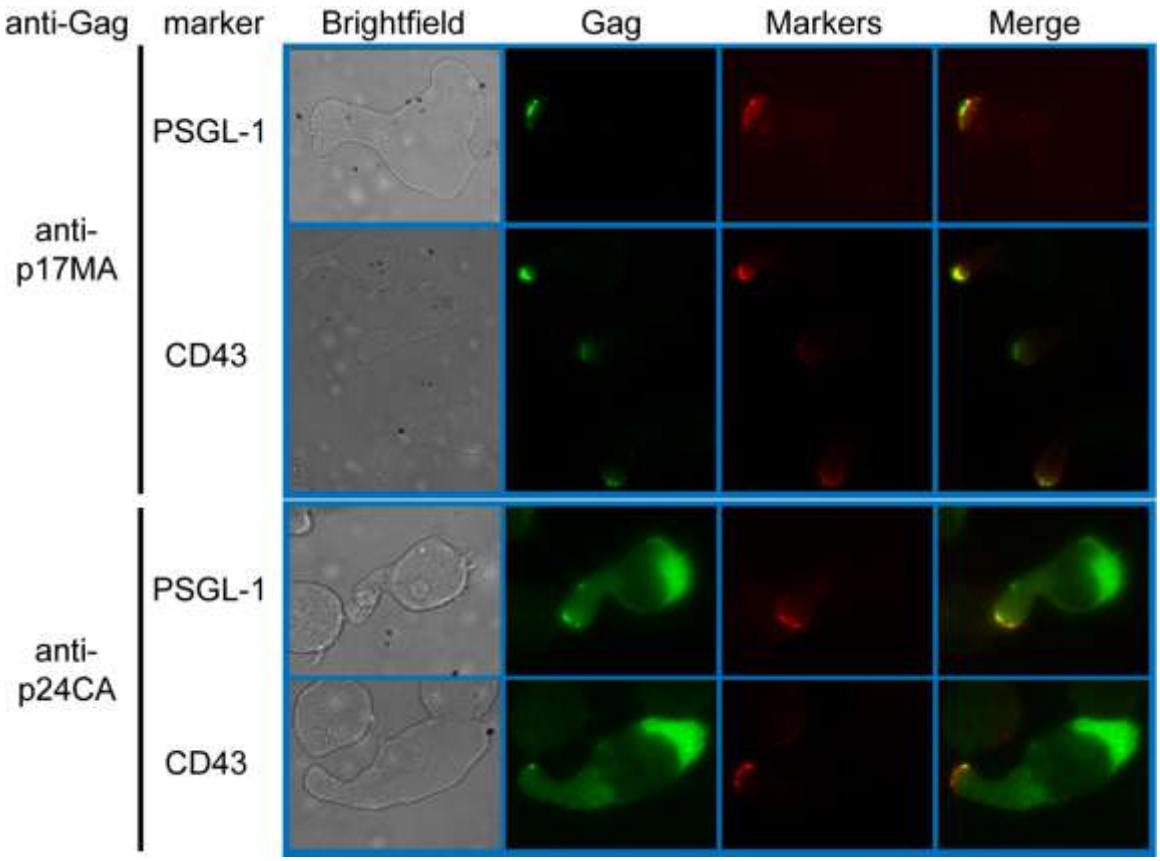

Figure 2.S1. Untagged Gag detected at the plasma membrane using anti-Gag antibodies shows strong colocalization with uropod markers.
P2 cells infected with wild type HIV-1 (NL4-3) were labeled with anti-PSGL-1 or anti-CD43 (red) prior to fixation. Fixed cells were permeabilized and immunostained with anti-p17MA or anti-p24CA (green). Note that when Gag is detected on the cell surface, it colocalized with uropod markers.

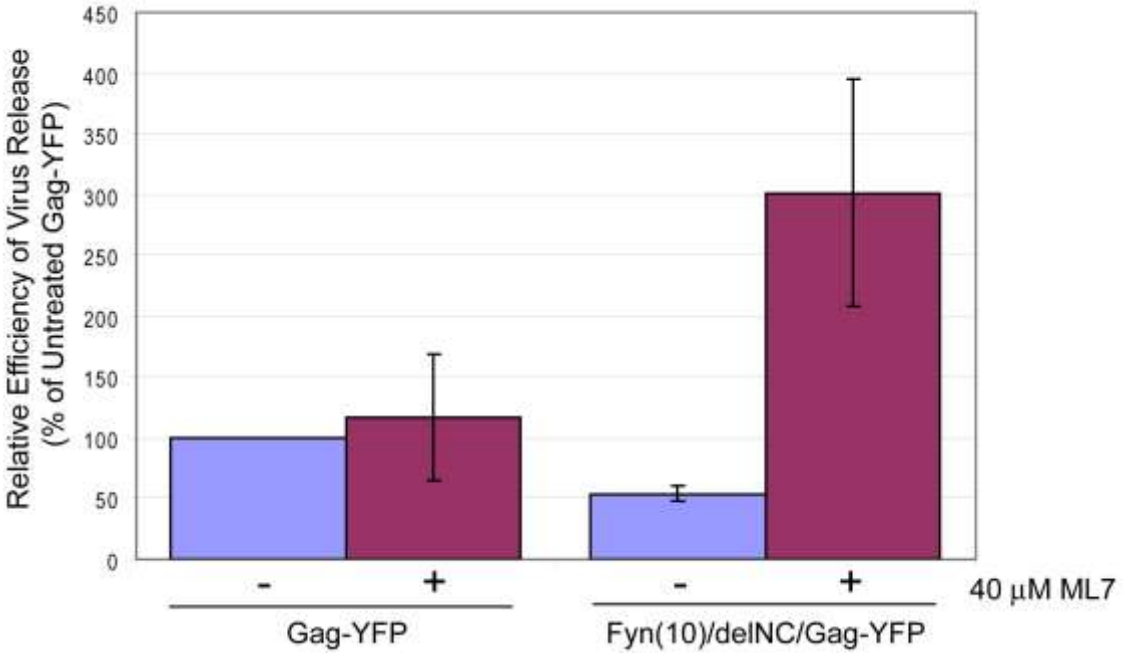

Figure 2.S2. Effects of ML7 on VLP release efficiency
P2 cells expressing Gag-YFP or Fyn(10)delNC Gag-YFP were metabolically labeled with [^{35}S] methionine/cysteine for 2 h in the presence of 40 μM ML7 (+) or DMSO (-). Cell and virus lysates were subjected to immunoprecipitation of viral proteins using HIV-Ig. Virus release efficiency was calculated as the amount of virion-associated Gag as a fraction of total (cell plus virion) Gag synthesized during a 2-h metabolic labeling period.

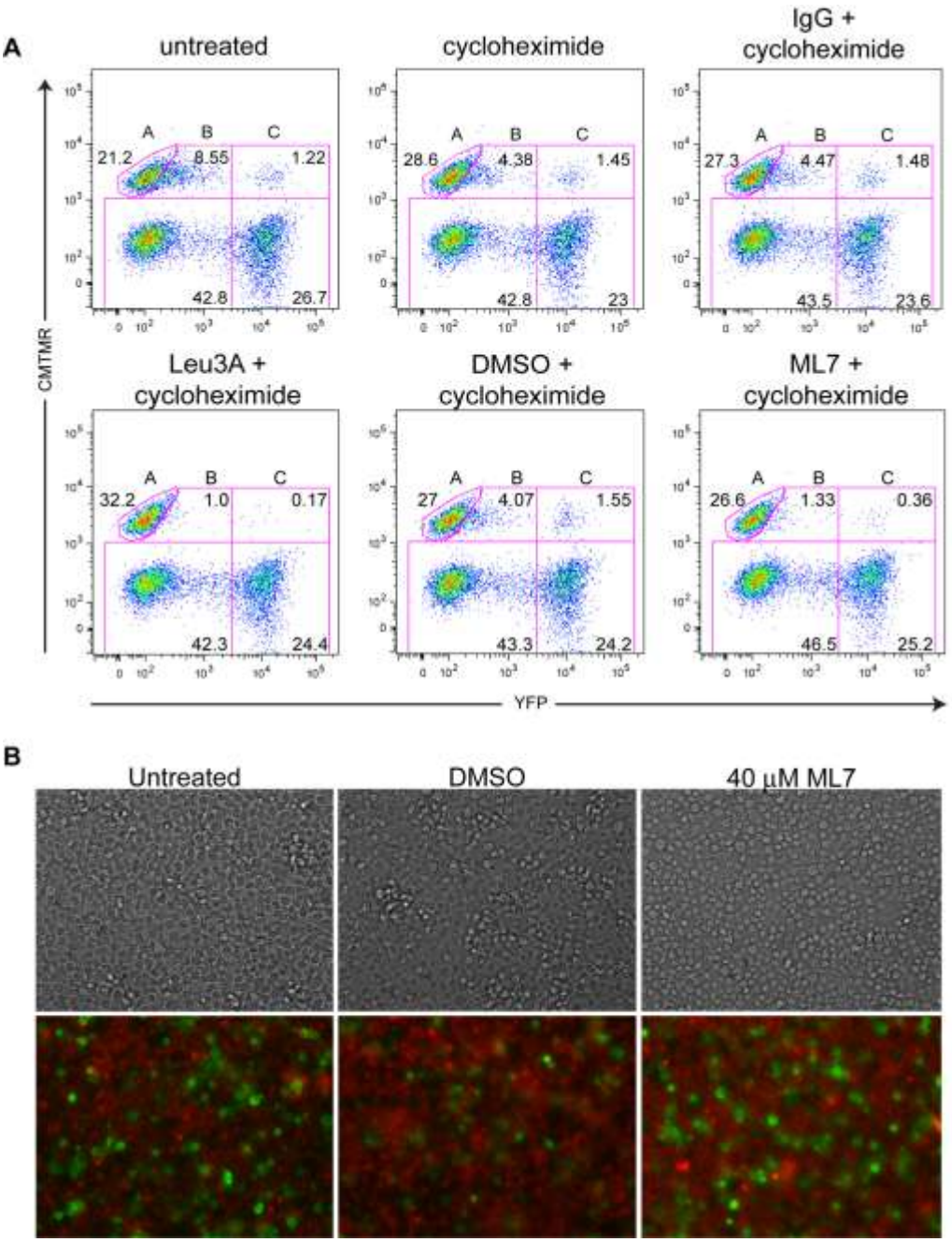

Figure 2.S3. Depolarization of T cells by ML7 treatment reduces cell-to-cell transfer of virus particles.

A) Transfer of Gag-YFP fluorescence from infected P2 cells to CMTMR-stained SupT1 target cells during a 3-h coculture period was measured by flow cytometry. ML7, DMSO, or antibodies, along with 10 µg/ml cycloheximide, were added at the beginning of the coculture period. Flow cytometry plots are shown. Gate A, CMTMR-labeled target cells; gate B, double positive cells representing target cells with transferred Gag-YFP particles; and gate C, YFP-expressing cells either fused or conjugated to CMTMR-labeled target cells. **B)** Representative brightfield (top panels) and fluorescence (bottom panels) images of cocultures untreated or treated with DMSO or ML7 are shown. Gag-YFP and CMTMR signals were shown in green and red, respectively.

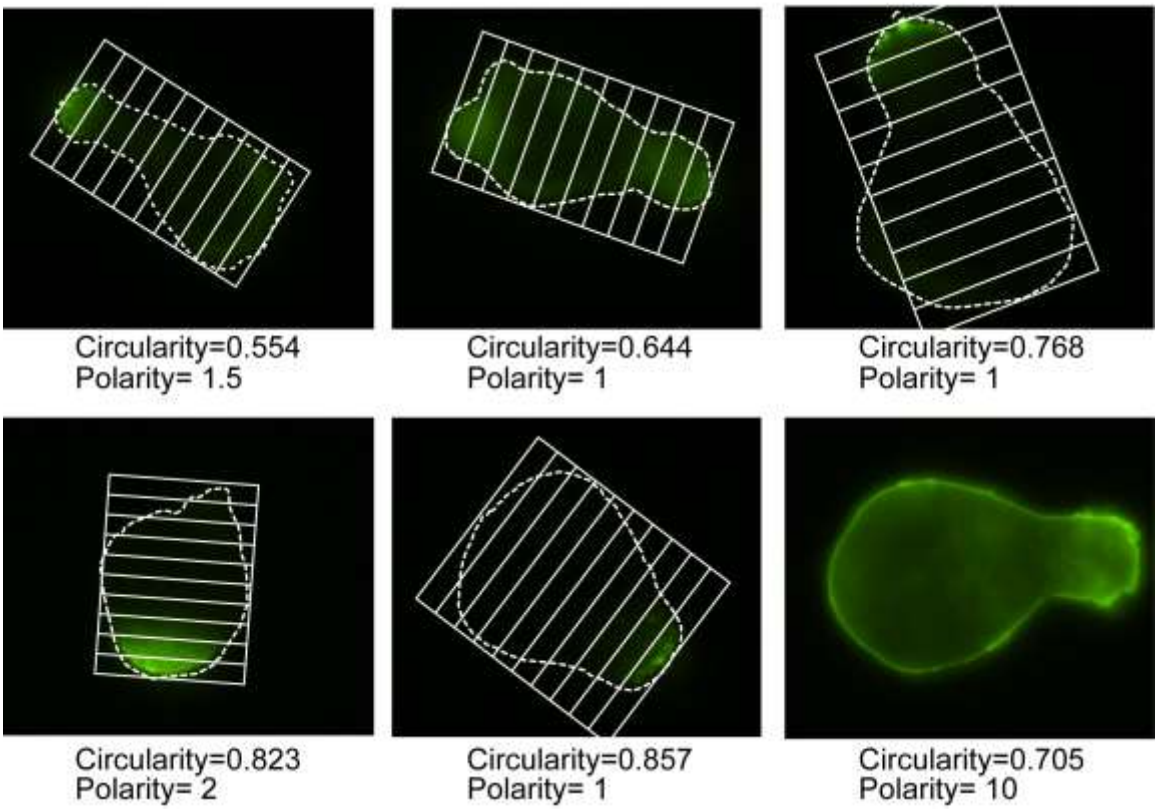

Figure 2.S4. Examples of polarity index calculations.
To measure morphological polarization of T cells, outlines of Gag-YFP-expressing P2 cells were determined by manually tracing the cell perimeter using the ImageJ program. Circularity values were then calculated based on this outline using the Measure function of ImageJ. The output values range between 0 and 1, with 1 representing a perfect circle. To quantify polarity of Gag localization, a 10-segmented grid was placed over each cell along the cell's longest axis. The number of segments that contained plasma-membrane-associated Gag was then used as the polarization index. For clarity, the outline and the grid were removed from the lower right panel.

Supplementary movies S1-S4: Available on PLoS Pathogens website: http://www.plospathogens.org/article/info%3Adoi%2F10.1371%2Fjournal.ppat.1001167#s5

References

1. Bajenoff, M., et al., *Stromal cell networks regulate lymphocyte entry, migration, and territoriality in lymph nodes.* Immunity, 2006. **25**(6): p. 989-1001.

2. Hugues, S., et al., *Distinct T cell dynamics in lymph nodes during the induction of tolerance and immunity.* Nat Immunol, 2004. **5**(12): p. 1235-42.

3. Mempel, T.R., S.E. Henrickson, and U.H. Von Andrian, *T-cell priming by dendritic cells in lymph nodes occurs in three distinct phases.* Nature, 2004. **427**(6970): p. 154-9.

4. Miller, M.J., et al., *Autonomous T cell trafficking examined in vivo with intravital two-photon microscopy.* Proc Natl Acad Sci U S A, 2003. **100**(5): p. 2604-9.

5. Miller, M.J., et al., *Two-photon imaging of lymphocyte motility and antigen response in intact lymph node.* Science, 2002. **296**(5574): p. 1869-73.

6. Mrass, P., et al., *Random migration precedes stable target cell interactions of tumor-infiltrating T cells.* J Exp Med, 2006. **203**(12): p. 2749-61.

7. Adamson, C.S. and E.O. Freed, *Human immunodeficiency virus type 1 assembly, release, and maturation.* Adv Pharmacol, 2007. **55**: p. 347-87.

8. Alfadhli, A., A. Still, and E. Barklis, *Analysis of human immunodeficiency virus type 1 matrix binding to membranes and nucleic acids.* J Virol, 2009. **83**(23): p. 12196-203.

9. Bryant, M. and L. Ratner, *Myristoylation-dependent replication and assembly of human immunodeficiency virus 1.* Proc Natl Acad Sci U S A, 1990. **87**(2): p. 523-7.

10. Chan, R., et al., *Retroviruses human immunodeficiency virus and murine leukemia virus are enriched in phosphoinositides.* J Virol, 2008. **82**(22): p. 11228-38.

11. Chukkapalli, V., et al., *Interaction between the human immunodeficiency virus type 1 Gag matrix domain and phosphatidylinositol-(4,5)-bisphosphate is essential for efficient gag membrane binding.* J Virol, 2008. **82**(5): p. 2405-17.

12. Chukkapalli, V., S.J. Oh, and A. Ono, *Opposing mechanisms involving RNA and lipids regulate HIV-1 Gag membrane binding through the highly basic region of the matrix domain.* Proc Natl Acad Sci U S A, 2010. **107**(4): p. 1600-5.

13. Dalton, A.K., et al., *Electrostatic interactions drive membrane association of the human immunodeficiency virus type 1 Gag MA domain.* J Virol, 2007. **81**(12): p. 6434-45.

14. Gottlinger, H.G., J.G. Sodroski, and W.A. Haseltine, *Role of capsid precursor processing and myristoylation in morphogenesis and infectivity of human immunodeficiency virus type 1.* Proc Natl Acad Sci U S A, 1989. **86**(15): p. 5781-5.

15. Hill, C.P., et al., *Crystal structures of the trimeric human immunodeficiency virus type 1 matrix protein: implications for membrane association and assembly.* Proc Natl Acad Sci U S A, 1996. **93**(7): p. 3099-104.

16. Ono, A., et al., *Phosphatidylinositol (4,5) bisphosphate regulates HIV-1 Gag targeting to the plasma membrane.* Proc Natl Acad Sci U S A, 2004. **101**(41): p. 14889-94.

17. Saad, J.S., et al., *Structural basis for targeting HIV-1 Gag proteins to the plasma membrane for virus assembly.* Proc Natl Acad Sci U S A, 2006. **103**(30): p. 11364-9.

18. Shkriabai, N., et al., *Interactions of HIV-1 Gag with assembly cofactors.* Biochemistry, 2006. **45**(13): p. 4077-83.

19. Tang, C., et al., *Entropic switch regulates myristate exposure in the HIV-1 matrix protein.* Proc Natl Acad Sci U S A, 2004. **101**(2): p. 517-22.

20. Zhou, W., et al., *Identification of a membrane-binding domain within the amino-terminal region of human immunodeficiency virus type 1 Gag protein which interacts with acidic phospholipids.* J Virol, 1994. **68**(4): p. 2556-69.

21. Burniston, M.T., et al., *Human immunodeficiency virus type 1 Gag polyprotein multimerization requires the nucleocapsid domain and RNA and is promoted by the capsid-dimer interface and the basic region of matrix protein.* J Virol, 1999. **73**(10): p. 8527-40.

22. Datta, S.A., et al., *Conformation of the HIV-1 Gag protein in solution.* J Mol Biol, 2007. **365**(3): p. 812-24.

23. Datta, S.A., et al., *Interactions between HIV-1 Gag molecules in solution: an inositol phosphate-mediated switch.* J Mol Biol, 2007. **365**(3): p. 799-811.

24. Ehrlich, L.S., B.E. Agresta, and C.A. Carter, *Assembly of recombinant human immunodeficiency virus type 1 capsid protein in vitro.* J Virol, 1992. **66**(8): p. 4874-83.

25. Franke, E.K., et al., *Specificity and sequence requirements for interactions between various retroviral Gag proteins.* J Virol, 1994. **68**(8): p. 5300-5.

26. Gamble, T.R., et al., *Structure of the carboxyl-terminal dimerization domain of the HIV-1 capsid protein.* Science, 1997. **278**(5339): p. 849-53.

27. Gross, I., et al., *N-Terminal extension of human immunodeficiency virus capsid protein converts the in vitro assembly phenotype from tubular to spherical particles.* J Virol, 1998. **72**(6): p. 4798-810.

28. Hogue, I.B., A. Hoppe, and A. Ono, *Quantitative fluorescence resonance energy transfer microscopy analysis of the human immunodeficiency virus type 1 Gag-Gag interaction: relative contributions of the CA and NC domains and membrane binding.* J Virol, 2009. **83**(14): p. 7322-36.

29. Joshi, A., K. Nagashima, and E.O. Freed, *Mutation of dileucine-like motifs in the human immunodeficiency virus type 1 capsid disrupts virus assembly, gag-gag interactions, gag-membrane binding, and virion maturation.* J Virol, 2006. **80**(16): p. 7939-51.

30. Li, H., et al., *Myristoylation is required for human immunodeficiency virus type 1 Gag-Gag multimerization in mammalian cells.* J Virol, 2007. **81**(23): p. 12899-910.

31. Momany, C., et al., *Crystal structure of dimeric HIV-1 capsid protein.* Nat Struct Biol, 1996. **3**(9): p. 763-70.

32. von Schwedler, U.K., et al., *Functional surfaces of the human immunodeficiency virus type 1 capsid protein.* J Virol, 2003. **77**(9): p. 5439-50.

33. Zhang, W.H., et al., *Gag-Gag interactions in the C-terminal domain of human immunodeficiency virus type 1 p24 capsid antigen are essential for Gag particle assembly.* J Gen Virol, 1996. **77 (Pt 4)**: p. 743-51.

34. D'Souza, V. and M.F. Summers, *How retroviruses select their genomes.* Nat Rev Microbiol, 2005. **3**(8): p. 643-55.

35. Campbell, S. and A. Rein, *In vitro assembly properties of human immunodeficiency virus type 1 Gag protein lacking the p6 domain.* J Virol, 1999. **73**(3): p. 2270-9.

36. Campbell, S. and V.M. Vogt, *Self-assembly in vitro of purified CA-NC proteins from Rous sarcoma virus and human immunodeficiency virus type 1.* J Virol, 1995. **69**(10): p. 6487-97.

37. Cimarelli, A., et al., *Basic residues in human immunodeficiency virus type 1 nucleocapsid promote virion assembly via interaction with RNA.* J Virol, 2000. **74**(7): p. 3046-57.

38. Dawson, L. and X.F. Yu, *The role of nucleocapsid of HIV-1 in virus assembly.* Virology, 1998. **251**(1): p. 141-57.

39. Derdowski, A., L. Ding, and P. Spearman, *A novel fluorescence resonance energy transfer assay demonstrates that the human immunodeficiency virus type 1*

Pr55Gag I domain mediates Gag-Gag interactions. J Virol, 2004. **78**(3): p. 1230-42.

40. Huseby, D., et al., *Assembly of human immunodeficiency virus precursor gag proteins.* J Biol Chem, 2005. **280**(18): p. 17664-70.

41. Sandefur, S., et al., *Mapping and characterization of the N-terminal I domain of human immunodeficiency virus type 1 Pr55(Gag).* J Virol, 2000. **74**(16): p. 7238-49.

42. Sandefur, S., V. Varthakavi, and P. Spearman, *The I domain is required for efficient plasma membrane binding of human immunodeficiency virus type 1 Pr55Gag.* J Virol, 1998. **72**(4): p. 2723-32.

43. Zabransky, A., E. Hunter, and M. Sakalian, *Identification of a minimal HIV-1 gag domain sufficient for self-association.* Virology, 2002. **294**(1): p. 141-50.

44. Demirov, D.G. and E.O. Freed, *Retrovirus budding.* Virus Res, 2004. **106**(2): p. 87-102.

45. Martin-Serrano, J., T. Zang, and P.D. Bieniasz, *Role of ESCRT-I in retroviral budding.* J Virol, 2003. **77**(8): p. 4794-804.

46. Morita, E. and W.I. Sundquist, *Retrovirus budding.* Annu Rev Cell Dev Biol, 2004. **20**: p. 395-425.

47. Krummel, M.F. and I. Macara, *Maintenance and modulation of T cell polarity.* Nat Immunol, 2006. **7**(11): p. 1143-9.

48. Sanchez-Madrid, F. and M.A. del Pozo, *Leukocyte polarization in cell migration and immune interactions.* Embo J, 1999. **18**(3): p. 501-11.

49. Sanchez-Madrid, F. and J.M. Serrador, *Bringing up the rear: defining the roles of the uropod.* Nat Rev Mol Cell Biol, 2009. **10**(5): p. 353-9.

50. Alonso-Lebrero, J.L., et al., *Polarization and interaction of adhesion molecules P-selectin glycoprotein ligand 1 and intercellular adhesion molecule 3 with moesin and ezrin in myeloid cells.* Blood, 2000. **95**(7): p. 2413-9.

51. Itoh, S., et al., *Redistribution of P-selectin glycoprotein ligand-1 (PSGL-1) in chemokine-treated neutrophils: a role of lipid microdomains.* J Leukoc Biol, 2007. **81**(6): p. 1414-21.

52. Ratner, S., W.S. Sherrod, and D. Lichlyter, *Microtubule retraction into the uropod and its role in T cell polarization and motility.* J Immunol, 1997. **159**(3): p. 1063-7.

53. Chen, P., et al., *Predominant mode of human immunodeficiency virus transfer between T cells is mediated by sustained Env-dependent neutralization-resistant virological synapses.* J Virol, 2007. **81**(22): p. 12582-95.

54. Nguyen, D.H. and J.E. Hildreth, *Evidence for budding of human immunodeficiency virus type 1 selectively from glycolipid-enriched membrane lipid rafts.* J Virol, 2000. **74**(7): p. 3264-72.

55. Pearce-Pratt, R., D. Malamud, and D.M. Phillips, *Role of the cytoskeleton in cell-to-cell transmission of human immunodeficiency virus.* J Virol, 1994. **68**(5): p. 2898-905.

56. Perotti, M.E., X. Tan, and D.M. Phillips, *Directional budding of human immunodeficiency virus from monocytes.* J Virol, 1996. **70**(9): p. 5916-21.

57. Phillips, D.M., *The role of cell-to-cell transmission in HIV infection.* AIDS, 1994. **8**(6): p. 719-31.

58. Chertova, E., et al., *Proteomic and biochemical analysis of purified human immunodeficiency virus type 1 produced from infected monocyte-derived macrophages.* J Virol, 2006. **80**(18): p. 9039-52.

59. Fais, S., et al., *Unidirectional budding of HIV-1 at the site of cell-to-cell contact is associated with co-polarization of intercellular adhesion molecules and HIV-1 viral matrix protein.* Aids, 1995. **9**(4): p. 329-35.

60. Gomez-Mouton, C., et al., *Segregation of leading-edge and uropod components into specific lipid rafts during T cell polarization.* Proc Natl Acad Sci U S A, 2001. **98**(17): p. 9642-7.

61. Jolly, C. and Q.J. Sattentau, *Human immunodeficiency virus type 1 virological synapse formation in T cells requires lipid raft integrity.* J Virol, 2005. **79**(18): p. 12088-94.

62. Ono, A. and E.O. Freed, *Role of lipid rafts in virus replication.* Adv Virus Res, 2005. **64**: p. 311-58.

63. del Pozo, M.A., et al., *Chemokines regulate cellular polarization and adhesion receptor redistribution during lymphocyte interaction with endothelium and extracellular matrix. Involvement of cAMP signaling pathway.* J Cell Biol, 1995. **131**(2): p. 495-508.

64. Serrador, J.M., et al., *CD43 interacts with moesin and ezrin and regulates its redistribution to the uropods of T lymphocytes at the cell-cell contacts.* Blood, 1998. **91**(12): p. 4632-44.

65. Tibaldi, E.V., R. Salgia, and E.L. Reinherz, *CD2 molecules redistribute to the uropod during T cell scanning: implications for cellular activation and immune surveillance.* Proc Natl Acad Sci U S A, 2002. **99**(11): p. 7582-7.

66. Dimitrov, D.S., et al., *Quantitation of human immunodeficiency virus type 1 infection kinetics.* J Virol, 1993. **67**(4): p. 2182-90.

67. Hubner, W., et al., *Quantitative 3D video microscopy of HIV transfer across T cell virological synapses.* Science, 2009. **323**(5922): p. 1743-7.

68. Martin, N., et al., *Virological synapse-mediated spread of human immunodeficiency virus type 1 between T cells is sensitive to entry inhibition.* J Virol, 2010. **84**(7): p. 3516-27.

69. Mazurov, D., et al., *Quantitative comparison of HTLV-1 and HIV-1 cell-to-cell infection with new replication dependent vectors.* PLoS Pathog, 2010. **6**(2): p. e1000788.

70. Sato, H., et al., *Cell-to-cell spread of HIV-1 occurs within minutes and may not involve the participation of virus particles.* Virology, 1992. **186**(2): p. 712-24.

71. Sourisseau, M., et al., *Inefficient human immunodeficiency virus replication in mobile lymphocytes.* J Virol, 2007. **81**(2): p. 1000-12.

72. Alfsen, A., et al., *HIV-1-infected blood mononuclear cells form an integrin- and agrin-dependent viral synapse to induce efficient HIV-1 transcytosis across epithelial cell monolayer.* Mol Biol Cell, 2005. **16**(9): p. 4267-79.

73. Arrighi, J.F., et al., *DC-SIGN-mediated infectious synapse formation enhances X4 HIV-1 transmission from dendritic cells to T cells.* J Exp Med, 2004. **200**(10): p. 1279-88.

74. Garcia, E., et al., *HIV-1 trafficking to the dendritic cell-T-cell infectious synapse uses a pathway of tetraspanin sorting to the immunological synapse.* Traffic, 2005. **6**(6): p. 488-501.

75. Gousset, K., et al., *Real-time visualization of HIV-1 GAG trafficking in infected macrophages.* PLoS Pathog, 2008. **4**(3): p. e1000015.

76. Groot, F., S. Welsch, and Q.J. Sattentau, *Efficient HIV-1 transmission from macrophages to T cells across transient virological synapses.* Blood, 2008. **111**(9): p. 4660-3.

77. Igakura, T., et al., *Spread of HTLV-I between lymphocytes by virus-induced polarization of the cytoskeleton.* Science, 2003. **299**(5613): p. 1713-6.

78. Jolly, C., et al., *HIV-1 cell to cell transfer across an Env-induced, actin-dependent synapse.* J Exp Med, 2004. **199**(2): p. 283-93.

79. McDonald, D., et al., *Recruitment of HIV and its receptors to dendritic cell-T cell junctions.* Science, 2003. **300**(5623): p. 1295-7.

80. Rudnicka, D., et al., *Simultaneous cell-to-cell transmission of human immunodeficiency virus to multiple targets through polysynapses.* J Virol, 2009. **83**(12): p. 6234-46.

81. Sherer, N.M., et al., *Retroviruses can establish filopodial bridges for efficient cell-to-cell transmission.* Nat Cell Biol, 2007. **9**(3): p. 310-5.

82. Sowinski, S., et al., *Membrane nanotubes physically connect T cells over long distances presenting a novel route for HIV-1 transmission.* Nat Cell Biol, 2008. **10**(2): p. 211-9.

83. Wang, J.H., C. Wells, and L. Wu, *Macropinocytosis and cytoskeleton contribute to dendritic cell-mediated HIV-1 transmission to CD4+ T cells.* Virology, 2008. **381**(1): p. 143-54.

84. Yu, H.J., M.A. Reuter, and D. McDonald, *HIV traffics through a specialized, surface-accessible intracellular compartment during trans-infection of T cells by mature dendritic cells.* PLoS Pathog, 2008. **4**(8): p. e1000134.

85. Majorovits, E., et al., *Human T-lymphotropic virus-1 visualized at the virological synapse by electron tomography.* PLoS One, 2008. **3**(5): p. e2251.

86. Pais-Correia, A.M., et al., *Biofilm-like extracellular viral assemblies mediate HTLV-1 cell-to-cell transmission at virological synapses.* Nat Med, 2010. **16**(1): p. 83-9.

87. Sherer, N.M. and W. Mothes, *Cytonemes and tunneling nanotubules in cell-cell communication and viral pathogenesis.* Trends Cell Biol, 2008. **18**(9): p. 414-20.

88. Jin, J., et al., *Assembly of the murine leukemia virus is directed towards sites of cell-cell contact.* PLoS Biol, 2009. **7**(7): p. e1000163.

89. Vasiliver-Shamis, G., et al., *Human immunodeficiency virus type 1 envelope gp120 induces a stop signal and virological synapse formation in noninfected CD4+ T cells.* J Virol, 2008. **82**(19): p. 9445-57.

90. Vasiliver-Shamis, G., et al., *Human immunodeficiency virus type 1 envelope gp120-induced partial T-cell receptor signaling creates an F-actin-depleted zone in the virological synapse.* J Virol, 2009. **83**(21): p. 11341-55.

91. Puigdomenech, I., et al., *On the steps of cell-to-cell HIV transmission between CD4 T cells.* Retrovirology, 2009. **6**: p. 89.

92. Sattentau, Q., *Avoiding the void: cell-to-cell spread of human viruses.* Nat Rev Microbiol, 2008. **6**(11): p. 815-26.

93. Haller, C. and O.T. Fackler, *HIV-1 at the immunological and T-lymphocytic virological synapse.* Biol Chem, 2008. **389**(10): p. 1253-60.

94. Piguet, V. and Q. Sattentau, *Dangerous liaisons at the virological synapse.* J Clin Invest, 2004. **114**(5): p. 605-10.

95. Sol-Foulon, N., et al., *ZAP-70 kinase regulates HIV cell-to-cell spread and virological synapse formation.* Embo J, 2007. **26**(2): p. 516-26.

96. Jolly, C., I. Mitar, and Q.J. Sattentau, *Adhesion molecule interactions facilitate human immunodeficiency virus type 1-induced virological synapse formation between T cells.* J Virol, 2007. **81**(24): p. 13916-21.

97. Arthos, J., et al., *HIV-1 envelope protein binds to and signals through integrin alpha4beta7, the gut mucosal homing receptor for peripheral T cells.* Nat Immunol, 2008. **9**(3): p. 301-9.

98. Kinashi, T. and K. Katagiri, *Regulation of lymphocyte adhesion and migration by the small GTPase Rap1 and its effector molecule, RAPL.* Immunol Lett, 2004. **93**(1): p. 1-5.

99. Hubner, W., et al., *Sequence of human immunodeficiency virus type 1 (HIV-1) Gag localization and oligomerization monitored with live confocal imaging of a replication-competent, fluorescently tagged HIV-1.* J Virol, 2007. **81**(22): p. 12596-607.

100. Ono, A., J.M. Orenstein, and E.O. Freed, *Role of the Gag matrix domain in targeting human immunodeficiency virus type 1 assembly.* J Virol, 2000. **74**(6): p. 2855-66.

101. Zhou, W. and M.D. Resh, *Differential membrane binding of the human immunodeficiency virus type 1 matrix protein.* J Virol, 1996. **70**(12): p. 8540-8.

102. Ruggiero, E., et al., *Virological consequences of early events following cell-cell contact between human immunodeficiency virus type 1-infected and uninfected CD4+ cells.* J Virol, 2008. **82**(16): p. 7773-89.

103. Puigdomenech, I., et al., *HIV transfer between CD4 T cells does not require LFA-1 binding to ICAM-1 and is governed by the interaction of HIV envelope glycoprotein with CD4.* Retrovirology, 2008. **5**: p. 32.

104. Blanco, J., et al., *High level of coreceptor-independent HIV transfer induced by contacts between primary CD4 T cells.* J Biol Chem, 2004. **279**(49): p. 51305-14.

105. Ono, A. and E.O. Freed, *Plasma membrane rafts play a critical role in HIV-1 assembly and release.* Proc Natl Acad Sci U S A, 2001. **98**(24): p. 13925-30.

106. Ding, L., et al., *Independent segregation of human immunodeficiency virus type 1 Gag protein complexes and lipid rafts.* J Virol, 2003. **77**(3): p. 1916-26.

107. Holm, K., et al., *Human immunodeficiency virus type 1 assembly and lipid rafts: Pr55(gag) associates with membrane domains that are largely resistant to Brij98 but sensitive to Triton X-100.* J Virol, 2003. **77**(8): p. 4805-17.

108. Lindwasser, O.W. and M.D. Resh, *Multimerization of human immunodeficiency virus type 1 Gag promotes its localization to barges, raft-like membrane microdomains.* J Virol, 2001. **75**(17): p. 7913-24.

109. Nydegger, S., et al., *Mapping of tetraspanin-enriched microdomains that can function as gateways for HIV-1.* J Cell Biol, 2006. **173**(5): p. 795-807.

110. Booth, A.M., et al., *Exosomes and HIV Gag bud from endosome-like domains of the T cell plasma membrane.* J Cell Biol, 2006. **172**(6): p. 923-35.

111. Grigorov, B., et al., *A role for CD81 on the late steps of HIV-1 replication in a chronically infected T cell line.* Retrovirology, 2009. **6**: p. 28.

112. Brugger, B., et al., *The HIV lipidome: a raft with an unusual composition.* Proc Natl Acad Sci U S A, 2006. **103**(8): p. 2641-6.

113. Jolly, C. and Q.J. Sattentau, *Human immunodeficiency virus type 1 assembly, budding, and cell-cell spread in T cells take place in tetraspanin-enriched plasma membrane domains.* J Virol, 2007. **81**(15): p. 7873-84.

114. Krementsov, D.N., et al., *Tetraspanins regulate cell-to-cell transmission of HIV-1.* Retrovirology, 2009. **6**: p. 64.

115. Manes, S., et al., *Membrane raft microdomains mediate front-rear polarity in migrating cells.* Embo J, 1999. **18**(22): p. 6211-20.

116. Rossy, J., et al., *Flotillins interact with PSGL-1 in neutrophils and, upon stimulation, rapidly organize into membrane domains subsequently accumulating in the uropod.* PLoS One, 2009. **4**(4): p. e5403.

117. Fabbri, M., et al., *Dynamic partitioning into lipid rafts controls the endo-exocytic cycle of the alphaL/beta2 integrin, LFA-1, during leukocyte chemotaxis.* Mol Biol Cell, 2005. **16**(12): p. 5793-803.

118. Pierini, L.M. and F.R. Maxfield, *Flotillas of lipid rafts fore and aft.* Proc Natl Acad Sci U S A, 2001. **98**(17): p. 9471-3.

119. Harder, T., et al., *Lipid domain structure of the plasma membrane revealed by patching of membrane components.* J Cell Biol, 1998. **141**(4): p. 929-42.

120. Janes, P.W., S.C. Ley, and A.I. Magee, *Aggregation of lipid rafts accompanies signaling via the T cell antigen receptor.* J Cell Biol, 1999. **147**(2): p. 447-61.

121. Gri, G., et al., *The inner side of T cell lipid rafts.* Immunol Lett, 2004. **94**(3): p. 247-52.

122. Lingwood, D., et al., *Plasma membranes are poised for activation of raft phase coalescence at physiological temperature.* Proc Natl Acad Sci U S A, 2008. **105**(29): p. 10005-10.

123. Meder, D., et al., *Phase coexistence and connectivity in the apical membrane of polarized epithelial cells.* Proc Natl Acad Sci U S A, 2006. **103**(2): p. 329-34.

124. Shvartsman, D.E., et al., *Differently anchored influenza hemagglutinin mutants display distinct interaction dynamics with mutual rafts.* J Cell Biol, 2003. **163**(4): p. 879-88.

125. Freed, E.O. and M.A. Martin, *Domains of the human immunodeficiency virus type 1 matrix and gp41 cytoplasmic tail required for envelope incorporation into virions.* J Virol, 1996. **70**(1): p. 341-51.

126. Mammano, F., et al., *Rescue of human immunodeficiency virus type 1 matrix protein mutants by envelope glycoproteins with short cytoplasmic domains.* J Virol, 1995. **69**(6): p. 3824-30.

127. Akari, H., T. Fukumori, and A. Adachi, *Cell-dependent requirement of human immunodeficiency virus type 1 gp41 cytoplasmic tail for Env incorporation into virions.* J Virol, 2000. **74**(10): p. 4891-3.

128. Murakami, T. and E.O. Freed, *Genetic evidence for an interaction between human immunodeficiency virus type 1 matrix and alpha-helix 2 of the gp41 cytoplasmic tail.* J Virol, 2000. **74**(8): p. 3548-54.

129. Murakami, T. and E.O. Freed, *The long cytoplasmic tail of gp41 is required in a cell type-dependent manner for HIV-1 envelope glycoprotein incorporation into virions.* Proc Natl Acad Sci U S A, 2000. **97**(1): p. 343-8.

130. Lopez-Verges, S., et al., *Tail-interacting protein TIP47 is a connector between Gag and Env and is required for Env incorporation into HIV-1 virions.* Proc Natl Acad Sci U S A, 2006. **103**(40): p. 14947-52.

131. Wyma, D.J., A. Kotov, and C. Aiken, *Evidence for a stable interaction of gp41 with Pr55(Gag) in immature human immunodeficiency virus type 1 particles.* J Virol, 2000. **74**(20): p. 9381-7.

132. Massanella, M., et al., *Antigp41 antibodies fail to block early events of virological synapses but inhibit HIV spread between T cells.* AIDS, 2009. **23**(2): p. 183-8.

133. Facke, M., et al., *A large deletion in the matrix domain of the human immunodeficiency virus gag gene redirects virus particle assembly from the plasma membrane to the endoplasmic reticulum.* J Virol, 1993. **67**(8): p. 4972-80.

134. Freed, E.O., et al., *Single amino acid changes in the human immunodeficiency virus type 1 matrix protein block virus particle production.* J Virol, 1994. **68**(8): p. 5311-20.

135. Yuan, X., et al., *Mutations in the N-terminal region of human immunodeficiency virus type 1 matrix protein block intracellular transport of the Gag precursor.* J Virol, 1993. **67**(11): p. 6387-94.

136. Hermida-Matsumoto, L. and M.D. Resh, *Localization of human immunodeficiency virus type 1 Gag and Env at the plasma membrane by confocal imaging.* J Virol, 2000. **74**(18): p. 8670-9.

137. Cannon, P.M., et al., *Structure-function studies of the human immunodeficiency virus type 1 matrix protein, p17.* J Virol, 1997. **71**(5): p. 3474-83.

138. Reil, H., et al., *Efficient HIV-1 replication can occur in the absence of the viral matrix protein.* Embo J, 1998. **17**(9): p. 2699-708.

139. Ono, A., *HIV-1 Assembly at the Plasma Membrane: Gag Trafficking and Localization.* Future Virol, 2009. **4**(3): p. 241-257.

140. Dou, J., et al., *Characterization of a myristoylated, monomeric HIV Gag protein.* Virology, 2009. **387**(2): p. 341-52.

141. Crist, R.M., et al., *Assembly properties of human immunodeficiency virus type 1 Gag-leucine zipper chimeras: implications for retrovirus assembly.* J Virol, 2009. **83**(5): p. 2216-25.

142. Accola, M.A., B. Strack, and H.G. Gottlinger, *Efficient particle production by minimal Gag constructs which retain the carboxy-terminal domain of human immunodeficiency virus type 1 capsid-p2 and a late assembly domain.* J Virol, 2000. **74**(12): p. 5395-402.

143. Zhang, Y., et al., *Analysis of the assembly function of the human immunodeficiency virus type 1 gag protein nucleocapsid domain.* J Virol, 1998. **72**(3): p. 1782-9.

144. Gillette, J.M., et al., *Intercellular transfer to signalling endosomes regulates an ex vivo bone marrow niche.* Nat Cell Biol, 2009. **11**(3): p. 303-11.

145. Jolly, C., I. Mitar, and Q.J. Sattentau, *Requirement for an intact T-cell actin and tubulin cytoskeleton for efficient assembly and spread of human immunodeficiency virus type 1.* J Virol, 2007. **81**(11): p. 5547-60.

146. Seveau, S., et al., *Neutrophil polarity and locomotion are associated with surface redistribution of leukosialin (CD43), an antiadhesive membrane molecule.* Blood, 2000. **95**(8): p. 2462-70.

147. Braun, J., et al., *Two distinct mechanisms for redistribution of lymphocyte surface macromolecules. I. Relationship to cytoplasmic myosin.* J Cell Biol, 1978. **79**(2 Pt 1): p. 409-18.

148. Kammer, G.M., E.I. Walter, and M.E. Medof, *Association of cytoskeletal re-organization with capping of the complement decay-accelerating factor on T lymphocytes.* J Immunol, 1988. **141**(9): p. 2924-8.

149. Fang, Y., et al., *Higher-order oligomerization targets plasma membrane proteins and HIV gag to exosomes.* PLoS Biol, 2007. **5**(6): p. e158.

150. Fisher, R.J., et al., *Sequence-specific binding of human immunodeficiency virus type 1 nucleocapsid protein to short oligonucleotides.* J Virol, 1998. **72**(3): p. 1902-9.

151. Hancock, J.F., *Lipid rafts: contentious only from simplistic standpoints.* Nat Rev Mol Cell Biol, 2006. **7**(6): p. 456-62.

152. Fujita, A., J. Cheng, and T. Fujimoto, *Segretation of GM1 and GM3 clusters in the cell membrane depends on the intact actin cytoskeleton.* Biochim Biophys Acta, 2009. **1791**(5): p. 388-396.

153. Katagiri, K., et al., *RAPL, a Rap1-binding molecule that mediates Rap1-induced adhesion through spatial regulation of LFA-1.* Nat Immunol, 2003. **4**(8): p. 741-8.

154. Morin, N.A., et al., *Nonmuscle myosin heavy chain IIA mediates integrin LFA-1 de-adhesion during T lymphocyte migration.* J Exp Med, 2008. **205**(1): p. 195-205.

155. Smith, A., et al., *A talin-dependent LFA-1 focal zone is formed by rapidly migrating T lymphocytes.* J Cell Biol, 2005. **170**(1): p. 141-51.

156. Deschambeault, J., et al., *Polarized human immunodeficiency virus budding in lymphocytes involves a tyrosine-based signal and favors cell-to-cell viral transmission.* J Virol, 1999. **73**(6): p. 5010-7.

157. Adachi, A., et al., *Production of acquired immunodeficiency syndrome-associated retrovirus in human and nonhuman cells transfected with an infectious molecular clone.* J Virol, 1986. **59**(2): p. 284-91.

158. Zacharias, D.A., et al., *Partitioning of lipid-modified monomeric GFPs into membrane microdomains of live cells.* Science, 2002. **296**(5569): p. 913-6.

159. Nagai, T., et al., *A variant of yellow fluorescent protein with fast and efficient maturation for cell-biological applications.* Nat Biotechnol, 2002. **20**(1): p. 87-90.

160. Rizzo, M.A., et al., *An improved cyan fluorescent protein variant useful for FRET.* Nat Biotechnol, 2004. **22**(4): p. 445-9.

161. Freed, E.O. and M.A. Martin, *The role of human immunodeficiency virus type 1 envelope glycoproteins in virus infection.* J Biol Chem, 1995. **270**(41): p. 23883-6.

162. Yee, J.K., T. Friedmann, and J.C. Burns, *Generation of high-titer pseudotyped retroviral vectors with very broad host range.* Methods Cell Biol, 1994. **43 Pt A**: p. 99-112.

163. Nieto, M., et al., *Polarization of chemokine receptors to the leading edge during lymphocyte chemotaxis.* J Exp Med, 1997. **186**(1): p. 153-8.

164. Wilkinson, P.C. and I. Newman, *Chemoattractant activity of IL-2 for human lymphocytes: a requirement for the IL-2 receptor beta-chain.* Immunology, 1994. **82**(1): p. 134-9.

165. Goebl, N.A., et al., *Neonatal Fc receptor mediates internalization of Fc in transfected human endothelial cells.* Mol Biol Cell, 2008. **19**(12): p. 5490-505.

166. Lachmanovich, E., et al., *Co-localization analysis of complex formation among membrane proteins by computerized fluorescence microscopy: application to immunofluorescence co-patching studies.* J Microsc, 2003. **212**(Pt 2): p. 122-31.

167. Hoppe, A., K. Christensen, and J.A. Swanson, *Fluorescence resonance energy transfer-based stoichiometry in living cells.* Biophys J, 2002. **83**(6): p. 3652-64.

168. Negulescu, P.A., et al., *Polarity of T cell shape, motility, and sensitivity to antigen.* Immunity, 1996. **4**(5): p. 421-30.

Chapter III

HIV-1 Gag Associates with a Specific Subset of Uropod-Directed Microdomains Determined by Matrix

Abstract

T cells are one of the natural targets of HIV-1, which primarily spreads in culture by cell-to-cell transmission. In lymphoid organs, where cell-to-cell transmission of HIV-1 likely occurs, T cells often adopt a polarized morphology. In chapter II, HIV-1 Gag was found to localize to a rear end protrusion called a uropod of polarized T cells. Uropod localization of Gag was driven by NC-mediated multimerization. Uropods participated in virological synapses that promote cell-to-cell transmission. Finally, Gag was found to associate with uropod-directed microdomains (UDMs), which comigrated rearward with Gag to the uropod as T cells polarized. However, the level of multimerization sufficient to drive uropod localization, the composition of UDMs and the viral determinants for Gag association with UDMs remained vague. Elucidating these mechanisms could lead to a better understanding of how HIV-1 traffics and spreads *in vivo*. In this chapter, a low level of multimerization and inner-leaflet binding of Gag to the plasma membrane was found to be sufficient to drive Gag localization to uropods. Gag also associated with a specific subset of UDMs enriched in the uropod proteins PSGL-1, CD43 and CD44,

while excluding other uropod proteins such as ICAM-1, ICAM-3 and the uropod-associated lipid raft marker CD59. Mechanistically, it was found that this specific UDM association is determined by the Gag structural domain matrix (MA).

Introduction

HIV-1 spread between cultured T cells is efficiently mediated by cell-to-cell transmission[1-5]. T cells in lymphoid organs, where cell-to-cell transmission likely occurs, adopt a polarized morphology[6-10]. Therefore, understanding the mechanisms of HIV-1 localization, assembly and transmission in polarized T cells could provide better insights into how HIV-1 is spread *in vivo*.

Polarized T cells form two ends, the leading edge at the front and a protrusion at the rear called a uropod. Uropods are enriched in several adhesion molecules including PSGL-1, CD43, CD44, ICAM-1, ICAM-3, CD44[11-15], as well as the lipid raft marker CD59[11]. Functionally, uropods are important for T cell migration and are known to mediate cell-cell contacts[16, 17]. In chapter II it was shown that HIV-1 Gag localizes to uropods in polarized T cells, which participated in virological synapses between HIV-1 infected and uninfected T cells.

The HIV-1 structural polyprotein Gag is sufficient to form virus like particles (VLPs)[18]. Starting at the N-terminus, Gag is composed of four structural domains: matrix (MA), capsid (CA), nucleocapsid (NC) and the late domain p6. MA mediates membrane targeting and binding. CA and NC mediate multimerization. CA mediates multimerization through a dimerization interface in its C-terminal region[19-23]. NC likely mediates multimerization of Gag by binding and utilizing RNA as a scaffold[19,

21, 24-26]. NC also recognizes and packages the viral RNA genome[27]. p6 facilitates pinching off of virus particles by recruiting the cellular ESCRT complex.

MA mediates binding of Gag to the plasma membrane through a bipartite signal. The first is an N-terminal myristate moiety that is normally sequestered within MA. Through a structural change, the myristate is exposed and inserted into the inner-leaflet of the plasma membrane, which increases membrane binding of Gag[28-32]. The second signal is a stretch of basic amino acids that form a highly basic region (HBR) on the surface of MA[30, 33-36]. The positive charge of the HBR is thought to increase Gag association with acidic lipids in the plasma membrane. Residues found within the HBR also mediate a direct interaction between Gag and a negatively charged phospholipid, phosphatidylinositol-(4,5)-bisphosphate [PI(4,5)P2], and thereby facilitate Gag membrane targeting and binding[37-39]. In this chapter, another function of MA is described in which it plays a role in determining microdomain association of Gag.

Plasma membrane microdomains are dynamic, sub-microscopic clusters of lipids and/or proteins. HIV-1 Gag associates with cholesterol and sphingomyelin-enriched microdomains called lipid rafts.. Consistent with this notion, Gag has been observed to colocalize with GM1[41, 43], a well-known lipid raft marker. Notably, lipid rafts have been found to be important for Gag membrane binding and virus assembly[40-42]. For example, disrupting lipid rafts by cholesterol depletion results in a reduction of HIV-1 virus release[41, 44, 45]. Also, another study found that multimerization of Gag facilitated its association with microdomains “barges” that were important for virus assembly[40]. In addition to lipid rafts, markers for other microdomains also colocalize with Gag. For example, tetraspanins such as CD9, CD63, CD81 and CD82, which homo-

or hetero-oligomerize to form tetraspanin-enriched microdomains (TEMs), have also shown strong colocalization with Gag[46]. Lipid rafts and TEMs are experimentally distinguishable by different sensitivities to cholesterol depletion[47] and by microscopy[46, 48]. Recently, it was shown by Hogue et. al. that Gag is able to reorganize the plasma membrane bring lipid rafts and TEMs together[48]. Therefore, Gag may drive the formation of unique microdomains on the plasma membrane.

In addition to the role lipid rafts play in virus assembly, TEMs also seem to play a role in virus spread. For example, knockdown of CD81 was observed to increase cell-to-cell transmission[49]. Tetraspanins have been found to be enriched in virological synapses[50] and appear to prevent Env-mediated cell-cell fusion[51]. Interestingly, knocking down CD81 also decreases virus release, but increases virus infectivity[52]. Thus, TEMs may serve a delicate balance of functions that both enhance and inhibit virus replication. Further studies are required to better define the function of different TEMs in virus spread.

Recently, it was observed that Gag associates with another group of microdomains termed exosomes/microvesicles (EMVs) or endosome-like domains (ELDs) from which exosomes are secreted[53, 54]. It was also determined that multimerization and membrane binding are sufficient to drive ELD association[54]. Because one of the markers for ELDs is the tetraspanin CD63, it is conceivable that the TEMs with which Gag associates represent the same microdomain as ELDs. Notably, these observations define a specific microdomain with which Gag associates with, show that multimerization is sufficient to drive this localization, and are consistent with a model in which the Gag-ELD association drives polarity of ELDs on the plasma

membrane[53, 54]. These findings are consistent with the observations and working model developed in this thesis.

In chapter II it was found that Gag associates with uropod-directed microdomains that could carry Gag to the uropod in polarized T cells and that NC-mediated multimerization is required for uropod localization. However, the composition of UDMs, how Gag associates with them, and the level of multimerization that is sufficient to drive Gag localization to uropods remained to be elucidated. Observations made in this chapter support a model in which multimerization at the level of tetramerization or higher is sufficient to drive Gag localization to uropods and that Gag associates with a specific subset of UDMs via an MA-dependent mechanism.

Results

Virus surfing and membrane curvature are not required for uropod localization.

In chapter II it was determined that NC-mediated multimerization drives uropod localization of Gag. However, what aspects of multimerization drive uropod localization were undefined. Gag multimerization is required for membrane curvature and particle formation. Virus particles are known to undergo virus surfing, in which they unidirectionally migrate on the outer leaflet of the plasma membrane in a receptor- and actin/myosin-dependent manner. For example, when Murine Leukemia Virus (MLV) particles, another retrovirus, were exogenously added to HEK293 cells, they were observed to move on the plasma membrane to the cell body[55]. This was also observed for HIV-1 as well as for virus particles pseudotyped with the envelope proteins of avian leukosis virus (ALV) or vesicular stomatitis virus (VSV). In addition to exogenously

added virus particles, newly formed MLV particles from infected HEK293 cells were also observed to undergo surfing[56]. In another study, what appeared to be newly formed HIV-1 particles were observed by spinning disk confocal microscopy to form outside of cell-cell contact sites followed by lateral localization of these particles to the contact sites, which is consistent with virus surfing[57]. Thus, while these experiments observed either MLV or HIV-1 in the context of adherent HEK293 cells, it is conceivable that this outer-leaflet surfing mechanism could also mediate uropod localization in polarized T cells.

To address the possibility that surfing of virus particles mediates HIV-1 localization to uropods, two fluorescently tagged CA mutants of Gag were utilized. P99A/Gag-YFP and EE75,76AA/Gag-YFP multimerize on the plasma membrane but do not efficiently curve the membrane or form virus particles[22, 48, 58](Fig. 3.1A). This phenotype is evident in electron micrographs showing electron dense patches of P99A/Gag-YFP and EE75,76AA/Gag-YFP in HeLa cells (Fig. 3.1B, images taken by Ferri Soheilian and Kunio Nagashima). It should be noted that, while the planar multimer phenotype likely also occurs in T cells based on the above micrographs, electron microscopy of these mutants should also be done in T cells.

P99A/Gag-YFP and EE75,76AA/Gag-YFP were expressed in P2 cells by spin infection and immunostained for the uropod marker PSGL-1 by copatching. Interestingly, both of these planar multimer mutants clearly localized to the uropod (Fig. 3.1C). These observations indicate that membrane curvature or particle formation, and hence virus surfing on the outer leaflet of the plasma membrane, are not required for uropod localization of Gag. Conversely this observation also indicates that multimerization and

association with the inner leaflet of the plasma membrane are sufficient for Gag to localize to the uropod.

Low level of multimerization is sufficient for Gag polarization towards the uropod.

For wild type Gag-YFP, multimerization requires both CA and NC. However, a Gag-YFP construct that replaces NC with a heterologous dimerizing leucine zipper(LZ) sequence (LZ/Gag-YFP) is still capable of multimerizing and forming virus-like particles (VLPs)[59-61]. In chapter II, it was shown that LZ/Gag-YFP localizes to the uropod. Disrupting the CA dimerization interface in this construct (Fyn(10)/LZ/WMAA/Gag-YFP), which should only allow LZ-mediated dimerization, caused a loss of uropod localization. Because the planar multimer mutants localized so strongly to the uropod, these results collectively suggest that uropod localization occurs early in the assembly process after Gag dimerization but before membrane curvature.

To test whether polarized localization of Gag occurs early in assembly, low-order Gag multimer mutants were examined. While the LZ sequence normally functions as a dimerization motif, specific mutations have been shown to change its oligomerization property from a dimer to a trimer(LZ3)[62] or tetramer(LZ4)[63]. Thus, to make trimeric and tetrameric Gag, these mutations were introduced into the dimeric LZ/WMAA/Gag-YFP construct (Fig. 3.2A). The WMAA CA mutations were introduced to ensure that LZ was the only interacting domain. However, theses CA mutations decrease multimerization and hence the number of myristates available for membrane binding[21, 64]. To overcome this membrane binding deficiency, the MA mutation 20LK, which is known to increase membrane binding[32, 65], was also introduced into the LZ mutant

constructs. A monomeric Gag construct containing this 20LK mutation and mutations of both the CA dimerization interface and the 15 basic residues of NC (20LK/WMAA/14A1G/Gag-YFP) was also examined. This construct is similar to a previously described monomeric Gag mutant[66]. 20LK/WMAA/14A1G/Gag-YFP (monomer), 20LK/WMAA/LZ/Gag-YFP (dimer), 20LK/WMAA/LZ3/Gag-YFP (trimer) and 20LK/WMAA/LZ4/Gag-YFP (tetramer) (Fig. 3.2A) will be referred to hereafter as monomeric/, LZ2/, LZ3/ and LZ4/Gag-YFP respectively.

When expressed in polarized P2 cells, the monomeric/, LZ2/ and LZ3/Gag-YFP constructs were observed to localize around the entire plasma membrane. In contrast, while LZ4/Gag-YFP was not as polarized as the 20LK/LZ/Gag-YFP positive control, it was significantly more polarized than monomeric/, LZ2/ or LZ3/Gag-YFP (Fig. 3.2B). Polarization of these mutants in P2 cells is quantified in Fig. 3.2C. These findings suggest that uropod localization of Gag occurs early in the assembly process after the multimerization of four or more Gag proteins.

Gag associates with a specific subset of uropod-directed microdomains.

Observations from chapter II suggest that Gag associates with uropod-directed microdomains, enriched in the uropod markers CD43 and PSGL-1, that could carry Gag to the uropod. Determining the composition of UDMs could lead to a better understanding of their function. Thus, in addition to PSGL-1 and CD43, copatching between Gag and other uropod-associated proteins ICAM-1, ICAM-3, CD44 and CD59[11-14] (Fig. 3.4A-D, top panels) was also examined in unpolarized P2 cells. Gag-YFP was observed to copatch with PSGL-1 and CD43 as previously observed (quantified

but images not shown) and also copatched with CD44 (Fig. 3.3D, lower panel). However, Gag did not copatch with ICAM-1, ICAM-3 or CD59 (Fig. 3.3A-C, lower panels). These observations are quantified in Fig. 3.3E and indicate that Gag associates with a specific subset of UDMs.

Membrane curvature is not required for recruitment of specific UDMs.

Because Gag appears to associate with a specific subset of UDMs, it is possible that association of Gag with these specific UDMs confers a selective advantage to virus replication compared to other UDMs. Thus, the mechanism of Gag association with specific UDMs requires further elucidation.

Membrane curvature can facilitate recruitment of some cell surface proteins[67]. It was also recently observed that Gag is able to coalesce microdomains, such as lipid rafts and TEMs, that do not normally colocalize. Because membrane curvature was also implicated in this Gag-mediated microdomain recruitment[48], it is conceivable that Gag associates with specific UDMs that are attracted to membrane curvature as opposed to those that are not.

To investigate whether specific UDM association by Gag is determined by membrane curvature, copatching between the planar multimer mutants P99A/Gag-YFP and EE75,76AA/Gag-YFP and the uropod markers PSGL-1, CD43 and CD59 was examined in unpolarized P2 cells. Almost identically to wild type Gag-YFP, both of the planar multimer mutants were observed to copatch with PSGL-1 and CD43 but not with CD59 (Fig. 3.4A-C). Copatching was quantified in Fig. 3.4D. These observations indicate that inhibition of membrane curvature does not disrupt the specific UDM

association observed for wild type Gag-YFP and that the specificity of UDM association is likely determined earlier in the HIV-1 assembly process.

MA determines specificity of UDM association.

It is conceivable that while multimerization is required for uropod localization, it may not drive the specificity of UDM association. Thus, it is possible that a viral component is required in conjunction with multimerization to determine specific UDM association. The most likely Gag component to determine UDM specificity would be MA because it is the domain of Gag that interacts directly with the plasma membrane. Thus, a Gag mutant in which MA was deleted (Fyn(10)/ΔMA/Gag-YFP) was expressed in P2 cells and examined for UDM association by copatching analysis. To control for the addition of Fyn(10), which is necessary to compensate for the loss of membrane binding in the absence of MA, Fyn(10)/ΔMA/Gag-YFP was compared to Fyn(10)/Gag-YFP. Strikingly, while Fyn(10)/Gag-YFP appears to associate with the same PSGL-1/CD43-enriched subset of UDMs as Gag-YFP (Fig. 3.5A), the loss of MA caused Gag to segregate from PSGL-1 and CD43 (Fig. 3.5B). Both Fyn(10)/Gag-YFP and Fyn(10)/ΔMA/Gag-YFP also did not copatch with ICAM-3 similar to WT (Fig. 3.5A-B). Interestingly, copatching between Fyn(10)/ΔMA/Gag-YFP and CD59 was enhanced when compared to Fyn(10)/Gag-YFP (Fig. 3.5A-B). Copatching is quantified in Fig. 3.5C. Together, these data indicate that MA determines the association of Gag with specific UDMs.

Discussion

Uropod localization of HIV-1 Gag requires multimerization. However, it was unknown what aspect of multimerization drove this localization. One potential mechanism of localization of HIV-1 on the plasma membrane is virus surfing. Surfing has been observed for virus particles containing envelope proteins of several viruses including MLV, ALV, VSV and HIV-1 in HEK293 cells[55]. However, because the planar mutants P99A/Gag-YFP and EE75,76AA/Gag-YFP were observed to localize to the uropod, it was determined that membrane curvature, and subsequently virus surfing on the plasma membrane, are not required for uropod localization of Gag in polarized T cells. It should be noted that, while these results indicate that inner leaflet association is sufficient for uropod localization of Gag, it does not exclude the possibility that HIV-1 virus particles could also surf on the outer leaflet of the plasma membrane to the uropod. For example, exogenously added Gag-YFP virus particles that are attached to the cell surface, but not fused to the membrane, also localize to the uropod (data not shown). This suggests that Gag-YFP particles can surf on the outer leaflet of the plasma membrane to the uropod in a manner consistent with the surfing observed for exogenously added HIV-1 and MLV particles in HEK293 cells[55]. Virus surfing could also explain the observation that unpolarized patches of Gag in unpolarized T cells localize to contact sites after the contacts are formed[3, 68]. However, because planar multimer mutants localize strongly to the uropod and tetrameric Gag tends to polarize on the plasma membrane, it suggests that uropod localization begins at an early stage of the assembly process. Supporting this model, the dynamics of HIV-1 assembly have been studied and found that after nucleation, a particle forms in roughly 8-9 minutes[69]. In chapter II (fig.

1) live cell analysis observing a Gag-YFP-expressing polarized T cell over 20 minutes did not show any particles or patches of Gag forming outside of the uropod. This observation is consistent with a model in which, in T cells that are already polarized, assembling virus particles reach the uropod before virus particle formation is completed.

It is also possible that virus surfing is not responsible for the localization of HIV-1 to the site of cell-cell contacts observed between HEK293 cells[57] or unpolarized T cells[3, 68]. For example, because planar multimers still form visible patches and puncta on the plasma membrane (Fig. 3.1 and Fig. 3.4) it can not be ruled out that these "particles" were not fully formed before the observed migration of HIV-1 to cell-cell contact sites occurred. Therefore, these potentially pre-formed particles could have utilized the inner-leaflet-associated mechanism that facilitates Gag localization to uropods in polarized T cells. Repeating those experiments with planar multimer mutants or performing correlative scanning electron microscopy of virus assembly in similar experiments is required to determine whether the observed polarized localization to contact sites between unpolarized T cells or HEK293 cells is truly due to virus surfing.

It was found that Gag associates with a specific subset of UDMs enriched in PSGL-1, CD43 and CD44 but not ICAM-1, ICAM-3 or the lipid raft marker CD59. Other microdomains, such as lipid rafts and TEMs, have been observed to be important for HIV-1 functions including virus assembly/release, spread, and localization[41-43, 46, 49]. Thus, a possible function of UDMs is to facilitate uropod localization on the plasma membrane. As discussed in chapter II, uropod localization of Gag is beneficial to the virus because uropods participate in virological synapses and promote cell-to-cell transfer of virus particles. However, because ICAM-1, ICAM-3 and CD59 also localize to the

uropod, it is conceivable that uropod localization of Gag would also be mediated if Gag associated with these uropod proteins. Thus, it is possible that there are other functions of CD43/PSGL-1/CD44-enriched UDMs that benefit HIV-1.

One potential benefit for Gag specifically associating with CD43/PSGL-1/CD44-enriched UDMs is that crosslinking PSGL-1 is known to activate a signaling pathway that results in the increased avidity of the adhesion molecule LFA-1 to its binding partner ICAM-1[70]. LFA-1 is enriched in the virological synapse and can promote its stability[71]. Thus, it is conceivable that Gag association with PSGL-1 could induce this signaling pathway to increase cell-cell adhesion and enhance HIV-1 cell-to-cell transmission. Association with other uropod proteins such as the adhesion molecules CD43 and CD44 could also enhance virus replication by increasing attachment to target cells.

Because of the potential impact of Gag association with specific UDMs on virus replication, it is important to elucidate the mechanism of this interaction. Membrane curvature has been implicated in Gag recruitment of different microdomains in HeLa cells[48]. However, it was found that MA, not membrane curvature, determined the association of Gag with a specific subset of UDMs. One possibility for this MA-mediated recruitment of specific UDMs could be the presence of a direct interaction between Gag and a UDM-associated protein. In chapter II, myosin was found to be required for polarized localization of Gag, indicating that the actin cytoskeleton is important for uropod localization. Uropod proteins are linked to the actin cytoskeleton by ERM proteins (ref). Thus, it is conceivable that an interaction between Gag and a uropod protein could also link multimerizing Gag to the actin cytoskeleton, enabling uropod

localization. Alternatively, it can be speculated that Gag association with specific UDMs is indirect. For example, the highly basic region (HBR) of MA associates with the phospholipid PI(4,5)P_2. If PSGL-1, CD43 and CD44 also have an affinity for PI(4,5)P_2, then it is conceivable that association of Gag with specific UDMs is based on this shared phospholipid association.

The finding that Fyn(10)/ΔMA/Gag-YFP localizes to the uropod but does not associate with the same specific subset of UDMs as Gag-YFP or Fyn(10)/Gag-YFP suggests that UDM association may not be required for Gag localization to the uropod. In conjunction with tetrameric Gag being more polarized than monomeric, dimeric or trimeric Gag, and planar multimers localizing to uropods, these observations could support a model in which Gag multimerization is the sole factor that drives its localization to uropods. However, it is also possible that association with alternative UDMs drives Fyn(10)/ΔMA/Gag-YFP localization to uropods. This model is supported by the observation that Fyn(10)/ΔMA/Gag-YFP copatches strongly with the uropod-associated lipid raft marker CD59. It is likely that the association of Fyn(10)/ΔMA/Gag-YFP with CD59 is driven by the Fyn(10) sequence, which encodes a myristoylation and two palmitoylation signals. These acylation signals have been observed to preferentially mediate cholesterol-dependent clustering of modified proteins on the plasma membrane. These modified proteins associated with DRMs[72], which suggests lipid raft association. Thus, it is conceivable that MA actively associates with specific UDMs and overcomes the affinity of Fyn(10) for CD59-enriched lipid rafts, while in the absence of MA, Fyn(10) facilitates Gag association with CD59-enriched lipid rafts that also transport Gag to the uropod.

Because of the observations that multimerization drives uropod localization and that MA determines specificity of UDM association, it is conceivable that any HIV-1 Gag mutant that multimerizes enough to polarize to the uropod and contains MA will associate with CD43/PSGL-1/CD44-enriched UDMs. Therefore, the increased polarization of LZ4/Gag-YFP suggests that multimerization at the level of a tetramerization or higher allows MA-mediated association of Gag with specific UDMs that then carry Gag to the uropod. Multimerization-mediated microdomain association is consistent with observations by the Gould group that show multimerization is required for association of HIV-1 Gag with ELD microdomains[53]. However, LZ4/Gag-YFP does not form visible patches or puncta on the cell surface and therefore cannot be examined by copatching analyses. Thus, super resolution microscopy, which can detect the correlation between two plasma membrane-associated proteins on a nanometer scale, is likely required to determine whether tetrameric Gag indeed associates with specific UDMs in the future.

The observations described in this chapter have further defined the relationship between Gag multimerization and uropod localization and the association between HIV-1 Gag and microdomains in biologically relevant polarized T cells. These findings lead to a more refined working model of HIV-1 in polarized T cells: When NC-mediated multimerizaton reaches the level of tetramerization or higher, Gag associates with specific uropod-directed microdomains enriched in CD43, PSGL-1 and CD44 via an MA-mediated mechanism. These Gag-associated UDMs then laterally localize on the membrane to the uropod where virus particles assemble and accumulate. Uropods then mediate contact and VS formation with target cells to facilitate cell-to-cell transmission.

(Fig. 3.6). Thus, this chapter defines in much greater detail the role of Gag multimerization in uropod localization and elucidates a novel function of MA in determining Gag association with a specific subset of uropod-directed microdomains, which could have a significant impact on virus replication and spread.

Materials and Methods

Plasmids

The HIV-1 molecular clone Gag-YFP was described previously[21, 37]. The YFP-tagged planar multimer mutants contain CA mutations P99A or EE75,76AA (P99A/Gag-YFP and EE75,76AA/Gag-YFP). They were constructed by standard molecular biology techniques to introduce the mutations as described previously[22, 48]. Derivatives of pNL4-3/Gag-YFP in which the start codon or the entire MA sequence was replaced by 10 amino acids that encode two palmitoyl and a myristoyl signal from Fyn kinase, Fyn(10)/Gag-YFP and Fyn(10)/ΔMA/Gag-YFP, respectively, have been described previously[37]. The LZ mutants 20LK/WMAA/LZ/Gag-YFP, 20LK/WMAA/LZ3/Gag-YFP, 20LK/WMAA/LZ4/Gag-YFP, (LZ2/, LZ3/, and LZ4/Gag-YFP respectively), were constructed by first introducing LZ into 20LK/Gag-YFP by standard molecular biology techniques followed by PCR mutagenesis of LZ. All mutants were in the context of the pNL4-3 molecular clone of HIV-1[73].

Copatching Assay

P2 cells, a polarized T cell line derived from A3.01 T cell line described previously[74], were cultured in RPMI media containing 10% FBS (RPMI-10). Gag-YFP

and its derivatives were expressed in P2 cells by spin infection with VSV-G pseudotyped virus stocks encoding the Gag derivatives as described previously[74]. Infected cells were maintained in RPMI-10 for 2 days. Cells were then resuspended in primary antibody, CD43, CD44, PSGL-1, ICAM-1, ICAM-3, or CD59 (BD Biosciences Pharmingen. San Diego, CA) and incubated for 30 min at 37°C. Cells were washed in RPMI-10 and resuspended in AlexaFluor-594-conjugated goat anti-mouse IgG secondary antibody (Invitrogen. Carlsbad, California) for 30 min at 37°C. Cells were then washed, fixed in 4% paraformaldehyde and processed for microscopy as previously described[74]. For Gag-YFP derivatives, copatching between Gag and UDM marker localized on the tops of cells were quantified as described in Chapter II. Because Fyn(10)/ΔMA/Gag-YFP localizes to internal compartments as well as the cell membrane, to ensure only plasma membrane-associated Gag was quantified for colocalization, images were taken of Fyn(10)/Gag-YFP and Fyn(10)/ΔMA/Gag-YFP-expressing cells through the center plain of the cell. Quantification was then calculated from Gag and UDM marker on the outer edge of the cell using ImageJ and the JaCop plugin as previously described[74].

Polarization calculation

Cells expressing monomeric/, LZ2/, LZ3/, LZ4/ or LZ/Gag-YFP were fixed in 4% PFA for 20min, washed with PBS-2%FBS and mounted on slides as described above. To quantify polarity of Gag localization, a 10-segmented grid was placed over each cell along the cell's longest axis. 10 minus the number of segments that contained plasma membrane-associated Gag was then used as the polarization index. Thus a higher number

corresponds to higher polarization, with 0 corresponding to Gag distributed over the entire plasma membrane.

Nucleofection

For Gag mutants encoding Fyn(10) on their N-terminus, nucleofection of the DNA by Amaxa kit V was used to express these mutants in P2 cells because virus stocks of these mutants have low infectivity. Briefly, $1x10^6$ P2 cells were resuspended in 100μl Amaxa V solution and transferred to a cuvette. Program C-016 was used to electroporate the samples. Transfected cells were added to 2ml RPMI-10 and cultured for 3 days before immunostaining experiments were performed.

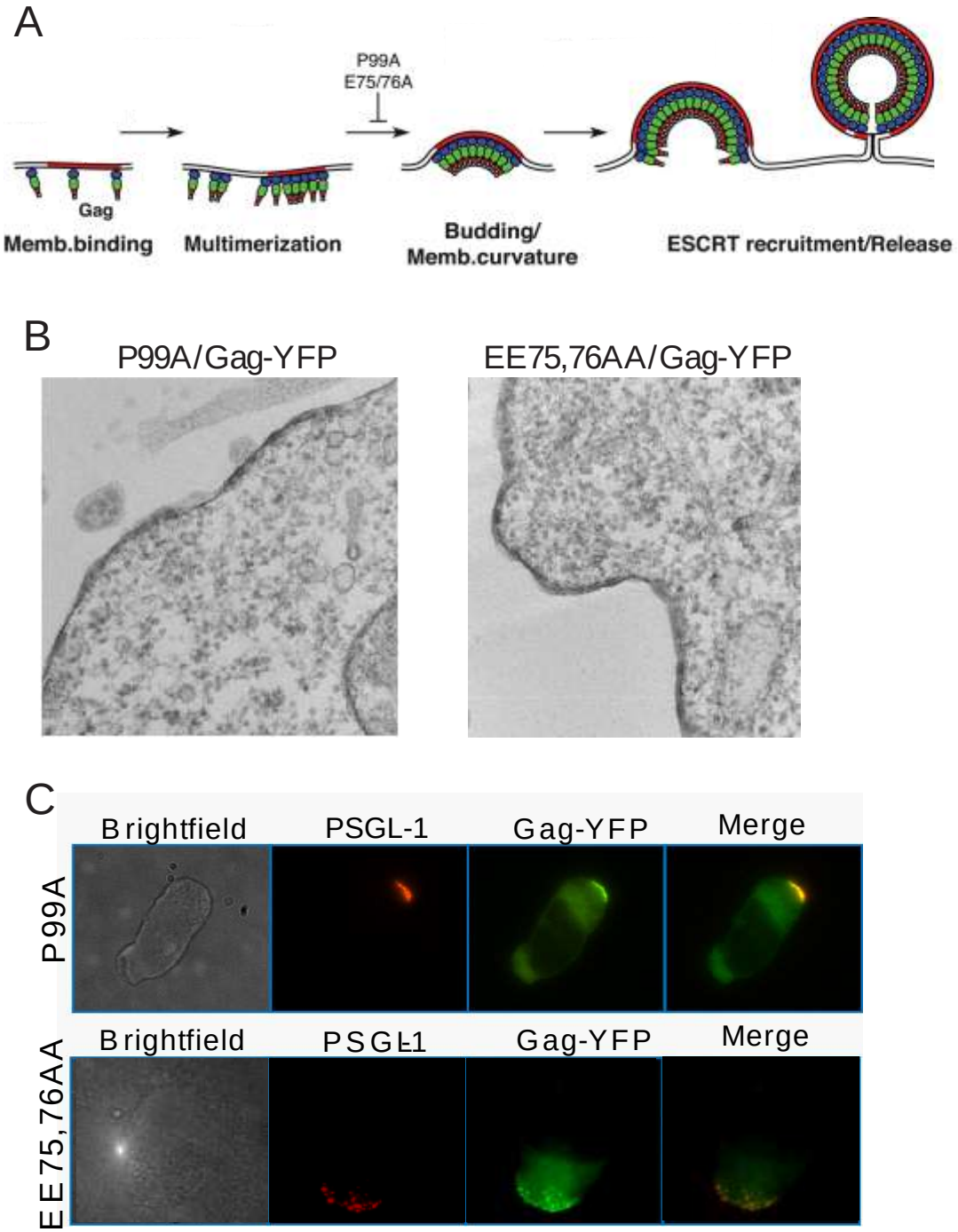

Figure 3.1. Membrane curvature or particle formation is not required for uropod localization. A) Cartoon indicating the step in Gag assembly that is inhibited by the CA mutations P99A and EE75,76AA. **B)** Electron micrographs of HeLa cells expressing P99A/Gag-YFP (left panel) or EE75,76AA/Gag-YFP (right panel). Note the electron dense patches of Gag but lack of virus-like particles. **C)** P2 were infected with VSVG-pseudotyped virus particles encoding P99A/Gag-YFP (upper panel) or EE75,76AA/Gag-YFP (lower panel) and immunostained for PSGL-1 by copatching. Infected polarized cells were observed to determine uropod localization.

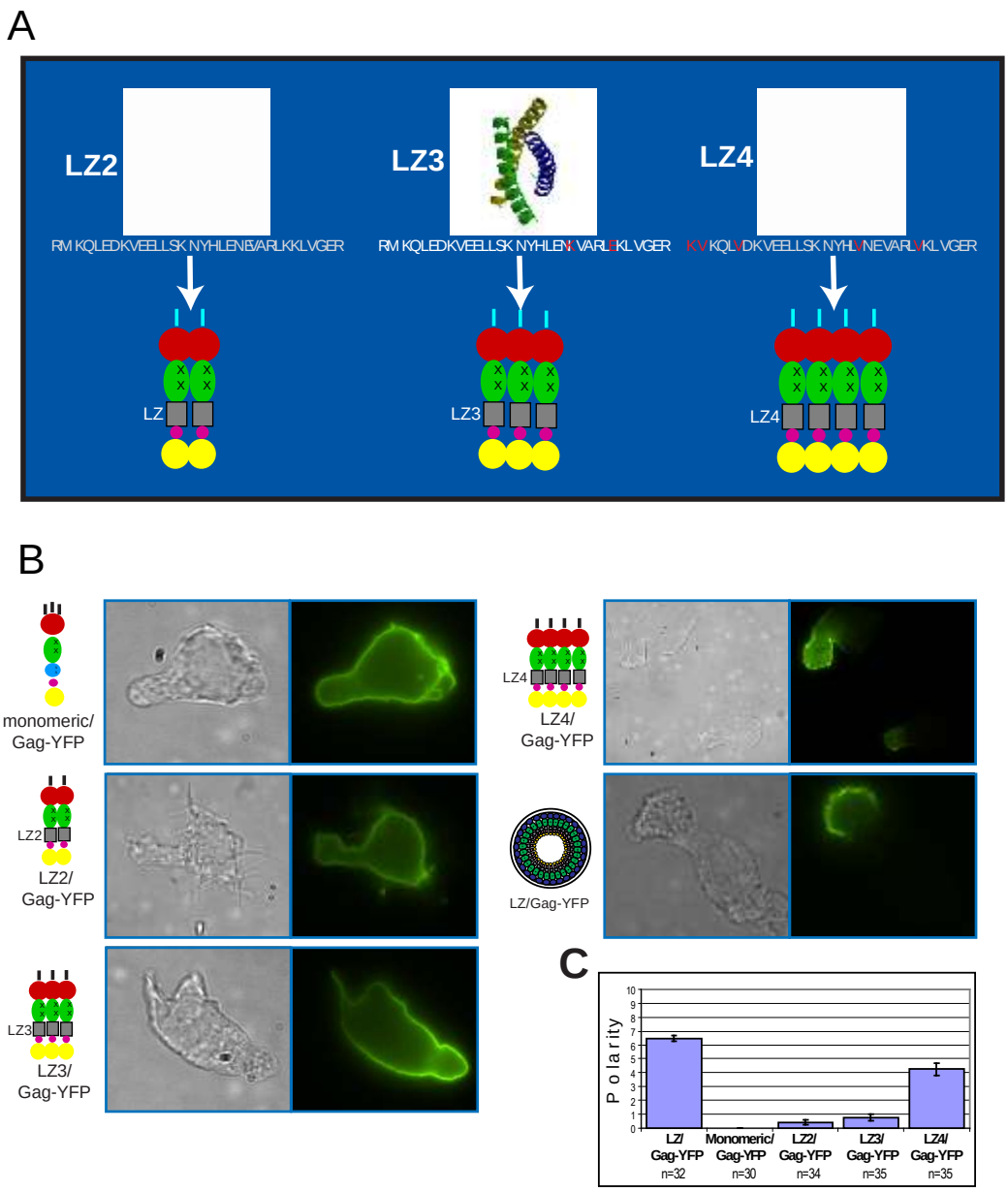

Figure 3.2. LZ4/Gag-YFP polarizes more than monomeric/, LZ2/ or LZ3/Gag-YFP. **A)** Illustration of low-order multimer Leucine Zipper (LZ) mutants. Mutations (denoted by red letters) were made in the sequence of the dimeric leucine zipper sequence to generate what are expected to be trimeric and tetrameric LZ sequences. These LZ sequences were inserted in place of NC. The CA mutation, WM184,185AA (WMAA, denoted by two X), prevents CA-mediated dimerization and was introduced into the constructs to ensure that LZ provides the only Gag-Gag interaction. All constructs contain the MA mutation 20LK, which increases membrane binding. **B)** Monomeric/Gag-YFP, containing mutations in the CA dimerization interface and 15 basic residues in NC, LZ2/, LZ3/, LZ4/Gag-YFP, and an LZ/Gag-YFP construct that multimerizes and forms particles were packaged into VSV-G-pseudotyped virus particles and used to infect P2 cells. **C)** Polarity of the mutants in polarized P2 cells was measured as the amount of cell perimeter not covered by Gag. Error bars represent standard error of the mean.

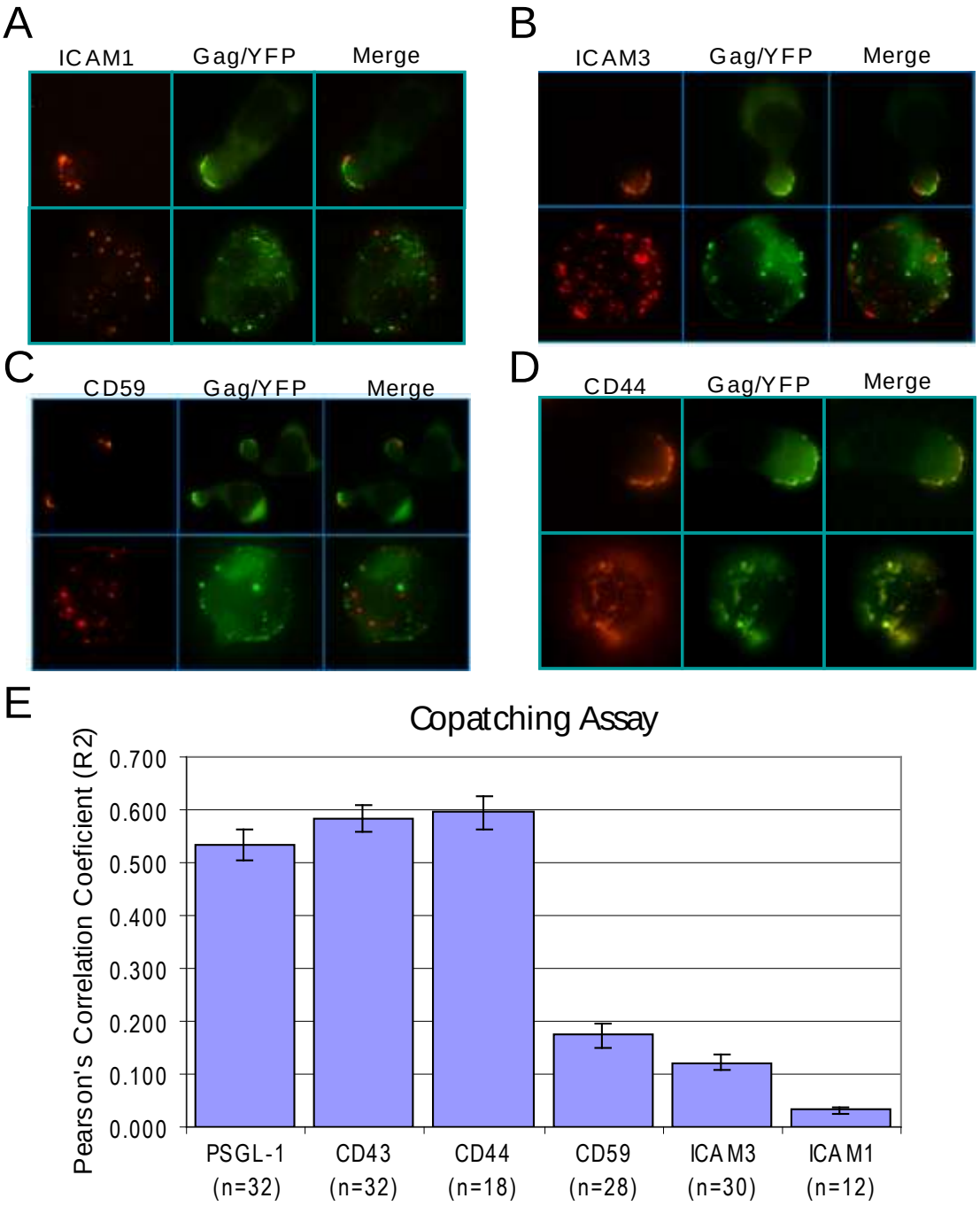

Figure 3.3. Gag associates with a specific subset of uropod-directed microdomains. P2 cells were infected with a VSVG-pseudotyped virus encoding Gag-YFP. Cells were immunostained by copatching assay for **A)** ICAM-1, **B)** ICAM-3, **C)** CD59 and **D)** CD44. Polarized cells were observed to confirm that the uropod proteins were enriched at the uropod (**A-D**, top panels) and unpolarized cells were examined to observe whether uropod markers were enriched in Gag-associated UDMs (**A-D**, bottom panels). **E)** The level of copatching between Gag and uropod markers was measured by the square of Pearson's correlation coefficient. n=the number of cells used in calculations. Error bars represent standard error of the mean.

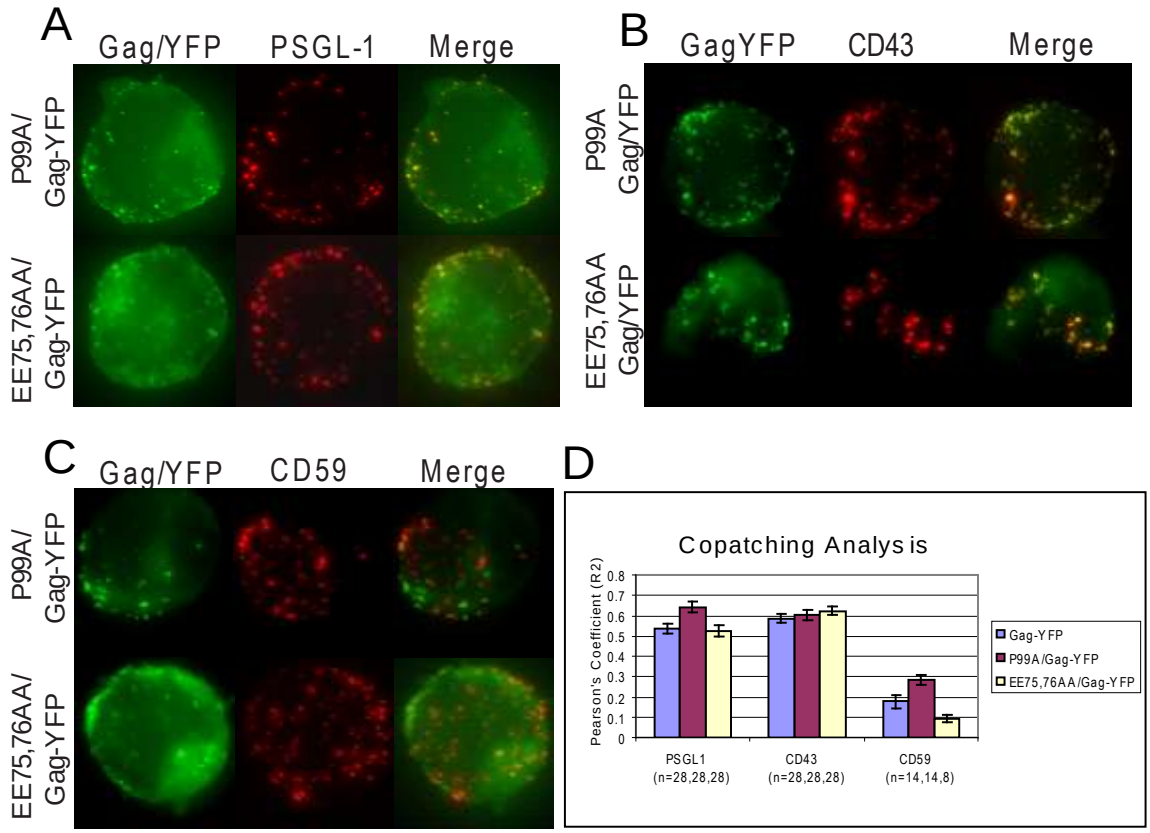

Figure 3.4. Membrane curvature is not required for specific UDM association.
P2 cells were infected with VSV-G-pseudotyped virus particles encoding the planar multimer mutants P99A/Gag-YFP (**A-C,** top panels) and EE75,76AA/Gag-YFP (**A-C,** bottom panels). These cells were immunostained for **A)** PSGL-1, **B)** CD43 or **C)** CD59 by copatching. **D)** The level of copatching between Gag and uropod markers was calculated using the square of Pearson's correlation coefficient. n=the number of cells used in calculations. Error bars represent standard error of the mean.

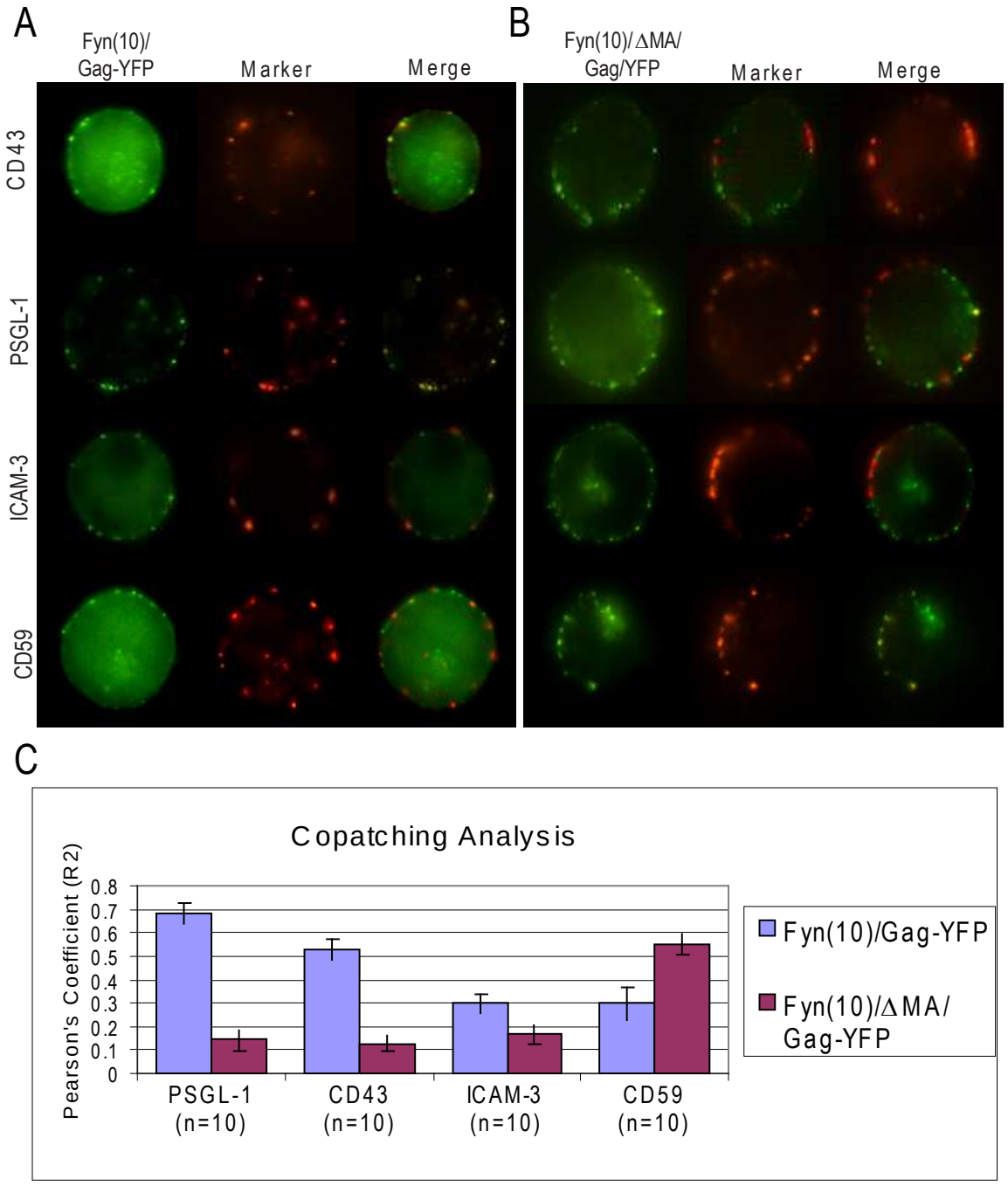

Figure 3.5. Gag association with specific UDMs is determined by MA.
P2 cells were transfected by Amaxa nucleofection with DNA encoding **A)** Fyn(10)/Gag-YFP or **B)** Fyn(10)/ΔMA/Gag-YFP. Cells were immunostained by copatching for PSGL-1, CD43, ICAM-3 or CD59. **C)** The level of copatching between Gag and uropod markers was calculated using the square of Pearson's correlation coefficient. n=the number of cells used in calculations. Error bars represent standard error of the mean.

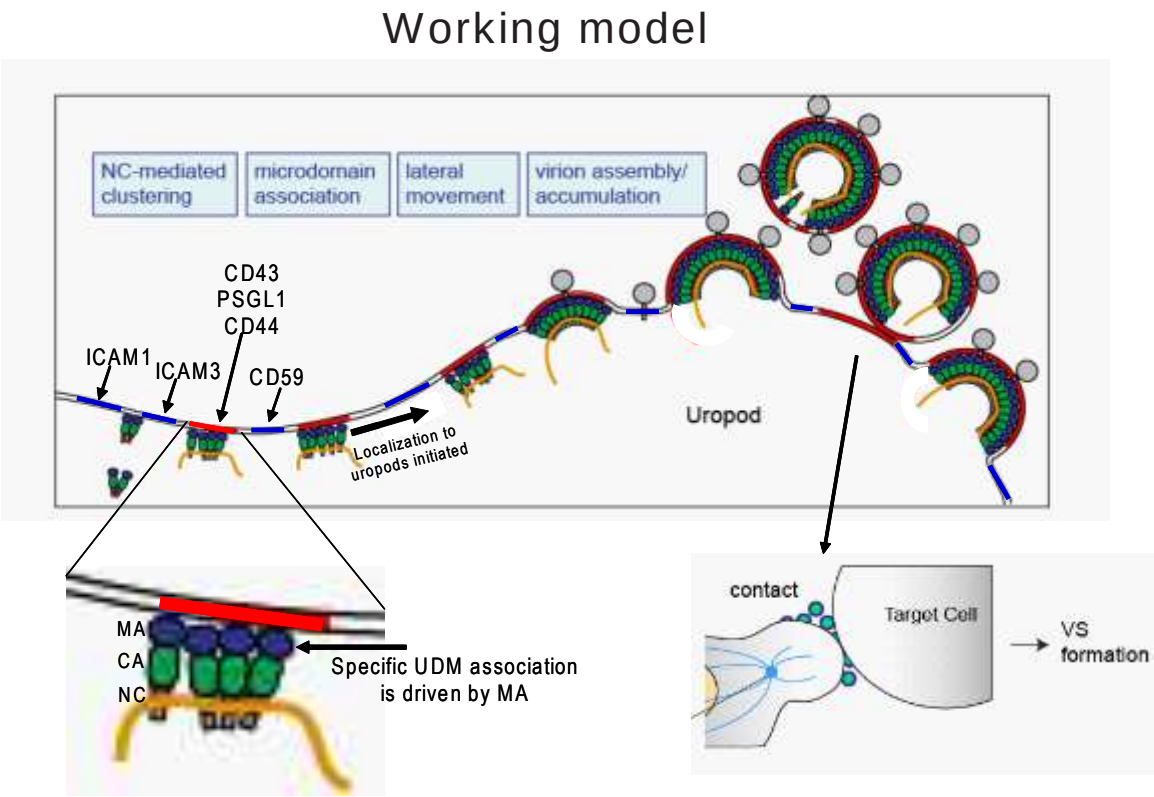

Figure 3.6. Working Model.

When NC-mediated multimerizaton reaches the level of tetramerization or higher, Gag associates with specific uropod-directed microdomains enriched in CD43, PSGL-1 and CD44 via an MA-mediated mechanism. These Gag-associated UDMs then laterally localize on the membrane to the uropod where virus particles assemble and accumulate. Uropods then mediate contact and VS formation with target cells to facilitate cell-to-cell transmission.

References

1. **Chen, P., et al.,** ***Predominant mode of human immunodeficiency virus transfer between T cells is mediated by sustained Env-dependent neutralization-resistant virological synapses.*** **Journal of Virology, 2007. 81(22): p. 12582-12595.**

2. **Dimitrov, D.S., et al.,** ***Quantitation of human immunodeficiency virus type 1 infection kinetics.*** **J Virol, 1993. 67(4): p. 2182-90.**

3. **Hubner, W., et al.,** ***Quantitative 3D Video Microscopy of HIV Transfer Across T Cell Virological Synapses.*** **Science, 2009. 323(5922): p. 1743-1747.**

4. **Martin, N., et al.,** ***Virological Synapse-Mediated Spread of Human Immunodeficiency Virus Type 1 between T Cells Is Sensitive to Entry Inhibition.*** **Journal of Virology, 2010. 84(7): p. 3516-3527.**

5. **Mazurov, D., et al.,** ***Quantitative Comparison of HTLV-1 and HIV-1 Cell-to-Cell Infection with New Replication Dependent Vectors.*** **Plos Pathogens, 2010. 6(2).**

6. **Bajenoff, M., et al.,** ***Stromal cell networks regulate lymphocyte entry, migration, and territoriality in lymph nodes.*** **Immunity, 2006. 25(6): p. 989-1001.**

7. **Hugues, S., et al.,** ***Distinct T cell dynamics in lymph nodes during the induction of tolerance and immunity.*** **Nat Immunol, 2004. 5(12): p. 1235-42.**

8. **Miller, M.J., et al.,** ***Autonomous T cell trafficking examined in vivo with intravital two-photon microscopy.*** **Proc Natl Acad Sci U S A, 2003. 100(5): p. 2604-9.**

9. **Miller, M.J., et al.,** ***Two-photon imaging of lymphocyte motility and antigen response in intact lymph node.*** **Science, 2002. 296(5574): p. 1869-73.**

10. **Mrass, P., et al.,** ***Random migration precedes stable target cell interactions of tumor-infiltrating T cells.*** **J Exp Med, 2006. 203(12): p. 2749-61.**

11. **Alonso-Lebrero, J.L., et al.,** ***Polarization and interaction of adhesion molecules P-selectin glycoprotein ligand 1 and intercellular adhesion molecule 3 with moesin and ezrin in myeloid cells.*** **Blood, 2000. 95(7): p. 2413-9.**

12. **Sanchez-Madrid, F. and M.A. del Pozo,** ***Leukocyte polarization in cell migration and immune interactions.*** **EMBO J, 1999. 18(3): p. 501-11.**

13. **Rosenman, S.J., et al.,** ***Syn-capping of human T lymphocyte adhesion/activation molecules and their redistribution during interaction with endothelial cells.*** **J Leukoc Biol, 1993. 53(1): p. 1-10.**

14. **del Pozo, M.A., et al.,** ***Chemokines regulate cellular polarization and adhesion receptor redistribution during lymphocyte interaction with endothelium and extracellular matrix. Involvement of cAMP signaling pathway.*** **Journal of Cell Biology, 1995. 131(2): p. 495-508.**

15. **Serrador, J.M., et al.,** ***A juxta-membrane amino acid sequence of P-selectin glycoprotein ligand-1 is involved in moesin binding and ezrin/radixin/moesin-directed targeting at the trailing edge of migrating lymphocytes.*** **Eur J Immunol, 2002. 32(6): p. 1560-6.**

16. **McFarland, W. and D.H. Heilman,** ***Lymphocyte Foot Appendage: Its Role in Lymphocyte Function and in Immunological Reactions.*** **Nature, 1965. 205: p. 887-8.**

17. **del Pozo, M.A., et al.,** ***ICAMs redistributed by chemokines to cellular uropods as a mechanism for recruitment of T lymphocytes.*** **Journal of Cell Biology, 1997. 137(2): p. 493-508.**

18. **Adamson, C.S. and I.M. Jones,** ***The molecular basis of HIV capsid assembly--five years of progress.*** **Rev Med Virol, 2004. 14(2): p. 107-21.**

19. **Burniston, M.T., et al.,** ***Human immunodeficiency virus type 1 Gag polyprotein multimerization requires the nucleocapsid domain and RNA and is promoted by the capsid-dimer interface and the basic region of matrix protein.*** **Journal of Virology, 1999. 73(10): p. 8527-8540.**

20. **Gamble, T.R., et al.,** ***Structure of the carboxyl-terminal dimerization domain of the HIV-1 capsid protein.*** **Science, 1997. 278(5339): p. 849-853.**

21. **Hogue, I.B., A. Hoppe, and A. Ono,** ***Quantitative fluorescence resonance energy transfer microscopy analysis of the human immunodeficiency virus type 1 Gag-Gag interaction: relative contributions of the CA and NC domains and membrane binding.*** **J Virol, 2009. 83(14): p. 7322-36.**

22. **von Schwedler, U.K., et al.,** ***Functional surfaces of the human immunodeficiency virus type 1 capsid protein.*** **Journal of Virology, 2003. 77(9): p. 5439-5450.**

23. **Zhang, W.H., et al.,** ***Gag-Gag interactions in the C-terminal domain of human immunodeficiency virus type 1 p24 capsid antigen are essential for Gag particle assembly.*** **Journal of General Virology, 1996. 77: p. 743-751.**

24. **Campbell, S. and V.M. Vogt,** ***Self-Assembly in-Vitro of Purified Ca-Nc Proteins from Rous-Sarcoma Virus and Human-Immunodeficiency-Virus Type-1.*** **Journal of Virology, 1995. 69(10): p. 6487-6497.**

25. Cimarelli, A., et al., ***Basic residues in human immunodeficiency virus type 1 nucleocapsid promote virion assembly via interaction with RNA.*** **Journal of Virology, 2000. 74(7): p. 3046-3057.**

26. Dawson, L. and X.F. Yu, ***The role of nucleocapsid of HIV-1 in virus assembly.*** **Virology, 1998. 251(1): p. 141-57.**

27. D'Souza, V. and M.F. Summers, ***How retroviruses select their genomes.*** **Nat Rev Microbiol, 2005. 3(8): p. 643-55.**

28. Bryant, M. and L. Ratner, ***Myristoylation-Dependent Replication and Assembly of Human Immunodeficiency Virus-1.*** **Proceedings of the National Academy of Sciences of the United States of America, 1990. 87(2): p. 523-527.**

29. Tang, C., et al., ***Entropic switch regulates myristate exposure in the HIV-1 matrix protein.*** **Proceedings of the National Academy of Sciences of the United States of America, 2004. 101(2): p. 517-522.**

30. Zhou, W.J., et al., ***Identification of a Membrane-Binding Domain within the Amino-Terminal Region of Human-Immunodeficiency-Virus Type-1 Gag Protein Which Interacts with Acidic Phospholipids.*** **Journal of Virology, 1994. 68(4): p. 2556-2569.**

31. Freed, E.O., et al., ***Single Amino-Acid Changes in the Human-Immunodeficiency-Virus Type-1 Matrix Protein Block Virus Particle-Production.*** **Journal of Virology, 1994. 68(8): p. 5311-5320.**

32. Ono, A. and E.O. Freed, ***Binding of human immunodeficiency virus type 1 Gag to membrane: Role of the matrix amino terminus.*** **Journal of Virology, 1999. 73(5): p. 4136-4144.**

33. Dalton, A.K., et al., ***Electrostatic interactions drive membrane association of the human immunodeficiency virus type 1 Gag MA domain.*** **Journal of Virology, 2007. 81(12): p. 6434-6445.**

34. Yuan, X., et al., ***Mutations in the N-Terminal Region of Human-Immunodeficiency-Virus Type-1 Matrix Protein Block Intracellular-Transport of the Gag Precursor.*** **Journal of Virology, 1993. 67(11): p. 6387-6394.**

35. Ono, A., J.M. Orenstein, and E.O. Freed, ***Role of the gag matrix domain in targeting human immunodeficiency virus type 1 assembly.*** **Journal of Virology, 2000. 74(6): p. 2855-2866.**

36. Chukkapalli, V., S.J. Oh, and A. Ono, ***Opposing mechanisms involving RNA and lipids regulate HIV-1 Gag membrane binding through the highly basic region of the matrix domain.*** **Proceedings of the National Academy of Sciences of the United States of America, 2010. 107(4): p. 1600-1605.**

37. Chukkapalli, V., et al., ***Interaction between the human immunodeficiency virus type 1 Gag matrix domain and phosphatidylinositol-(4,5)-bisphosphate is essential for efficient gag membrane binding.*** **J Virol, 2008. 82(5): p. 2405-17.**

38. Ono, A., et al., ***Phosphatidylinositol (4,5) bisphosphate regulates HIV-1 gag targeting to the plasma membrane.*** **Proceedings of the National Academy of Sciences of the United States of America, 2004. 101(41): p. 14889-14894.**

39. Saad, J.S., et al., ***Structural basis for targeting HIV-1 Gag proteins to the plasma membrane for virus assembly.*** **Proceedings of the National Academy of Sciences of the United States of America, 2006. 103(30): p. 11364-11369.**

40. Lindwasser, O.W. and M.D. Resh, ***Multimerization of human immunodeficiency virus type 1 Gag promotes its localization to barges, raft-like membrane microdomains.*** **J Virol, 2001. 75(17): p. 7913-24.**

41. Ono, A. and E.O. Freed, ***Plasma membrane rafts play a critical role in HIV-1 assembly and release.*** **Proc Natl Acad Sci U S A, 2001. 98(24): p. 13925-30.**

42. Ding, L., et al., ***Independent segregation of human immunodeficiency virus type 1 Gag protein complexes and lipid rafts.*** **J Virol, 2003. 77(3): p. 1916-26.**

43. Nguyen, D.H. and J.E. Hildreth, ***Evidence for budding of human immunodeficiency virus type 1 selectively from glycolipid-enriched membrane lipid rafts.*** **J Virol, 2000. 74(7): p. 3264-72.**

44. Ono, A. and E.O. Freed, ***Role of lipid rafts in virus replication.*** **Adv Virus Res, 2005. 64: p. 311-58.**

45. Jolly, C. and Q.J. Sattentau, ***Human immunodeficiency virus type 1 virological synapse formation in T cells requires lipid raft integrity.*** **J Virol, 2005. 79(18): p. 12088-94.**

46. Nydegger, S., et al., ***Mapping of tetraspanin-enriched microdomains that can function as gateways for HIV-1.*** **Journal of Cell Biology, 2006. 173(5): p. 795-807.**

47. Claas, C., C.S. Stipp, and M.E. Hemler, ***Evaluation of prototype transmembrane 4 superfamily protein complexes and their relation to lipid rafts.*** **Journal of Biological Chemistry, 2001. 276(11): p. 7974-7984.**

48. Hogue, I.B., et al., ***Gag induces the coalescence of clustered lipid rafts and tetraspanin-enriched microdomains at HIV-1 assembly sites on the plasma membrane.*** **J Virol, 2011. 85(19): p. 9749-66.**

49. Krementsov, D.N., et al., ***Tetraspanins regulate cell-to-cell transmission of HIV-1.*** **Retrovirology, 2009. 6.**

50. Jolly, C. and Q.J. Sattentau, *Human immunodeficiency virus type 1 assembly, budding, and cell-cell spread in T cells take place in tetraspanin-enriched plasma membrane domains.* J Virol, 2007. 81(15): p. 7873-84.

51. Weng, J., et al., *Formation of syncytia is repressed by tetraspanins in human immunodeficiency virus type 1-producing cells.* J Virol, 2009. 83(15): p. 7467-74.

52. Grigorov, B., et al., *A role for CD81 on the late steps of HIV-1 replication in a chronically infected T cell line.* Retrovirology, 2009. 6: p. 28.

53. Shen, B., et al., *Biogenesis of the Posterior Pole Is Mediated by the Exosome/Microvesicle Protein-Sorting Pathway.* J Biol Chem, 2011.

54. Fang, Y., et al., *Higher-order oligomerization targets plasma membrane proteins and HIV gag to exosomes.* PLoS Biol, 2007. 5(6): p. e158.

55. Lehmann, M.J., et al., *Actin- and myosin-driven movement of viruses along filopodia precedes their entry into cells.* Journal of Cell Biology, 2005. 170(2): p. 317-325.

56. Sherer, N.M., J. Jin, and W. Mothes, *Directional spread of surface-associated retroviruses regulated by differential virus-cell interactions.* J Virol, 2010. 84(7): p. 3248-58.

57. Jin, J., F. Li, and W. Mothes, *Viral determinants of polarized assembly for the murine leukemia virus.* J Virol, 2011. 85(15): p. 7672-82.

58. Kong, L.B., et al., *Cryoelectron microscopic examination of human immunodeficiency virus type 1 virions with mutations in the cyclophilin A binding loop.* J Virol, 1998. 72(5): p. 4403-7.

59. Crist, R.M., et al., *Assembly properties of human immunodeficiency virus type 1 Gag-leucine zipper chimeras: implications for retrovirus assembly.* J Virol, 2009. 83(5): p. 2216-25.

60. Accola, M.A., B. Strack, and H.G. Gottlinger, *Efficient particle production by minimal Gag constructs which retain the carboxy-terminal domain of human immunodeficiency virus type 1 capsid-p2 and a late assembly domain.* J Virol, 2000. 74(12): p. 5395-402.

61. Zhang, Y., et al., *Analysis of the assembly function of the human immunodeficiency virus type 1 gag protein nucleocapsid domain.* J Virol, 1998. 72(3): p. 1782-9.

62. Jawhari, H., Honnappa, S., Steinmetz, M.O, *Crystal structure of trimeric coiled coil GCN4 leucine zipper.* PDB database. To be published, 2011.

63. **Liu, J., et al.,** ***A parallel coiled-coil tetramer with offset helices.*** **Biochemistry, 2006. 45(51): p. 15224-31.**

64. **Ono, A., et al.,** ***Association of human immunodeficiency virus type 1 gag with membrane does not require highly basic sequences in the nucleocapsid: Use of a novel gag multimerization assay.*** **Journal of Virology, 2005. 79(22): p. 14131-14140.**

65. **Guo, X.F., et al.,** ***Mutation of the SP1 sequence impairs both multimerization and membrane-binding activities of human immunodeficiency virus type 1 Gag.*** **Journal of Virology, 2005. 79(3): p. 1803-1812.**

66. **Dou, J., et al.,** ***Characterization of a myristoylated, monomeric HIV Gag protein.*** **Virology, 2009. 387(2): p. 341-52.**

67. **Ursell, T.S., W.S. Klug, and R. Phillips,** ***Morphology and interaction between lipid domains.*** **Proceedings of the National Academy of Sciences of the United States of America, 2009. 106(32): p. 13301-13306.**

68. **Rudnicka, D., et al.,** ***Simultaneous cell-to-cell transmission of human immunodeficiency virus to multiple targets through polysynapses.*** **J Virol, 2009. 83(12): p. 6234-46.**

69. **Ivanchenko, S., et al.,** ***Dynamics of HIV-1 assembly and release.*** **PLoS Pathog, 2009. 5(11): p. e1000652.**

70. **Zarbock, A., C.A. Lowell, and K. Ley,** ***Spleen tyrosine kinase Syk is necessary for E-selectin-induced alpha(L)beta(2) integrin-mediated rolling on intercellular adhesion molecule-1.*** **Immunity, 2007. 26(6): p. 773-83.**

71. **Jolly, C., I. Mitar, and Q.J. Sattentau,** ***Adhesion molecule interactions facilitate human immunodeficiency virus type 1-induced virological synapse formation between T cells.*** **J Virol, 2007. 81(24): p. 13916-21.**

72. **Zacharias, D.A., et al.,** ***Partitioning of lipid-modified monomeric GFPs into membrane microdomains of live cells.*** **Science, 2002. 296(5569): p. 913-916.**

73. **Adachi, A., et al.,** ***Production of acquired immunodeficiency syndrome-associated retrovirus in human and nonhuman cells transfected with an infectious molecular clone.*** **J Virol, 1986. 59(2): p. 284-91.**

74. **Llewellyn, G.N., et al.,** ***Nucleocapsid promotes localization of HIV-1 gag to uropods that participate in virological synapses between T cells.*** **PLoS Pathog, 2010. 6(10): p. e1001167.**

Chapter IV

Discussion

Rationale

HIV-1 was discovered to be the causative agent of AIDS almost 30 years ago. Since then, a vast amount of research has been done to elucidate the mechanisms by which HIV-1 assembles, interacts with its host cells and the immune system, and how HIV-1 spreads between people and among the natural target cells within those people. Cell-to-cell transmission between T cells is now recognized as the primary mode of HIV-1 spread in tissue culture, as it is up to several thousand times more efficient than cell-free transmission[1-5]. In lymphoid organs, where cell-to-cell transmission likely occurs, T cells often adopt a polarized morphology[6-11]. Thus, determining the relationship between HIV-1 and polarized T cells could help elucidate how the virus spreads *in vivo*. However, few studies have been conducted to determine the mechanisms of HIV-1 localization and spread in polarized T cells. The work done in this thesis defines the mechanisms of Gag localization to a rear end protrusion of polarized T cells called a uropod, the role uropods play in cell-cell transfer of virus particles and the relationship between Gag and uropod-directed microdomains on the plasma membrane.

Summary of results

Chapter II

In chapter II, it was shown that Gag localizes to uropods in polarized T cells by immunostaining Gag-YFP-expressing primary T cells and a polarized T cell line, P2, for three uropod markers. It was also shown that patches of Gag at the uropod contain proteolytically cleaved MA as well as the Env glycoprotein, indicating that a subset of these uropod-localized Gag patches contain mature and likely infectious HIV-1 particles. This uropod localization was also stably maintained in live migrating T cells observed for over 20 minutes.

Uropods in uninfected T cells are enriched in adhesion molecules and are known to mediate contact with other cells[12-14]. It was determined in chapter II that HIV-1 Gag-containing uropods could also maintain stable contacts with target cells using live cell analyses. A cell-cell contact assay also showed that uropods of HIV-1-infected T cells preferentially mediated contacts with target cells over non-uropod contacts by a 2:1 ratio. This was especially significant considering the uropod accounts for only 20-30% of the cell surface. It was then examined whether any of these contacts formed virological synapses (VSs), which are contact junctions between infected and uninfected cells that mediate cell-to-cell transmission[1, 3, 15-18]. VS formation was identified by the accumulation of the virus receptor CD4 on target cells. Gag-YFP-expressing P2 cells, immunostained for the uropod marker CD43, were co-cultured with SupT1 cells that were immunostained for CD4 and cell-cell contacts were observed after 3 hours. This experiment revealed that CD4 was enriched at contacts containing Gag and CD43 but not at non-CD43-containing contacts or CD43 contacts of uninfected cells, indicating that

uropods participate in virological synapses. Furthermore, a myosin light chain kinase inhibitor ML7 that depolarizes cells and Gag was found to inhibit cell-cell transfer of virus particles. This indicates that the cytoskeleton plays a role in Gag polarization and that uropods or cell polarity enhance cell-to-cell transfer of virus particles.

The observations above indicate that the uropod plays an important biological function for HIV-1 transmission. Thus, understanding the mechanism by which uropod localization occurs is important. In chapter II, by copatching and live cell analyses, it was found that Gag associates with uropod-directed microdomains (UDMs). Specifically, Gag copatched with the uropod markers PSGL-1 and CD43 in both polarized and unpolarized T cells, and Gag/PSGL-1 patches were observed by live-cell microscopy to move rearward to the uropod as T cells polarized. Together, these data suggest that Gag associates with UDMs that carry Gag to the uropod.

To determine the viral components required to drive uropod localization, mutational analyses of Gag were performed. MA, CA and Env were found to be dispensable for localization of Gag to the uropod. However, deleting NC or mutating the basic residues of NC caused Gag to localize around the entire plasma membrane. This observation indicated that NC is required for uropod localization of Gag. It was possible that NC-dependent uropod localization was due to either NC-mediated multimerization, driven by NC utilizing RNA as a scaffold[19-25], or a protein-NC interaction. Thus, the mechanism of NC-mediated uropod localization was further elucidated by replacing NC with a heterologous dimerizing sequence, leucine zipper (LZ). This LZ mutant (LZ/Gag-YFP) multimerizes and forms particles[26-28], but LZ has no sequence homology to NC. LZ/Gag-YFP, but not the dimeric LZ/WMAA/Gag-YFP, rescued localization of Gag to

the uropod. Thus, NC-mediated higher-order multimerization (more than a dimer), and not an interaction between a cellular protein and NC, is required for uropod localization.

Chapter III

While multimerization drives uropod localization of Gag, the exact aspect of multimerization and the level of multimerization required for uropod localization were unknown. Also, while Gag was observed to associate with UDMs, the composition of the UDMs and the mechanisms that facilitate UDM association of Gag were undefined. Thus, chapter III aimed to further elucidate the mechanisms of multimerization-mediated uropod localization of Gag, the composition of UDMs and the viral determinants of UDM association.

A possible mechanism for uropod localization is that fully formed particles, which require Gag multimerization, could be caught in retrograde membrane actin flow or "surf" on the outer leaflet of the plasma membrane. However, it was observed that two Gag mutants containing CA mutations that allow multimerization but inhibit membrane curvature and particle formation, P99A[29-31] and EE75,76AA[32, 33], localized to the uropod. This indicates that membrane curvature, and hence virus particle formation or surfing of completed particles, is not necessary for uropod localization of Gag. It also indicates that multimerization and an association with the inner-leaflet of the plasma membrane is sufficient to drive uropod localization.

Because membrane curvature is not required for uropod localization, it was possible that uropod localization of Gag occurs at an early stage in virus assembly. To determine what level of multimerization is sufficient to drive uropod localization of Gag,

the localization of monomeric/, LZ2/, LZ3/ and LZ4/Gag-YFP, which are expected to be monomeric, dimeric, trimeric and tetrameric Gag respectively, was examined in polarized T cells. LZ4/Gag-YFP was observed to be much more polarized than monomeric/, LZ2/ or LZ3/Gag-YFP, suggesting that a relatively low order of multimerization is sufficient to drive localization of Gag to the uropod.

Gag association with UDMs was established in chapter II based on the copatching of Gag with two uropod markers, PSGL-1 and CD43. However, there are several other known uropod proteins that UDMs could be composed of including CD44, ICAM-1, ICAM-3 and the lipid raft marker CD59. Interestingly, CD44 was found to copatch with Gag similarly to PSGL-1 and CD43 while ICAM-1, ICAM-3 and CD59 did not. These results indicate that Gag associates with only a specific subset of UDMs.

Previous studies have shown that Gag is able to coalesce lipid rafts and tetraspanins together that normally segregate in HeLa cells[31, 34], but that a planar multimer mutant does not mediate this coalescence[31]. This suggests that Gag differentially recruits various microdomains in a step-wise manner that could be based on membrane curvature. Thus, it was conceivable that membrane curvature could facilitate recruitment of CD43/PSGL-1/CD44-enriched UDMs but not ICAM-1, ICAM-3 or CD59-enriched UDMs. However, it was found that the planar multimer mutants P99A/Gag-YFP and EE75,76AA/Gag-YFP associated with PSGL-1- and CD43- but not CD59-enriched UDMs similar to wild type Gag-YFP, indicating that UDM association occurs earlier in assembly before membrane curvature and by an alternative mechanism.

Because MA mediates membrane binding through its myristoyl group and highly basic region (HBR)[35-42], it was the likeliest part of Gag to facilitate specific UDM

association. Therefore, it was tested whether deleting MA would decrease CD43/PSGL-1/CD44-enriched UDM association. Interestingly, while Fyn(10)/Gag-YFP associated with CD43- and PSGL-1-enriched UDMs similarly to WT Gag-YFP, it was observed that Fyn(10)/ΔMA/Gag-YFP did not. Also, Fyn(10)/ΔMA/Gag-YFP showed an increase in CD59-enriched UDM association, which was not observed for WT Gag-YFP or Fyn(10)/Gag-YFP. Together, these data indicate that Gag associates with specific UDMs by an MA-dependent mechanism.

The findings from Chapter II and chapter III lead to a current working model for how HIV-1 localizes and is spread in polarized T cells: When NC-mediated multimerizaton reaches the level of tetramerization or higher, Gag associates with specific uropod-directed microdomains enriched in CD43, PSGL-1 and CD44 via an MA-mediated mechanism. These Gag-associated UDMs then laterally localize on the membrane to the uropod where virus particles assemble and accumulate. Uropods then mediate contact and VS formation with target cells to facilitate cell-to-cell transmission.

Thus, the observations described in this thesis provide new and biologically relevant insights into the potential mechanisms that HIV-1 utilizes to localize and spread between T cells *in vivo* and enhance our understanding of the relationship between Gag and the plasma membrane.

Future Directions

What are the dynamics of uropod-mediated contacts and VS formation?

VSs between T cells were found to be enriched in the uropod marker CD43, indicating that uropods participate in virological synapses. However, there are unanswered questions about the dynamics of uropod association with the VS. In particular, it remains unknown whether uropods mediate initial contact in the formation of the VS. Uropods are enriched in adhesion molecules, and uropods of HIV-1 infected T cells appear to preferentially mediate contacts with target cells at steady state. Thus, it is conceivable that uropods of HIV-1 infected T cells mediate initial contact with target cells. In this model, uropods would act as preformed platforms that form a VS soon after contact occurs. However, a mechanism of VS formation in which the initial contact occurs at another part of the cell is also possible. For example, the initial contact by an HIV-1 infected T cell could primarily occur at its leading edge, followed by reorientation of the cell to subsequently attach to the target cell via its uropod. In unpolarized cells, it has been shown that Gag patches can localize to a cell-cell contact site after contact occurs[3, 17]. This mechanism of Gag polarization to the VS in morphologically unpolarized T cells could utilize the same cellular machinery required to form uropods. Thus, the VSs that form between unpolarized cells could represent the polar cap where a uropod would form if the T cell were to polarize. Therefore, the original cell-cell interaction observed in these previous studies could represent a "non-uropod contact," followed by subsequent reorientation of the cell and cell machinery to form the "uropod contact" and the VS. Because T cells are constantly migrating and adopt a polarized morphology in lymphoid organs[6-11], determining the frequency of uropod and non-

uropod contacts and how they affect the formation of the VS would help to better understand the dynamics of HIV-1 cell-to-cell transmission *in vivo*.

To determine the dynamic relationship between uropods and VS formation, long-term live-cell microscopy could be used. Gag-YFP-expressing T cells could be immunostained for uropod markers such as PSGL-1 and co-cultured with another T cell line constitutively expressing fluorescently tagged CD4 (CD4-YFP). To prevent off target activation effects that could be caused by antibody crosslinking, Fab fragments that do not cause crosslinking could be used as the primary antibody. These co-cultured cells would then be observed by live-cell microscopy to determine the dynamics of uropod-mediated cell-cell contacts and VS formation. The time frame likely required to observe VS formation would be up to 3 hours based on the experiments in chapter II, in which virological synapses were observed after 3 hours of co-culture.

In the virological synapse studies that were discussed in chapter II, CD4-expressing target cells were immunostained with a fluorescently tagged primary antibody. In this approach, only one image of each cell was required for identifying VSs. However, the fluorescence signal of the FITC-conjugated CD4 antibody used in this approach was low and photobleached quickly, presenting a major obstacle to long-term live-cell microscopy. In contrast, YFP that is tagged to CD4 fluoresces more brightly than the FITC-conjugated antibody and does not photobleach as quickly. These properties make CD4-YFP more useful than CD4 immunostaining for long-term live-cell microscopy analyses of VS formation. To ensure that tagging of CD4 with YFP does not affect its function, HeLa and T cells were transfected with a plasmid encoding CD4-YFP. As expected of functioning CD4, CD4-YFP was found to be localized on the plasma

membrane in both transfected HeLa cells and in T cells (Fig. 4.1A-B). Furthermore, expression of CD4-YFP also increased the susceptibility of HeLa cells, which do not normally express CD4, to infection by pNL4-3-derived HIV-1 virus particles to a similar level as untagged CD4 (Fig. 4.1C). Together, these observations indicate that the addition of YFP to CD4 does not inhibit its function as a receptor for HIV-1 and thus could be used to study virological synapses.

For long-term live-cell microscopy, maintaining cell viability is critical. Three factors that affect cell health and viability are temperature, phototoxicity and pH changes that occur when cell culture medium is exposed to the air while on the microscope stage. While culture at room temperature is not lethal to the cells, cell processes slow down, and cell morphology can be altered. Maintaining cells at 37°C while on the microscope stage can be accomplished by utilizing a temperature-controlled closed chamber. CO_2 is required to maintain the pH of commonly used culture media buffered with $NaHCO_3$. Thus, when exposed to the air, this culture medium can become alkaline and adversely affect cells. Overcoming the loss of CO_2 can be achieved by placing the cells in a closed chamber and adding 5% CO_2 directly into it. Alternatively, CO_2-independent media containing HEPES or phosphate buffer, which resists pH changes without CO_2, is commercially available. While not all cells grow well in this media, similar studies that examined cell-cell transfer of virus particles between T cells by live-cell microscopy have utilized CO_2-independent media[3]. Finally, phototoxicity occurs when the excitation light splits oxygen molecules (O_2) into singlet oxygen or other reactive oxygen species that are harmful to cells. Shorter exposure times, longer periods between exposures and lower energy levels of the excitation light can be used to mitigate phototoxicity. In

conjunction with these steps, the oxygen level of the media can be reduced either through scavengers such as ascorbic acid or a derivative of vitamin E called Trolox or by a commercially available oxygen depletion system such as Oxyrase. The microscope itself has a major impact on the level of light required to clearly observe fluorescence. Spinning disc confocal microscopes can detect very low levels of light compared to epifluorescence microscopes, drastically reducing phototoxicity and photobleaching. However, an epifluorescence microscope was also successfully used in chapter II to observe live cells. While the time frame for those experiments, 30 min to 1 hour, was shorter than the 3 hour time frame likely required for the long-term live-cell microscopy experiments proposed above, the implementation of oxygen-reducing systems and addition of CO_2 and/or CO_2-independent media would allow a greatly increased time frame to observe cell-cell contacts and VS formation.

Under these conditions, long-term live-cell microscopy could be used to quantify 1) the ratio of initial contacts mediated by uropods to initial contacts mediated by the leading edge of Gag/YFP-expressing T cells, 2) whether Gag/YFP-expressing T cells reorient themselves to form uropod contacts if the initial contact is not mediated by the uropod, and if so, how long this process takes, and 3) the time to VS formation after the initial contact is made as measured by CD4 accumulation. Depending on the level of success of increasing the length of time that cells could be observed, the average duration of the VS could also be measured. Thus, these observations would determine whether uropods act as preformed platforms for HIV-1 that directly contacts target cells to form a VS, and provide insights into the mechanism and dynamics of VS formation in biologically relevant polarized T cells.

What is the mechanism by which MA determines specific UDM association?

In chapter III, MA was found to determine the specificity of UDM association by Gag. In the presence of MA, Fyn(10)/Gag-YFP associated with PSGL-1/CD43-enriched UDMs, and segregated from CD59- and ICAM-3-enriched UDMs. In the absence of MA, Gag lost its association with PSGL-1 and CD43, stayed segregated from ICAM-3, but gained an association with CD59. These observations elucidated a new function of MA in which MA determines Gag association with a specific subset of UDMs. Understanding this mechanism could lead to better insights into the relationship between Gag and plasma membrane microdomains and their function, specifically the role of UDMs in HIV-1 replication in polarized T cells.

Even though Fyn(10)/Gag-YFP and Fyn(10)/ΔMA/Gag-YFP have both had the acylation status of their MA altered by the addition of Fyn(10), these two mutants associated with different UDMs. Thus, the specificity of UDM association is likely due to the MA sequence itself and not the acylation status of MA. One of the other features of MA is the highly basic region (HBR). The HBR is known to be important for membrane binding[35, 37-39, 41, 42]. Potentially, the positively charged amino acids in the HBR could interact with specific negatively charged phospholipids to which some, but not all, uropod proteins are also attracted. Thus, it is conceivable that when Gag multimerizes, it clusters these acidic phospholipids and specific uropod proteins together. For example, the HBR mediates binding of Gag to the acidic phospholipid phosphoinositol-(4,5)-bisphosphate [$PI(4,5)P_2$], which has been observed to mediate clustering of plasma membrane proteins into microdomains[43]. Thus, it is conceivable that $PI(4,5)P_2$, which Gag directly binds to, mediates clustering of PSGL-1, CD43 and CD44, but not ICAM-1,

ICAM-3 or CD59. Alternatively, a direct interaction between a UDM protein and MA could also determine specific UDM association of Gag. Further mutational analysis of MA, discussed below, can be done to distinguish these possibilities.

First, to determine whether the HBR plays a role in specific UDM association, the 8 basic residues within the HBR of Fyn(10)/Gag-YFP could be mutated to neutral amino acids like alanine and threonine (Fyn(10)/6A2T/Gag-YFP). If Fyn(10)/6A2T/Gag-YFP lost its association with CD43/PSGL-1/CD44-enriched UDMs similarly to Fyn(10)/ΔMA/Gag-YFP, then it would indicate that the HBR is required for specific UDM association. In this case, to determine whether it is the positive charge of the HBR that determines specific UDM association, an HBR R/K switch mutant could be made in which the two Lys(K) are mutated to Arg(R) and the six Arg are mutated to Lys (HBR/RKswitch/Gag-YFP). This mutant would maintain the same overall charge as wild type Gag-YFP, but likely disrupt any direct interactions between Gag and UDM-associated proteins. If this mutant associated with CD43/PSGL-1/CD44-enriched UDMs, it would indicate that the positive charge of the HBR plays a major role in specific UDM recruitment. If HBR/RKswitch/Gag-YFP did not copatch with CD43/PSGL-1/CD44-enriched UDMs, it would suggest that a direct interaction between the HBR and either $PI(4,5)P_2$ or a UDM protein was occurring. To determine whether Gag association with $PI(4,5)P_2$ is required for specific UDM association, a mutant in which MA is replaced by the $PI(4,5)P_2$-binding PH-domain could be examined for UDM association. If this construct, which should bind $PI(4,5)P_2$ but lacks MA, was observed to copatch with CD43/PSGL-1/CD44-enriched UDMs it would indicate that $PI(4,5)P_2$ association of Gag

determines UDM association. If not, it would suggest instead that specific UDM association of Gag is determined by an interaction between MA and a UDM protein.

Alternatively, if the HBR mutant Fyn(10)/6A2T/Gag-YFP still associated with CD43/PSGL-1/CD44-enriched UDMs in T cells, then it would be concluded that another part of MA, not the HBR, determines specific UDM association. This would also suggest that a direct interaction between a UDM protein and some part of MA was occurring. In this case, deletion mutants could be made to determine the region of MA required for specific UDM association.

In the cases suggesting a direct interaction between MA and a UDM protein, once the region of MA that determines specific UDM association was identified, co-immunoprecipitation experiments between uropod proteins and these mutants, with WT Gag-YFP as the positive control, could be done to determine which, if any, uropod proteins MA interacts with. Candidate proteins would include the UDM markers with which Gag has already been observed to associate (PSGL-1, CD43 and CD44). Other candidates would include the Ezrin/Radixin/Moesin (ERM) proteins. ERMs are scaffolding proteins that are known to link the cytoplasmic tails of uropod-associated proteins, including PSGL-1, CD43 and CD44, to the actin cytoskeleton and are involved in their localization to uropods[44-47].

If a direct interaction between Gag and a uropod-associated protein is found, shRNA knockdowns of the identified protein could be done to determine whether this association mediates specific UDM recruitment and/or uropod localization of Gag. If the specificity of UDM association and/or uropod localization of Gag are found to be mediated by this direct interaction, it would then be possible to test the importance of

specific UDM association and/or uropod localization of Gag to virus replication. For example, T cells that express wild type Gag-YFP, and in which the identified UDM protein is knocked down by shRNA, could be used in functional assays such as cell-cell transfer, virus release and infectivity of virus particles.

Do individual UDM proteins enhance virus replication and spread?

It is conceivable that the benefit of Gag association with specific UDMs is conferred by a single UDM protein, such as CD43, PSGL-1 or CD44. If this is the case, it is also possible that knocking down that beneficial UDM protein disrupts a process other than Gag association with UDMs or uropod localization. Thus, while disrupting UDM association of wild type Gag is the best way to determine the role of UDMs in virus replication, it is possible and valuable to test the role of individual UDM proteins in these processes as well. For example, because the UDM proteins that Gag associates with are adhesion molecules, it is possible that these particular adhesion molecules promote cell-to-cell transfer of HIV-1 between T cells. Thus, to determine whether PSGL-1, CD43 or CD44 enhance cell-cell transfer of virus particles, T cells in which these UDM proteins are knocked down by shRNA can be used as donor cells in the cell-cell transfer assay described in chapter II.

The first candidate to be tested would be PSGL-1, because activation of PSGL-1 has been observed to cause a signaling cascade that results in increased avidity of LFA-1 to its binding partner ICAM-1[48, 49]. LFA-1 is an important adhesion molecule that has been observed to promote cell-to-cell transmission by stabilizing VSs, where it has been found to be enriched[50]. LFA-1 and its binding partner ICAM-1 have also been

implicated in virus infectivity and spread[51]. Because PSGL-1 has been observed to be activated by antibody crosslinking[49], it is conceivable that multimerizing Gag could also activate PSGL-1 and in turn lead to increased avidity of LFA-1, thereby enhancing cell-to-cell transmission.

To determine whether Gag facilitates PSGL-1-mediated signaling of LFA-1 activation in order to enhance cell-to-cell transmission, the first step would be to examine whether PSGL-1 enhances cell-to-cell transfer of virus particles. Gag-YFP-expressing P2 cells, in which PSGL-1 is knocked down, could be used as donor cells in the cell-cell transfer assay described in chapter II. If cell-to-cell transfer of virus particles is unaffected by PSGL-1 knockdown, then other uropod proteins would be individually tested for an effect on cell-to-cell transfer of virus particles. But if cell-to-cell transfer of virus particles is found to be reduced when PSGL-1 is knocked down, it would indicate that PSGL-1 enhances cell-cell transfer, potentially through activation of LFA-1. If so, a series of experiments could be done to determine whether PSGL-1-mediated enhancement of cell-to-cell virus transfer was due to LFA-1 activation (see figure 4.2 for flow chart).

The next step would be to determine whether Gag/YFP leads to the activation of LFA-1. This could be done by immunostaining Gag-YFP-expressing T cells with an antibody specific to activated LFA-1. If LFA-1 was not activated in the Gag/YFP-expressing T cells, then it would be likely that PSGL-1 enhances cell-to-cell transfer based on its own adhesive properties or that PSGL-1 activates other signaling pathways that facilitate cell-to-cell virus transfer. But if LFA-1 was found to be activated in T cells when Gag-YFP was expressed, whether this Gag-YFP-mediated LFA-1 activation was

due to PSGL-1 could then be determined by knocking down PSGL-1 in Gag-YFP-expressing T cells and observing whether LFA-1 remained activated. If LFA-1 was not activated in Gag/YFP-expressing cells in which PSGL-1 is knocked down, it would indicate that LFA-1 is activated by HIV-1 through another mechanism, possibly by another HIV-1 protein. But if LFA-1 activation was observed to be decreased in Gag/YFP-expressing cells when PSGL-1 is knocked down, whether LFA-1 enhances cell-cell transfer of virus particles could then be tested directly. This could be done by knocking down LFA-1 in donor cells expressing Gag-YFP and observing whether cell-to-cell transfer to target cells was decreased. If cell-to-cell transfer of virus particles is not affected by LFA-1 knockdown, it would indicate that LFA-1 activation is likely an off-target effect of Gag-YFP-mediated PSGL-1 activation but not involved in virus spread and that PSGL-1 enhances cell-to-cell transfer by another mechanism. But if cell-to-cell transmission of HIV-1 is decreased when LFA-1 is knocked down it would be possible that LFA-1 and PSGL-1 independently enhance cell-to-cell transfer of virus particles. Thus, if LFA-1 was observed to enhance cell-to-cell transfer of virus particles, the efficiency of cell-to-cell transfer of virus particles could be compared between donor cells in which PSGL-1 and LFA-1 are individually or simultaneously knocked down. If no or little difference is observed between cells that have both PSGL-1 and LFA-1 knocked down and cells with PSGL-1 or LFA-1 knocked down individually, then these observations combined would define a mechanism in which Gag crosslinks PSGL-1, which signals LFA-1 to increase its avidity to its binding partners, thereby enhancing cell-to-cell transfer of virus particles.

Does Gag associate with pre-existing uropod-directed microdomains?

In chapter III it was observed that Gag associates with PSGL-1/CD43/CD44-enriched UDMs but not ICAM-1-, ICAM-3- or CD59-enriched UDMs by an MA-dependent mechanism. However, it is unknown whether this association is driven by Gag recruitment of these UDMs or whether CD43/PSGL-1/CD44-enriched UDMs exist on the membrane even in the absence of Gag. Notably, it was recently shown that Gag coalesces existing microdomains that do not normally associate with each other in HeLa cells[31, 34]. Thus, it is possible that a similar mechanism occurs in T cells in which Gag coalesces separate UDMs.

It is of note however, that the relationship between Gag and microdomains are likely different between HeLa and T cells. For example, Gag colocalizes with CD59 in HeLa cells[31], but not in T cells. It is conceivable that this difference in microdomain association is caused by a differential expression of proteins important for microdomain association. For example, Gag associates with PSGL-1-enriched UDMs in T cells. However, HeLa cells do not express PSGL-1 (Fig. 4.3A). Thus, if PSGL-1 is a driving factor for Gag association with UDMs in T cells, the lack of PSGL-1 could account for the CD59 association of Gag in HeLa cells. Interestingly, when PSGL-1 is expressed via DNA plasmid in HeLa cells (Fig. 4.3B) it colocalizes with Gag (Fig. 4.3C), recapitulating the UDM association of Gag observed in T cells. It would thus also be interesting to examine whether this PSGL-1 expression disrupts Gag colocalization with CD59 in HeLa cells.

To determine whether UDMs pre-exist in the absence of Gag, or whether Gag coalesces different UDMs together, copatching analysis of UDM proteins in uninfected

P2 cells could be done. By utilizing different antibody isotypes with isotype-specific secondary antibodies, it could be determined whether CD43/PSGL-1/CD44-enriched microdomains exist in the absence of Gag or whether Gag coalesces these uropod proteins together.

In preliminary experiments, it was tested whether CD44 copatches with itself (positive control), CD43, PSGL-1, ICAM-1 or ICAM-3. It was observed that CD44 copatched with itself, PSGL-1 and CD43 and segregated from ICAM-1 (Fig. 4.4A-D). These observations would be expected if Gag-associated UDMs pre-exist on the plasma membrane. However, an interesting result was also observed in which CD44 copatched with ICAM-3 (Fig. 4.4E). These results are quantified in Fig. 4.4F. ICAM-3 does not copatch with Gag, as described in chapter III. Thus, this observation indicates that Gag associates with a specific pre-existing UDM and then reorganizes it by actively excluding some proteins from that UDM. Supporting this conclusion, it was observed that in cells expressing Gag-CFP, Gag copatched with CD44, but the colocalization of CD44 and ICAM-3 that had been observed in uninfected P2 cells was lost (Fig. 4.5A-B). These results are quantified in Fig. 4.5C.

To further examine this mechanism, Fyn(10)/ΔMA/Gag-YFP could be used. Because Fyn(10)/ΔMA/Gag-YFP does not copatch with CD43/PSGL-1/CD44-enriched UDMs, it would be expected that CD44 and ICAM-3 should remain copatched in cells expressing Fyn(10)/ΔMA/Gag-YFP similarly to uninfected cells. . If this was observed, combined with the previous observations, it would show that Gag reorganizes the plasma membrane by recruiting CD43, PSGL-1, and CD44, but actively segregating ICAM-3 from pre-existing UDMs and that this mechanism is dependant on MA. However, if it

was observed that ICAM-3 and CD44 did not copatch in the presence of Fyn(10)/ΔMA/Gag-YFP it would also be interesting as it would indicate that another HIV-1 protein could be playing a crucial role in plasma membrane microdomain organization and potentially open a major new direction in HIV-1 research.

While reorganization of plasma membrane microdomains has been observed previously, in which different microdomains are coalesced by Gag[31, 34], this process could be attributed to a non-specific mechanism in which multimerization on the membrane simply attracts various microdomains. However, in this case the observation that Gag could split existing microdomains apart reveals a new and novel mechanism by which HIV-1 actively rearranges the plasma membrane.

When does UDM association occur?

In chapter III, it was observed that LZ4/Gag-YFP polarizes more than monomeric/, LZ2/ or LZ3/Gag-YFP. In the working model, it is hypothesized that UDMs carry Gag to the uropod. If so, the increased LZ4/Gag-YFP polarization suggests that UDM association and uropod localization occur early in assembly. Thus, it would be expected that the increased polarization of LZ4/Gag-YFP would correlate to a stronger UDM association than monomeric/, LZ2/ or LZ3/Gag-YFP. However, because these low-order multimers do not form patches or puncta, the copatching assay performed with wild type Gag-YFP can not be used. Another method to determine whether LZ4/Gag-YFP associates with UDMs more than monomeric/, LZ2/ or LZ3/Gag-YFP is super resolution microscopy, which was recently optimized in collaboration with the Veatch lab to observe Gag and tetherin colocalization[33].

Super resolution microscopy is capable of 10-30nm resolution and thus, unlike conventional light microscopy, can observe microdomains in their native state[33, 52-54]. This is accomplished by linking a protein of interest to a photo-switchable tag such as mEos2[55] or labeling a primary antibody with a fluorescent secondary antibody capable of reversible photobleaching such as Alexafluor647[56]. Total internal reflection fluorescence (TIRF) microscopy[57] can then be used to observe only the cell surface-associated proteins. MEos2 switches between green and red fluorescence when stimulated by laser light and AlexaFluor647 switches between fluorescence and non fluorescence when stimulated by laser light in a reducing buffer. This "blinking" allows only a small subset of fluorophores to be observed in each image. Roughly 5000 images are then taken and compiled into a single image that pinpoints, to a high precision, the location of the fluorescent proteins. Cross correlation analysis, which calculates the likelihood of a protein being within a certain distance of another protein[58], can then be performed to determine whether the two proteins are associated with each other.

TIRF microscopy requires that the observed cells are in contact with the glass coverslip because the excitation laser is set to slightly below the critical angle, which is the angle that causes total reflection of the laser when it reaches the coverslip/sample interface. Thus, the evanescent wave generated at the coverslip/sample interface only penetrates approximately 100 nanometers past the glass/media interface into the cells. This method has been previously used to study HIV-1 membrane association and assembly[59-62]. Because of the necessity of cell adherence to the coverslip, the first experiments would be conducted using mEos2-tagged constructs in HeLa cells, which have been used previously for super resolution microscopy by Grover et. al[33]. In

contrast to HeLa cells, T cells are non-adherent, making TIRF difficult to achieve. However, developing this assay to observe Gag-mEos2-derived mutants in T cells may also be possible if T cells can be adhered to glass coverslips. For example, coating coverslips with either poly-L-lysine or fibronectin can promote T cell adherence to coverslips. If the adherence generated by this method does not significantly alter T cell morphology, then super resolution microscopy could be used to observe the level of association between UDMs and monomeric/, LZ2/, LZ3/ and LZ4/Gag-mEos2 in the more biologically relevant T cells.

If LZ4/Gag-mEos2 was observed to associate with UDMs to a higher degree than monomeric/, LZ2/ or LZ3/Gag-mEos2 in either HeLa or T cells, it would support the hypothesis that UDM association occurs early in assembly and that UDMs carry Gag to the uropod. However, if monomeric/Gag-mEos2 is observed to associate with UDMs as effectively as LZ4/Gag-mEos2 and at similar levels as wild type Gag-mEos2, it would also indicate that UDM association occurs early in assembly but that UDM association by itself does not drive uropod localization. Finally, if UDM association is observed for the wild type Gag-mEos2 control but not observed for LZ4/Gag-mEos2 or other LZ mutants, it would indicate both that UDM association is not required for uropod localization and that UDM association occurs later in assembly.

What are the dynamics of assembly, localization and UDM association of Gag in polarized T cells?

The above experiments would provide compelling evidence for when Gag association with UDMs occurs. However, the results would be based on fixed cells,

which represent a static snapshot of the processes that are occurring. Thus, they do not reveal the dynamics of when UDM association occurs relative to uropod localization. To examine the dynamics of these processes, live cell TIRF analyses could be used in conjunction with a drug-inducible Gag multimerization mutant. This assay could be used to determine where and when de-novo assembly of Gag and UDM association occur in polarized T cells and the relationship between UDM association and uropod localization.

The drug-inducible Gag multimerization mutant was constructed by replacing CA with a dimerization motif derived from the variant FKBP protein (VF1) (ΔCA/VF1/Gag-YFP). VF1 dimerization is induced by the addition of a small molecule drug, AP20187. Thus, when AP20187 is added, ΔCA/VF1/Gag-YFP multimerizes (Fig. 4.6A). This was observed in a preliminary experiment showing that ΔCA/VF1/Gag-YFP was mostly cytosolic before the addition of AP20187 (Fig. 4.6B), likely due to a membrane binding defect caused by a lack of multimerization. However, 30 minutes or longer after the addition of AP20187, ΔCA/VF1/Gag-YFP was observed to localize on the plasma membrane and to uropods in the majority of cells (Fig. 4.6C), indicating a restoration of multimerization. These results are quantified in Fig. 4.6D. If the experiments utilizing super resolution microscopy in T cells described in the previous section are successful, the same technique could be applied to living cells. T cells expressing ΔCA/FV1/Gag-mEos2 could be immunostained for PSGL-1 or other UDM proteins with an Fab antibody fragment conjugated to AlexaFluor647. After the addition of AP20187, images could be taken over 30min or 1hr. Unlike the previously proposed super resolution microscopy experiments of fixed cells, fewer pictures would have to be taken for each time point as living cells may migrate. Thus, some resolution would be sacrificed. However, the

resolution would still be enough to resolve single virus particle formation and UDM recruitment over time. This experiment would allow real time observation of whether forming Gag particles recruit UDM markers before or after they begin migrating to the uropod. Another possibility is that virus particles preferentially begin forming at the uropod in already polarized cells. Thus, these experiments could provide novel observations about the dynamics of how, when and where Gag assembly and UDM association occurs in polarized T cells.

Perspective

The research presented in this thesis could be used to expand our understanding of retrovirology in general. For example, HTLV-1 is another retrovirus that replicates in T cells. Like HIV-1, HTLV-1 Gag is thought to multimerize on the plasma membrane. Thus, based on the work presented in this thesis, HTLV-1 Gag could also localize to uropods in polarized T cells. Similarly to HIV-1, HTLV-1 spread is also primarily mediated through cell-to-cell transmission. Moreover, it was recently found that the uropod marker CD43 enhances cell-to-cell transmission of HTLV-1 [63]. These observations are consistent with the possibility that uropods are also important for the spread of other retroviruses. Thus, future studies could determine whether uropod-mediated cell-to-cell transmission represents a common mode of transmission for viruses that bud from polarized lymphoid cells.

In the context of HIV-1, further studies on the role of uropods for transmission of HIV-1 between other cell types would also broaden our understanding of HIV-1 spread *in vivo*. For example, dendritic cells are another target cell of HIV-1. It is conceivable that

uropods of uninfected T cells could also mediate contact with HIV-1-infected dendritic cells. If such uropod-mediated contact was observed, it would be consistent with the possibility that uropods not only play a role in transferring virus particles to target cells but also act as a site of virus entry. Similarly, investigating whether uropods play a role in cell-to-cell transmission between T cells and macrophages could also enhance our understanding of HIV-1 spread between the natural targets of HIV-1 *in vivo*.

The outcomes of future studies on the mechanisms of uropod localization and UDM association described in this chapter could also provide opportunities to examine the role of uropods in HIV-1 spread *in vivo*. For example, it could be found that uropod localization or UDM association of HIV-1 is dependent on a particular uropod protein, such as PSGL-1 or CD43. If this were found, human hematopoietic stem cells could be engineered to not express this protein and then used to generate humanized mice. These humanized mice would then contain human T cells that are polarized but do not concentrate HIV-1 at their uropods when infected. These humanized mice could then be used to study HIV-1 spread when HIV-1 does not localize to uropods in an *in vivo* context. If an interaction between Gag and a uropod protein was found to be important for spread of the virus *in vivo*, this humanized mouse system could also be used to test the therapeutic value of small molecule drugs that target this interaction.

Conclusion

Generally, the goal of science is to understand, at a fundamental level, the ways in which life and the world work. In the case of HIV-1 research, we strive to understand the details of how HIV-1 replicates and spreads within the human body. The strength of the

findings presented in this thesis are that they define mechanisms of HIV-1 localization and spread in T cells that are in the same biologically relevant, morphologically polarized state as most T cells in lymphoid organs. Thus, the observations that HIV-1 localizes to uropods in polarized cells and that uropods play a role in cell-to-cell transfer of virus particles, represent significant steps forward in our understanding of how HIV-1 is transmitted between T cells *in vivo*. The observations that multimerization is required for polarized localization and that MA determines the association of Gag with specific microdomains also represent new insights into the relationship between HIV-1 and the plasma membrane in biologically relevant polarized T cells. Therefore, these studies represent significant progress towards an ever deepening understanding of HIV-1 and how it operates within the human body.

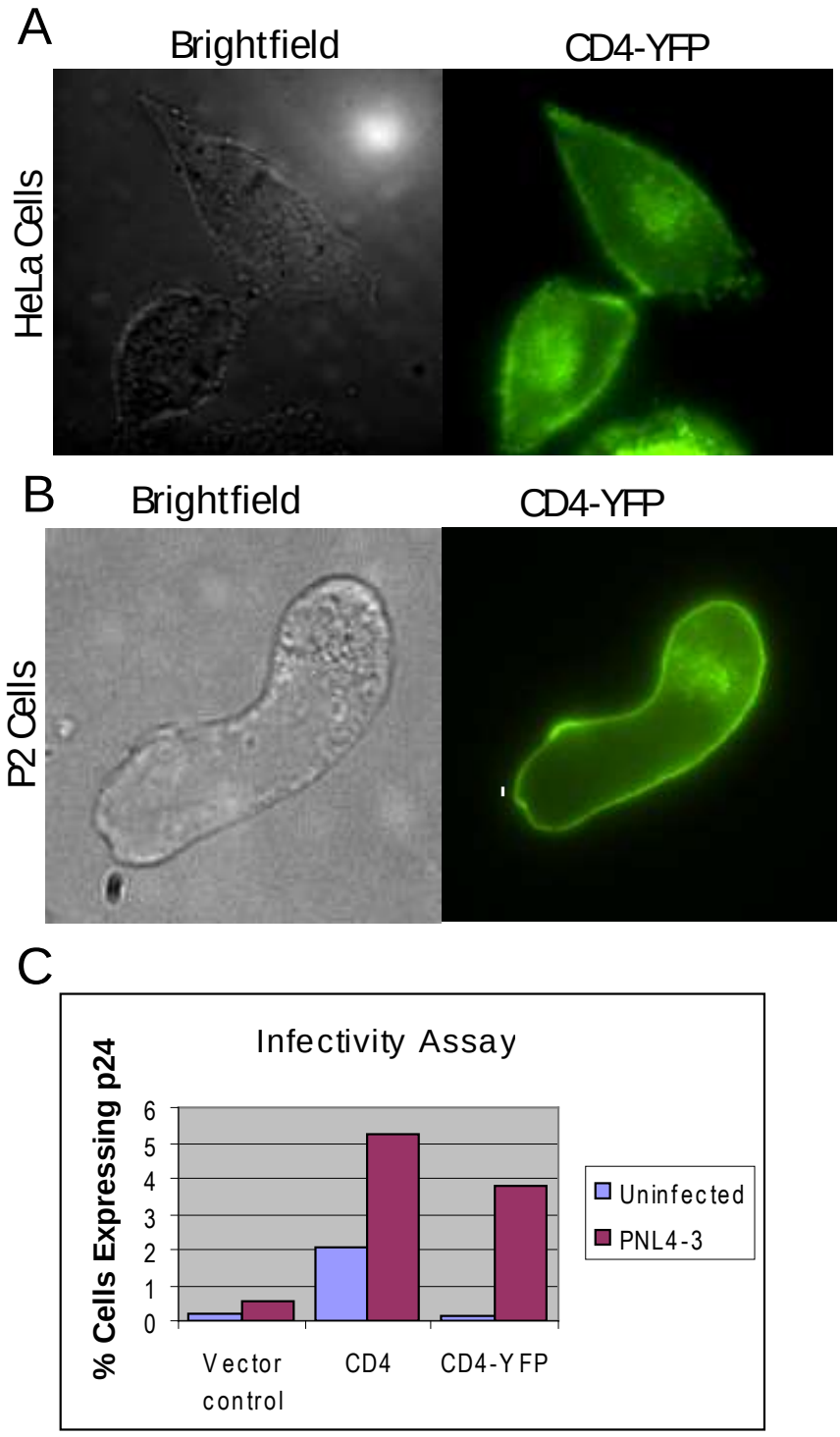

Figure 4.1. CD4-YFP promotes infection by HIV-1.
An expression plasmid encoding CD4-YFP was transfected into **A)** HeLa cells by lipofectamine or into **B)** P2 cells by amaxa nucleofection. **C)** HeLa cells expressing vector without CD4, or untagged CD4 or YFP-tagged CD4 were uninfected or mock infected with pNL4-3 virus particles. Two days post infection, p24 levels were measured by flow cytometry.

Model: HIV-1 Gag crosslinks PSGL-1, which activates LFA-1 that then enhances cell-cell transfer of virus particles.

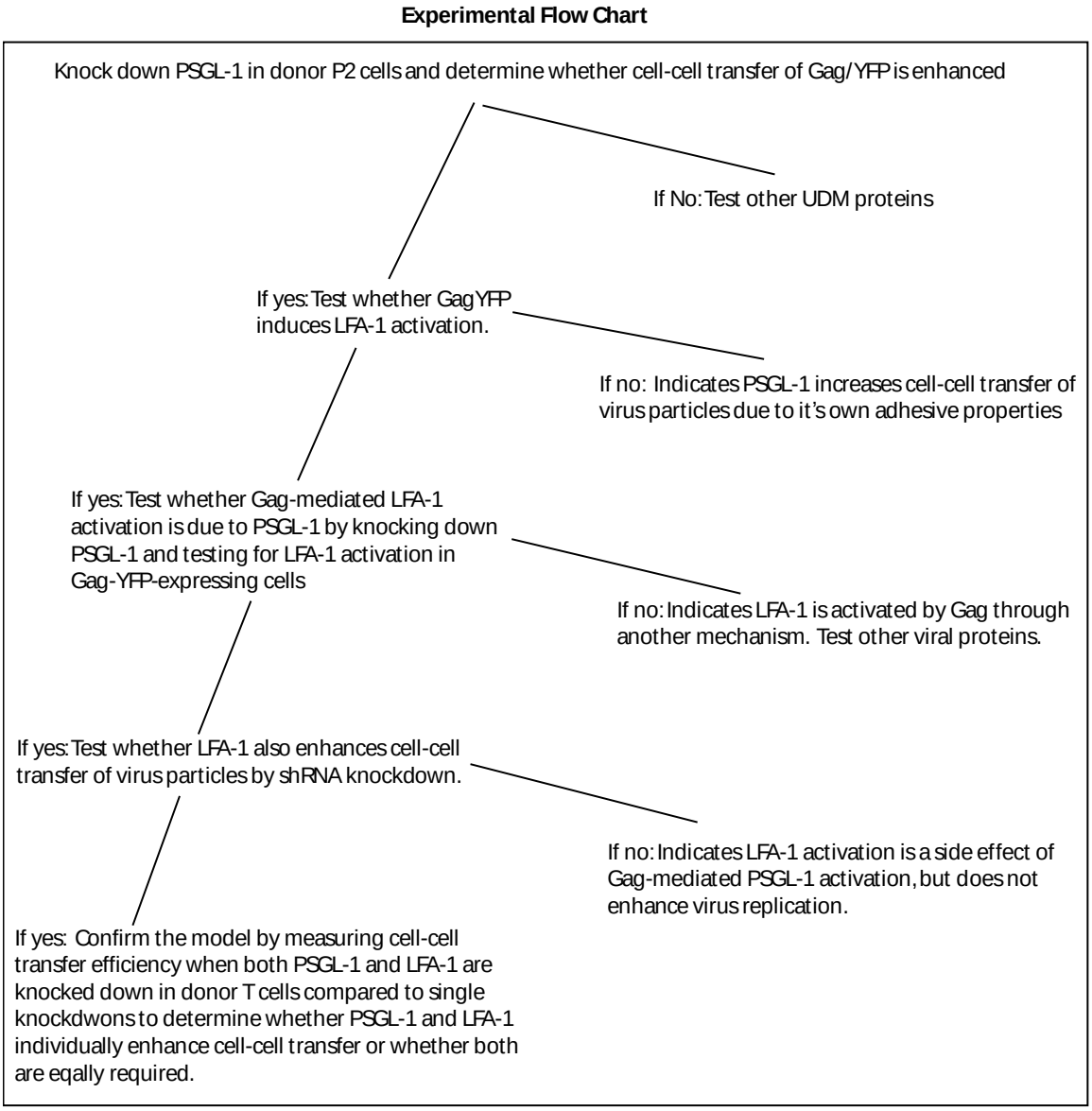

Figure 4.2. Experimental flow chart.
This flow chart outlines the experiments required to determine whether Gag/YFP activates PSGL-1 that then increases cell-cell transfer of virus particles by signaling LFA-1 to become more adhesive to its binding partners.

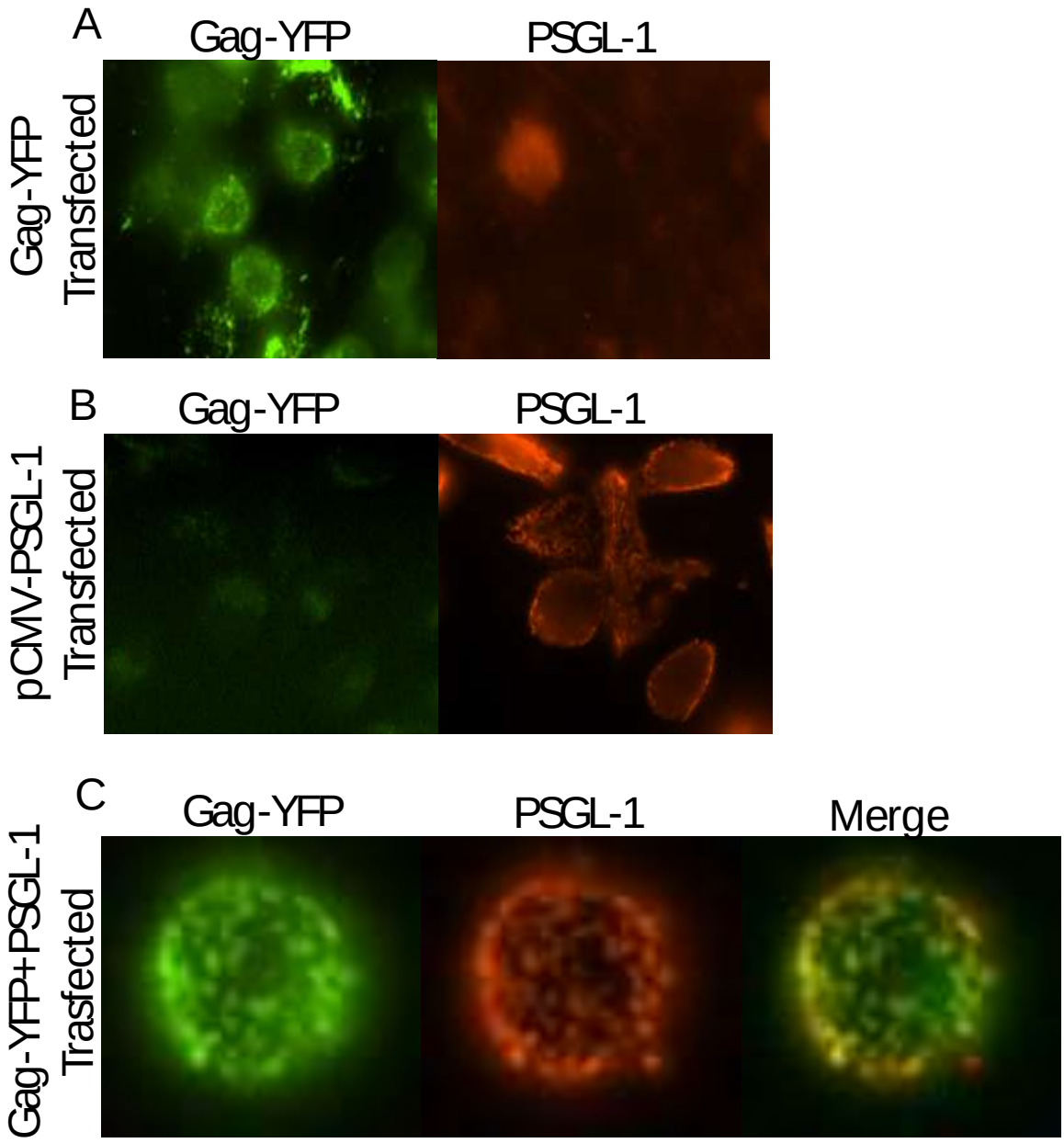

Figure 4.3. HeLa cells do not express PSGL-1 unless transfected. PSGL-1 in transfected HeLa cells copatch with Gag.
A) HeLa cells were transfected with Gag-YFP and immunostained by copatching for PSGL-1. **B)** HeLa cells were transfected with pCMV6-AC-PSGL-1 and immunostained for PSGL-1 by copatching. **C)** HeLa cells were transfected with both Gag-YFP and pCMV6-AC-PSGL-1 and immunostained for PSGL-1 by copatching.

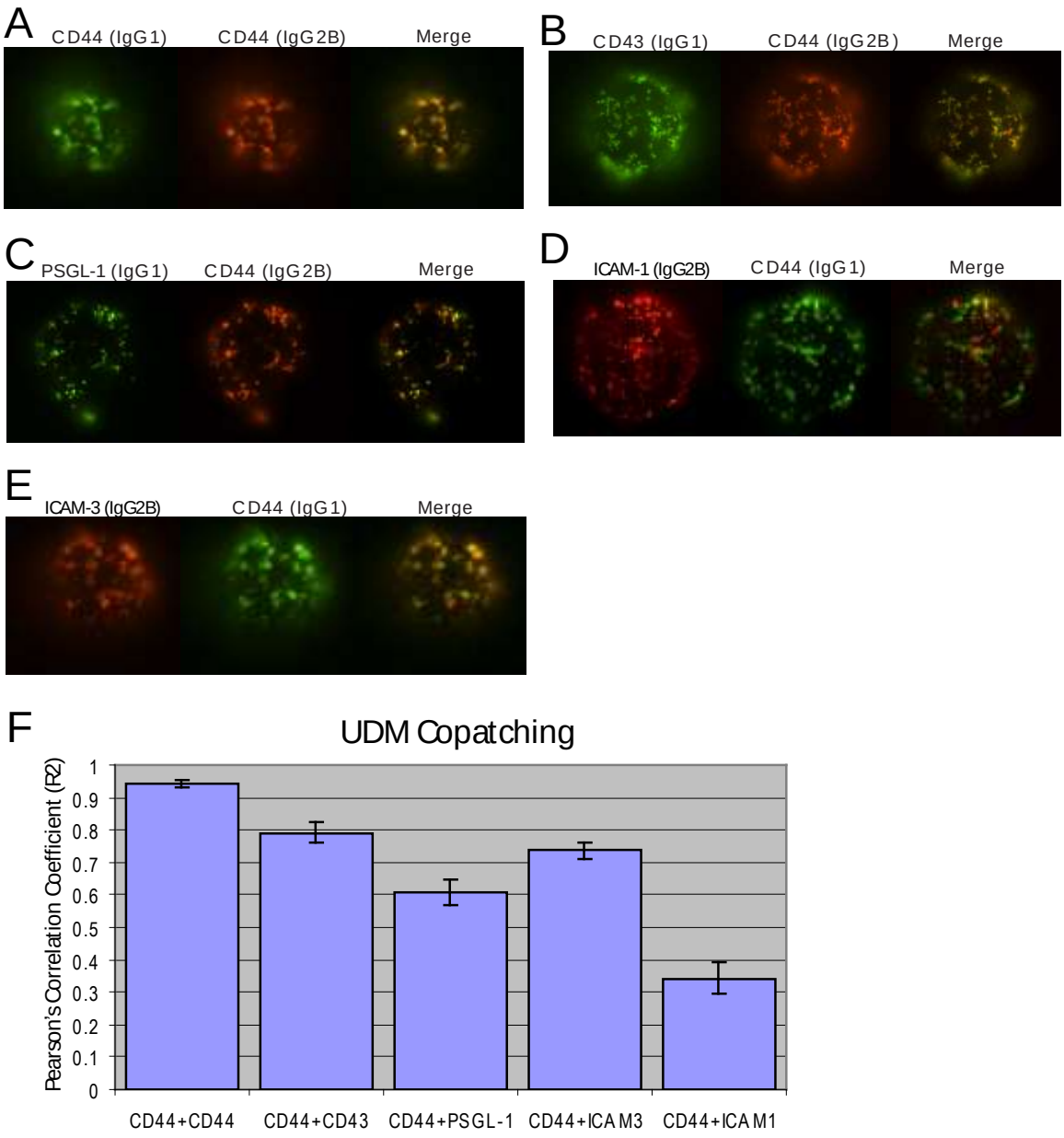

Figure 4.4. CD43/PSGL-1/CD44-enriched UDMs pre-exist, but also include ICAM-3.

Uninfected P2 cells were co-immunostained by copatching assay for CD44 and UDM proteins utilizing isotype specific secondary antibodies. **A)** As a positive control, CD44 copatches with itself. **B)** CD44 also copatches well with CD43 and **C)** PSGL-1. **D)** CD44 segregates from ICAM-1. **E)** CD44 also copatches with ICAM-3. **F)** Images taken of the tops of cells were quantified using the Pearson's coefficient. Error bars represent SEM.

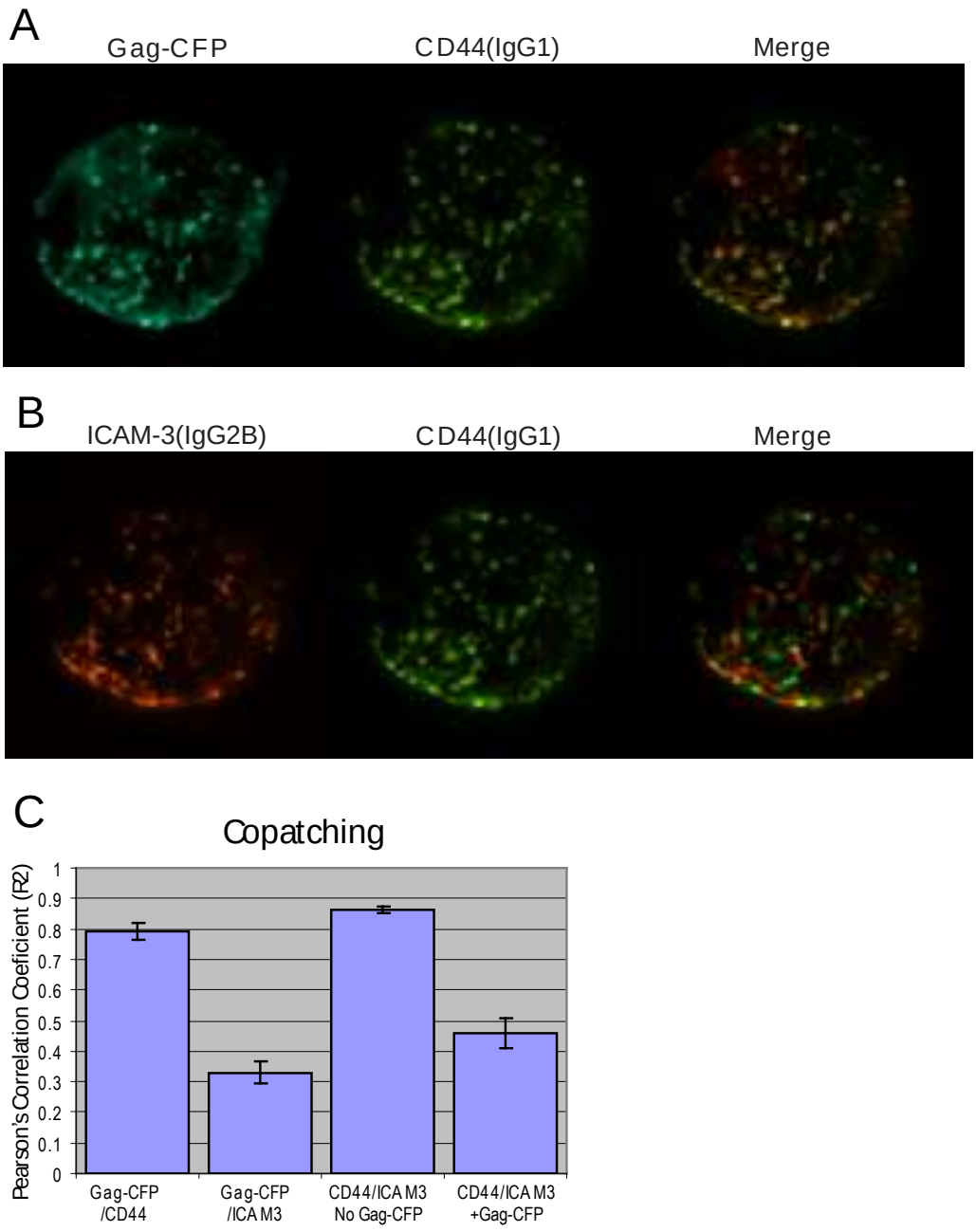

Figure 4.5. CD44/ICAM3 copatching is lost in the presence of Gag-CFP.
P2 cells were infected with VSV-G pseudotyped viral particles encoding Gag-CFP. Cells were immunostained by copatching and the tops of cells were imaged for **A)** CD44(IgG1) and Gag-CFP (red in the merged image) and **B)** CD44(IgG1) and ICAM-3(IgG2B). The image for (**A**) and (**B**) are of the same cell. **C)** Quantification of copatching was done using Pearson's coefficient. The first and fourth columns were quantified from the same Gag-CFP expressing cells immunostained for both ICAM-3 and CD44, while the second column was quantified from cells expressing Gag-CFP and only immunostained for ICAM-3, and the third column was quantified from uninfected cells immunostained for ICAM-3 and CD44.

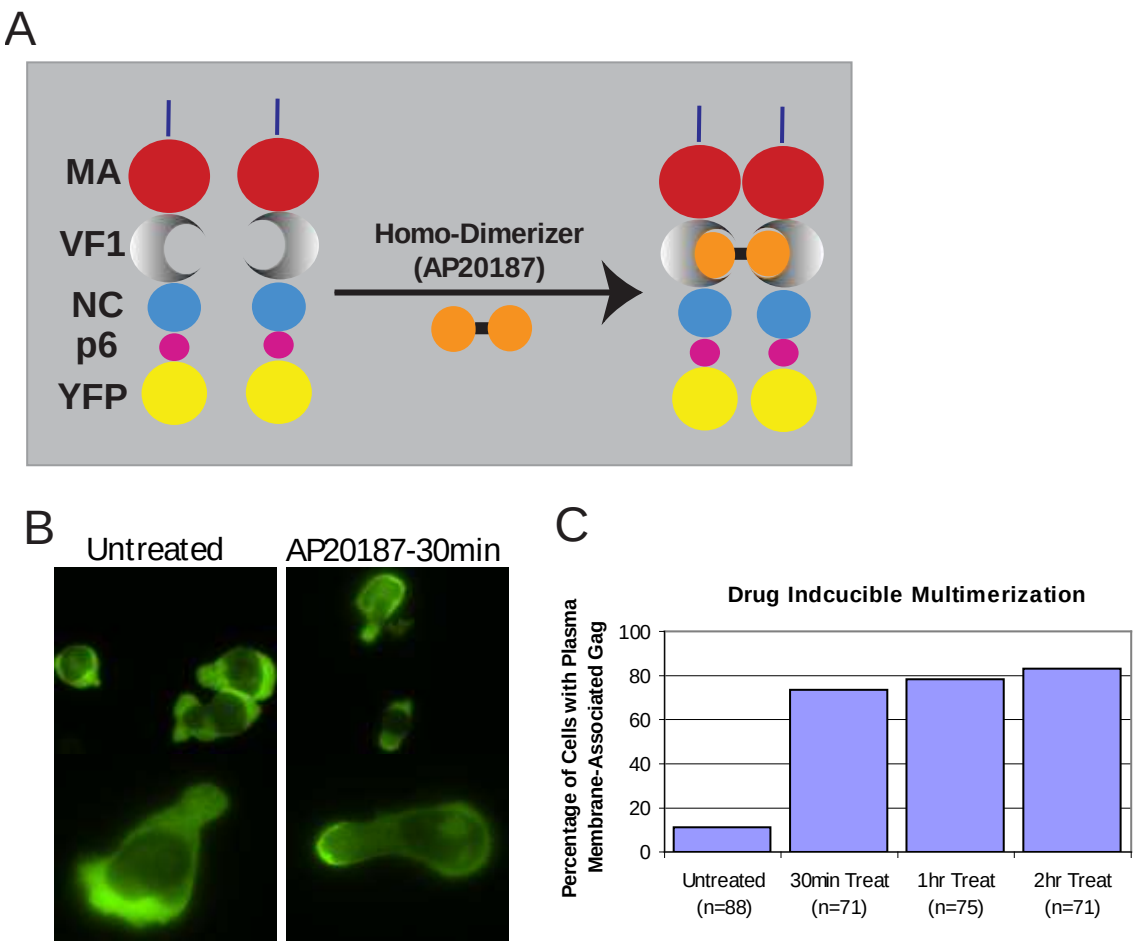

Figure 4.6. Drug inducible multimerization system.
A) Illustration of AP20187 induced multimerization of Gag containing the FV1 dimerization motif in place of CA (ΔCA/VF1/Gag-YFP). **B)** P2 cells were infected by VSV-G pseudotyped virus particles encoding ΔCA/VF1/Gag-YFP. 2 days post infection ΔCA/VF1/Gag-YFP is observed in the cytoplasm but not on the membrane (left panel), but after 30 minutes of AP20187 treatment, ΔCA/VF1/Gag-YFP is observed on the plasma membrane. **C)** Quantification of the percentage of observed with ΔCA/FV1/Gag-YFP on the membrane with or without AP20187 treatment. n=number of cells quantified.

References

1. Chen, P., et al., *Predominant mode of human immunodeficiency virus transfer between T cells is mediated by sustained Env-dependent neutralization-resistant virological synapses.* Journal of Virology, 2007. **81**(22): p. 12582-12595.

2. Dimitrov, D.S., et al., *Quantitation of Human-Immunodeficiency-Virus Type-1 Infection Kinetics.* Journal of Virology, 1993. **67**(4): p. 2182-2190.

3. Hubner, W., et al., *Quantitative 3D Video Microscopy of HIV Transfer Across T Cell Virological Synapses.* Science, 2009. **323**(5922): p. 1743-1747.

4. Martin, N., et al., *Virological Synapse-Mediated Spread of Human Immunodeficiency Virus Type 1 between T Cells Is Sensitive to Entry Inhibition.* Journal of Virology, 2010. **84**(7): p. 3516-3527.

5. Mazurov, D., et al., *Quantitative Comparison of HTLV-1 and HIV-1 Cell-to-Cell Infection with New Replication Dependent Vectors.* Plos Pathogens, 2010. **6**(2).

6. Bajenoff, M., et al., *Stromal cell networks regulate lymphocyte entry, migration, and territoriality in lymph nodes.* Immunity, 2006. **25**(6): p. 989-1001.

7. Hugues, S., et al., *Distinct T cell dynamics in lymph nodes during the induction of tolerance and immunity.* Nature Immunology, 2004. **5**(12): p. 1235-1242.

8. Miller, M.J., et al., *Autonomous T cell trafficking examined in vivo with intravital two-photon microscopy.* Proceedings of the National Academy of Sciences of the United States of America, 2003. **100**(5): p. 2604-2609.

9. Miller, M.J., et al., *Two-photon imaging of lymphocyte motility and antigen response in intact lymph node.* Science, 2002. **296**(5574): p. 1869-1873.

10. Mrass, P., et al., *Random migration precedes stable target cell interactions of tumor-infiltrating T cells.* Journal of Experimental Medicine, 2006. **203**(12): p. 2749-2761.

11. Mempel, T.R., S.E. Henrickson, and U.H. Von Andrian, *T-cell priming by dendritic cells in lymph nodes occurs in three distinct phases.* Nature, 2004. **427**(6970): p. 154-9.

12. Delpozo, M.A., et al., *Chemokines Regulate Cellular-Polarization and Adhesion Receptor Redistribution during Lymphocyte Interaction with Endothelium and Extracellular-Matrix - Involvement of Camp Signaling Pathway.* Journal of Cell Biology, 1995. **131**(2): p. 495-508.

13. Serrador, J.M., et al., *CD43 interacts with moesin and ezrin and regulates its redistribution to the uropods of T lymphocytes at the cell-cell contacts.* Blood, 1998. **91**(12): p. 4632-4644.

14. Tibaldi, E.V., R. Salgia, and E.L. Reinherz, *CD2 molecules redistribute to the uropod during T cell scanning: Implications for cellular activation and immune surveillance.* Proceedings of the National Academy of Sciences of the United States of America, 2002. **99**(11): p. 7582-7587.

15. Sourisseau, M., et al., *Inefficient human immunodeficiency virus replication in mobile lymphocytes.* Journal of Virology, 2007. **81**(2): p. 1000-1012.

16. Jolly, C., et al., *HIV-1 cell to cell transfer across an Env-induced, actin-dependent synapse.* Journal of Experimental Medicine, 2004. **199**(2): p. 283-93.

17. Rudnicka, D., et al., *Simultaneous Cell-to-Cell Transmission of Human Immunodeficiency Virus to Multiple Targets through Polysynapses.* Journal of Virology, 2009. **83**(12): p. 6234-6246.

18. Sol-Foulon, N., et al., *ZAP-70 kinase regulates HIV cell-to-cell spread and virological synapse formation.* Embo Journal, 2007. **26**(2): p. 516-526.

19. Burniston, M.T., et al., *Human immunodeficiency virus type 1 Gag polyprotein multimerization requires the nucleocapsid domain and RNA and is promoted by the capsid-dimer interface and the basic region of matrix protein.* Journal of Virology, 1999. **73**(10): p. 8527-8540.

20. Hogue, I.B., A. Hoppe, and A. Ono, *Quantitative Fluorescence Resonance Energy Transfer Microscopy Analysis of the Human Immunodeficiency Virus Type 1 Gag-Gag Interaction: Relative Contributions of the CA and NC Domains and Membrane Binding.* Journal of Virology, 2009. **83**(14): p. 7322-7336.

21. Campbell, S. and A. Rein, *In vitro assembly properties of human immunodeficiency virus type 1 Gag protein lacking the p6 domain.* Journal of Virology, 1999. **73**(3): p. 2270-2279.

22. Campbell, S. and V.M. Vogt, *Self-Assembly in-Vitro of Purified Ca-Nc Proteins from Rous-Sarcoma Virus and Human-Immunodeficiency-Virus Type-1.* Journal of Virology, 1995. **69**(10): p. 6487-6497.

23. Cimarelli, A., et al., *Basic residues in human immunodeficiency virus type 1 nucleocapsid promote virion assembly via interaction with RNA.* Journal of Virology, 2000. **74**(7): p. 3046-3057.

24. Dawson, L. and X.F. Yu, *The role of nucleocapsid of HIV-1 in virus assembly.* Virology, 1998. **251**(1): p. 141-157.

25. Sandefur, S., V. Varthakavi, and P. Spearman, *The I domain is required for efficient plasma membrane binding of human immunodeficiency virus type 1 Pr55(Gag).* Journal of Virology, 1998. **72**(4): p. 2723-2732.

26. Crist, R.M., et al., *Assembly Properties of Human Immunodeficiency Virus Type 1 Gag-Leucine Zipper Chimeras: Implications for Retrovirus Assembly.* Journal of Virology, 2009. **83**(5): p. 2216-2225.

27. Accola, M.A., B. Strack, and H.G. Gottlinger, *Efficient particle production by minimal gag constructs which retain the carboxy-terminal domain of human immunodeficiency virus type 1 capsid-p2 and a late assembly domain.* Journal of Virology, 2000. **74**(12): p. 5395-5402.

28. Zhang, Y.Q., et al., *Analysis of the assembly function of the human immunodeficiency virus type 1 gag protein nucleocapsid domain.* Journal of Virology, 1998. **72**(3): p. 1782-1789.

29. Franke, E.K., H.E.H. Yuan, and J. Luban, *Specific Incorporation of Cyclophilin-a into Hiv-1 Virions.* Nature, 1994. **372**(6504): p. 359-362.

30. Kong, L.B., et al., *Cryoelectron microscopic examination of human immunodeficiency virus type 1 virions with mutations in the cyclophilin A binding loop.* Journal of Virology, 1998. **72**(5): p. 4403-4407.

31. Hogue, I.B., et al., *Gag Induces the Coalescence of Clustered Lipid Rafts and Tetraspanin-Enriched Microdomains at HIV-1 Assembly Sites on the Plasma Membrane.* Journal of Virology, 2011. **85**(19): p. 9749-9766.

32. von Schwedler, U.K., et al., *Functional surfaces of the human immunodeficiency virus type 1 capsid protein.* Journal of Virology, 2003. **77**(9): p. 5439-5450.

33. Jonathan R. Grover, G.N.L., Ferri Soheilian, Kunio Nagashima, Sarah L. Veatch, Akira Ono, *The ESCRT complex promotes recruitment of tetherin to HIV-1 assembly sites.* In Revision, 2012.

34. Krementsov, D.N., et al., *HIV-1 Assembly Differentially Alters Dynamics and Partitioning of Tetraspanins and Raft Components.* Traffic, 2010. **11**(11): p. 1401-1414.

35. Alfadhli, A., A. Still, and E. Barklis, *Analysis of human immunodeficiency virus type 1 matrix binding to membranes and nucleic acids.* Journal of Virology, 2009. **83**(23): p. 12196-203.

36. Bryant, M. and L. Ratner, *Myristoylation-Dependent Replication and Assembly of Human Immunodeficiency Virus-1.* Proceedings of the National Academy of Sciences of the United States of America, 1990. **87**(2): p. 523-527.

37. Chukkapalli, V., et al., *Interaction between the human immunodeficiency virus type 1 Gag matrix domain and phosphatidylinositol-(4,5)-bisphosphate is essential for efficient Gag membrane binding.* Journal of Virology, 2008. **82**(5): p. 2405-2417.

38. Chukkapalli, V., S.J. Oh, and A. Ono, *Opposing mechanisms involving RNA and lipids regulate HIV-1 Gag membrane binding through the highly basic region of the matrix domain.* Proceedings of the National Academy of Sciences of the United States of America, 2010. **107**(4): p. 1600-1605.

39. Dalton, A.K., et al., *Electrostatic interactions drive membrane association of the human immunodeficiency virus type 1 Gag MA domain.* Journal of Virology, 2007. **81**(12): p. 6434-6445.

40. Ono, A., et al., *Phosphatidylinositol (4,5) bisphosphate regulates HIV-1 Gag targeting to the plasma membrane.* Proc Natl Acad Sci U S A, 2004. **101**(41): p. 14889-94.

41. Saad, J.S., et al., *Structural basis for targeting HIV-1 Gag proteins to the plasma membrane for virus assembly.* Proceedings of the National Academy of Sciences of the United States of America, 2006. **103**(30): p. 11364-11369.

42. Zhou, W.J., et al., *Identification of a Membrane-Binding Domain within the Amino-Terminal Region of Human-Immunodeficiency-Virus Type-1 Gag Protein Which Interacts with Acidic Phospholipids.* Journal of Virology, 1994. **68**(4): p. 2556-2569.

43. van den Bogaart, G., et al., *Membrane protein sequestering by ionic protein-lipid interactions.* Nature, 2011. **479**(7374): p. 552-555.

44. Alonso-Lebrero, J.L., et al., *Polarization and interaction of adhesion molecules P-selectin glycoprotein ligand 1 and intercellular adhesion molecule 3 with moesin and ezrin in myeloid cells.* Blood, 2000. **95**(7): p. 2413-9.

45. Yonemura, S., et al., *Ezrin/radixin/moesin (ERM) proteins bind to a positively charged amino acid cluster in the juxta-membrane cytoplasmic domain of CD44, CD43, and ICAM-2.* Journal of Cell Biology, 1998. **140**(4): p. 885-95.

46. Serrador, J.M., et al., *A novel serine-rich motif in the intercellular adhesion molecule 3 is critical for its ezrin/radixin/moesin-directed subcellular targeting.* J Biol Chem, 2002. **277**(12): p. 10400-9.

47. Serrador, J.M., et al., *A juxta-membrane amino acid sequence of P-selectin glycoprotein ligand-1 is involved in moesin binding and ezrin/radixin/moesin-directed targeting at the trailing edge of migrating lymphocytes.* Eur J Immunol, 2002. **32**(6): p. 1560-6.

48. Zarbock, A., C.A. Lowell, and K. Ley, *Spleen tyrosine kinase Syk is necessary for E-selectin-induced alpha(L)beta(2) integrin-mediated rolling on intercellular adhesion molecule-1.* Immunity, 2007. **26**(6): p. 773-83.

49. Urzainqui, A., et al., *ITAM-based interaction of ERM proteins with Syk mediates signaling by the leukocyte adhesion receptor PSGL-1.* Immunity, 2002. **17**(4): p. 401-12.

50. Jolly, C., I. Mitar, and Q.J. Sattentau, *Adhesion molecule interactions facilitate human immunodeficiency virus type 1-induced virological synapse formation between T cells.* Journal of Virology, 2007. **81**(24): p. 13916-21.

51. Tardif, M.R. and M.J. Tremblay, *LFA-1 is a key determinant for preferential infection of memory CD4(+) T cells by human immunodeficiency virus type 1.* Journal of Virology, 2005. **79**(21): p. 13714-13724.

52. Machta, B.B., et al., *Minimal model of plasma membrane heterogeneity requires coupling cortical actin to criticality.* Biophys J, 2011. **100**(7): p. 1668-77.

53. Betzig, E., et al., *Imaging intracellular fluorescent proteins at nanometer resolution.* Science, 2006. **313**(5793): p. 1642-5.

54. Rust, M.J., M. Bates, and X. Zhuang, *Sub-diffraction-limit imaging by stochastic optical reconstruction microscopy (STORM).* Nat Methods, 2006. **3**(10): p. 793-5.

55. McKinney, S.A., et al., *A bright and photostable photoconvertible fluorescent protein.* Nat Methods, 2009. **6**(2): p. 131-3.

56. Endesfelder, U., et al., *Chemically induced photoswitching of fluorescent probes--a general concept for super-resolution microscopy.* Molecules, 2011. **16**(4): p. 3106-18.

57. Axelrod, D., T.P. Burghardt, and N.L. Thompson, *Total internal reflection fluorescence.* Annu Rev Biophys Bioeng, 1984. **13**: p. 247-68.

58. Hammond, S., et al., *Roles for SH2 and SH3 domains in Lyn kinase association with activated Fc epsilon RI in RBL mast cells revealed by patterned surface analysis.* Journal of Structural Biology, 2009. **168**(1): p. 161-167.

59. Jouvenet, N., et al., *Plasma membrane is the site of productive HIV-1 particle assembly.* PLoS Biol, 2006. **4**(12): p. e435.

60. Jouvenet, N., P.D. Bieniasz, and S.M. Simon, *Imaging the biogenesis of individual HIV-1 virions in live cells.* Nature, 2008. **454**(7201): p. 236-40.

61. Ivanchenko, S., et al., *Dynamics of HIV-1 assembly and release.* Plos Pathogens, 2009. **5**(11): p. e1000652.

62. Jouvenet, N., S.M. Simon, and P.D. Bieniasz, *Imaging the interaction of HIV-1 genomes and Gag during assembly of individual viral particles.* Proc Natl Acad Sci U S A, 2009. **106**(45): p. 19114-9.

63. Mazurov, D., et al., *The role of O-glycosylation and expression of CD43 and CD45 on the surface of effector T cells in HTLV-1 cell-to-cell infection.* Journal of Virology, 2011.

Acknowledgements: The only one I'll thank is Chaelin Wang. I'm sorry for what happened, it was my fault. But you are the **best** thing that ever happened to my life. Thank you for everything, and I will forever love you.